COALESCENCE OF POSTPOLYMERIZATION MODIFICATION AND CLICK CHEMISTRY: THE DEVELOPMENT OF A POWERFUL METHOD TO GENERATE COMPLEX SURFACES

by

RACHELLE MARIE ARNOLD

(Under the Direction of Jason Locklin)

ABSTRACT

Using polymer science as a fundamental platform allows for a true interdisciplinary approach to create sophisticated and adaptable surfaces when combined with biology, materials science, and organic chemistry. Polymer thin films offer a wide range of possibilities to intricately design and tune the interfacial properties of specialized surfaces. Postpolymerization modification (PPM) through click reactions provides simple methods to easily create complex surfaces that bare spatially resolved chemical functionalities and incorporate very delicate components such as biomacromolecules or nanostructures. A stable, highly-reactive polymer, poly(pentafluorophenyl acrylate) (poly(PFPA)), was studied as a universal scaffold for the generation of these complex surfaces. The kinetics of the surface-initiated free radical polymerization of poly(PFPA) films were analyzed by varying the monomer concentration and the reaction time. Subsequently, the pseudo-first order reaction kinetics of aminolysis was determined via *ex situ* UV-vis. Patterned surfaces of PFPA and a second monomer containing a protected alkyne were produced through sequential surface-initiated free radical polymerizations.

The orthogonality of the aminolysis and copper(I)-catalyzed azide-alkyne cycloaddition reactions allowed for a one-pot, self-sorting modification reaction to be performed without cross contamination. Finally, poly(PFPA) was grafted directly onto oxide substrates through covalent attachment to surface silanol functional groups. Hydrolysis and anhydride formation was observed when thermal annealing was performed in ambient conditions, but under inert conditions, no side reactions were detected. Reactive microcapillary printing on the graft to poly(PFPA) films provided two areas of distinct chemistry that could be further functionalized to yield patterns with high resolution.

INDEX WORDS: CLICK CHEMISTRY, SURFACE-BOUND POLYMERS, POSTPOLYMERIZATION MODIFICATION, COMPLEX SURFACES, PATTERNED SURFACES

COALESCENCE OF POSTPOLYMERIZATION MODIFICATION AND CLICK CHEMISTRY: THE DEVELOPMENT OF A POWERFUL METHOD TO GENERATE COMPLEX SURFACES

by

RACHELLE MARIE ARNOLD

B.S., University of Indianapolis, 2009

A Dissertation Submitted to the Graduate Faculty of The University of Georgia in Partial Fulfillment of the Requirements for the Degree

DOCTOR OF PHILOSOPHY

ATHENS, GEORGIA

2014

COALESCENCE OF POSTPOLYMERIZATION MODIFICATION AND CLICK CHEMISTRY: THE DEVELOPMENT OF A POWERFUL METHOD TO GENERATE COMPLEX SURFACES

by

RACHELLE MARIE ARNOLD

Major Professor: Jason Locklin

Committee: Geoffrey Smith
John Stickney

Electronic Version Approved:

Julie Coffield
Interim Dean of the Graduate School
The University of Georgia
August 2014

DEDICATION

My dissertation is dedicated to Uncle Bob, who was my inspiration for attending graduate school. I'm pretty sure he had a bazillion degrees, and we always joked that he was a permanent student. Knowing that, I always thought of him when grad school got rough. If he could survive that many PhDs, I knew I would get through this one.

ACKNOWLEDGEMENTS

First and foremost, I want to thank my family. Mom, Dad, and Brandon, there is no way for me to show you how grateful and blessed I am to have you in my life. I'm the luckiest person in the world to have a family who supports my nerdiness as much as you do. You guys have been my anchor to keep me grounded, my shelter when the storms came, and my reason to keep trucking. I'll guess I could think about buying that house with a lake and a guesthouse because you have definitely have earned it. I love you guys more than anything. To all of my other family, and those who I call family, thank you from the bottom of my heart for all your support. There are way too many of you to name, or I would. But you know who you are. You all mean the world to me, and I am so appreciative for everything you have done for me.

Next, I would like to thank my PI, Jason Locklin, for being a constant role model and friend. Thank you for all the amazing opportunities you have given me, for believing in me when I had no confidence, and for never giving up on me. Your constant drive and high expectations have helped me grow not only as a scientist, but also as a person. I don't know many people who would put up with my sass and stubbornness for as long as you have. I truly appreciate everything. I would also like to thank my committee, John Stickney and Geoff Smith, for their time, knowledge, and push to help me reach my full potential.

To all the lab mates whom I have had the privilege to work with; Sara, Kristen, Vikram, Shameem, Kyle, Gareth, Eric, Evan, Joe, Jenna, Anandi, Jing, Jeremy, Josh,

Alex, Karson, and Deb. You have all helped mold me as a person and a leader, especially those who considered me the “Lab Mom”. I appreciate the support and opportunities you have given me over the years. I would especially like to thank Sara, who was my mentor when I started graduate school. Thank you for showing me how awesome activated esters are and for guiding me toward my dissertation project. Gareth, who got me in trouble for buying 23 boxes of aluminum foil, 9 Teflon flow cells, and many other things in unnecessarily large quantities. Thank you for always being there to bounce ideas off of and for helping me keep my sanity. Joe, who has been my brother from another mother. Thank you for always being there for me, no matter what it was. (I know my parents thank you for that, too!) I’m very excited to become your coworker at DaniMer after all of this is said and done. Anandi and Deb, who have become dear friends and an important part of my posse. The adventures we have had and the time we have spent together means the world to me. You have helped me more than you could ever know this past year. I look forward to future shenanigans! To several others; Evan, Josh, Sean, Tom, Chris, Dewey, Brandon, Henry, David, Brian, and Theresa. I will cherish all the memories and fun times we have had outside of lab. I feel like I have been through a lot with you, and grad school has definitely been better over the years because of it.

TABLE OF CONTENTS

Page

APPENDICES

LIST OF TABLES

Page

LIST OF FIGURES

Page

CHAPTER 1

INTRODUCTION AND LITERATURE REVIEW[1,2]

[1] Arnold, R. M.; Huddleston, N. E.; Locklin, J., *J. Mater. Chem.* **2012**, *22*, 19357-19365. Adapted with permission from The Royal Society of Chemistry.
[2] Adapted from review submitted to Accounts of Chemical Research.

Polymer Thin Films

Polymer thin films are robust, nano- and microstructured coatings that are attached to solid substrates and allow precise control over interfacial properties such as wettability, adhesion, friction, and absorption of biomolecules.[1-3] Polymer coatings can be generated in two ways, through physical deposition (physisorption) or covalent immobilization (chemisorption). Physisorption relies on weak intermolecular forces, such as hydrogen bonding, electrostatic interactions, and hydrophilic/hydrophobic interactions, between the polymer and the substrate. In most cases, the application of these coatings (i.e. spray coating, spin coating, or dip coating) requires a solvent to evaporate after the molecule is cast from a solution onto the substrate. The major disadvantage of using physisorption as the attachment mechanism is breakdown of the films under non-ideal conditions due to dewetting, delamination, desorption, or displacement.[2] The paint used on the side of a house that is peeling due to harsh weather conditions is an example of a physisorbed polymer coating that has failed.

Covalently attaching a polymer to a surface through chemisorption provides a more robust film. The added stability of the coating expands the number of applications for which these films can be used. Attachment can be accomplished through a "grafting to" method in which a polymer with a reactive functional group at one chain end, or several reactive groups along the backbone, is synthesized in solution. The chains can then adsorb and covalently attach to a complimentary functional group on the surface (Figure 1.1). One major advantage of using the grafting to method is that the polymer can be fully characterized (molecular weight, dispersity, etc.) before grafting. However, this thermodynamically and kinetically self-limiting process keeps polymer grafting densities

low and limits the degree of chain extension (Figure 1.2). The lack of chain interactions yields insufficient energy to overcome the entropically favored random coil configuration that the polymer adopts in solution. The polymer chains remain coiled once attached to the surface, which is commonly referred to as the mushroom regime, resulting in films less than 10 nm in thickness.[2]

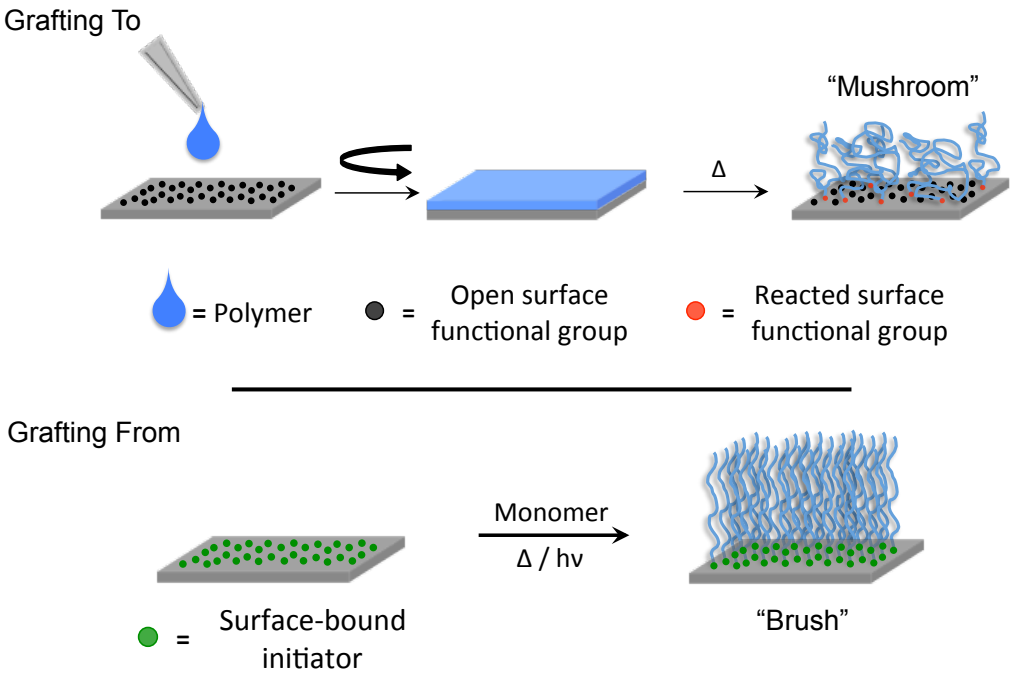

Figure 1.1. Schematic of example grafting to and grafting from processes.

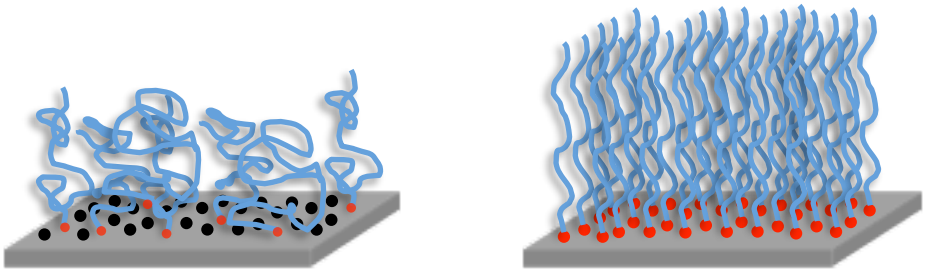

Figure 1.2. Polymer chain conformations in thin films. Mushroom regime (left). Polymer brush (right).

When grafting polymers to a surface, it is common to use a "primer layer" to provide increased reactivity at the interface. A primer layer consists of an anchoring polymer that is reactive towards both the substrate and the polymer to be bound to the surface.[4] One example of an anchoring polymer is poly(glycidyl methacrylate) (PGMA). The reactive epoxy functional group can ring open under the appropriate conditions to form a covalent bond with carboxyl, hydroxyl, amino, or anhydride functionalities. The amplified number of increased reactive sites on the surface can improve the grafting density of these films, although film thicknesses are usually still below 15 nm.

A "grafting from" method, where a polymer initiator is tethered to the surface using self-assembly and the polymerization proceeds directly from the substrate, can also be used to make polymer thin films. As the polymerization progresses, steric crowding and excluded volume effects cause the polymer chains to stretch away from the surface due to the densely packed initiators. These extended conformations are known as polymer brushes (Figure 1.2). The benefits of grafting from techniques include thicker films, a greater volume of functional groups, and unique interfacial properties that result from the polymer chain conformation.

Surface-initiated Free Radical Polymerization

Free radical polymerizations follow a chain growth mechanism consisting of three steps: initiation, propagation, and termination.[5] Initiation has two separate reactions. The first is homolytic dissociation of the initiator to produce primary radicals (Eq. 1.1), followed by the addition of a monomer unit, referred to as a radical center (Eq. 1.2).[5] In most cases, the first step of initiation is rate determining, as generating a radical center

occurs rapidly once the primary radical is formed. The work in this dissertation utilizes azobisisobutyronitrile (AIBN), or a derivative thereof, as the initiator species. Azo-based initiators undergo homolytic cleavage when activated by temperatures above 50 °C or by 300-350 nm UV light. In surface-initiated polymerizations, the azo group decomposes to produce both a surface-tethered radical and a free solution radical while releasing nitrogen gas (Scheme 1.1, Step 1). Unlike solution initiation, initiator efficiency tends to decrease with increasing initiator conversion on the surface due to restricted radical diffusion out of solvent and monomer cages even though the tethered radical is at the end of a flexible alkyl chain. This leads to an enhancement of direct deactivation between two primary radicals. The increased viscosity at the interface due to the high concentration of polymer favors recombination of primary radicals, also reducing initiation efficiency.[5]

$$I \xrightarrow{k_d} R\cdot \qquad \text{(Eq. 1.1)}$$

$$R\cdot + M \xrightarrow{k_i} M_1\cdot \qquad \text{(Eq. 1.2)}$$

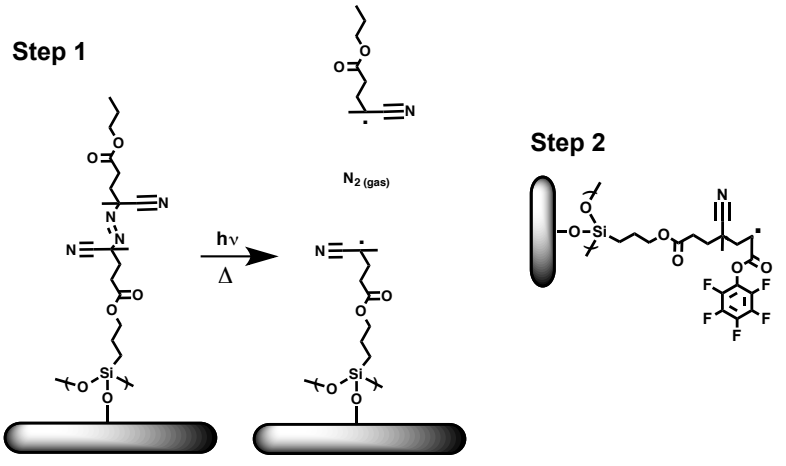

Scheme 1.1. Thermal or photoinitiation of surface-bound azo-based initiator.

Once the primary radicals escape the solvent/monomer cage, propagation occurs, adding one monomer unit at a time (Scheme 1.1, Step 2). With chain growth polymerizations, high molecular weight polymer is formed rapidly and remains essentially constant for the rest of the polymerization. Even though the molecular weight stays constant, the concentration of monomer is reduced with time, thus increasing conversion. While surface-initiated free radical polymerizations generate both surface-bound and free polymer in solution, it is theorized that the molecular weight and dispersity cannot be directly compared due to a difference in the polymerization rates because of dissimilar environments.[6]

During free radical polymerizations, termination can occur through two different bimolecular reactions.[5] The first is a radical combination or coupling. The second, called disproportionation, occurs when a hydrogen beta to the radical center is transferred to a different radical center, resulting in a dead chain end. Even though the rate constant for termination is several orders of magnitude greater than that of propagation (10^6 - 10^8 $M^{-1}s^{-1}$ compared to 10^2 - 10^4 $M^{-1}s^{-1}$, respectively), the polymerization can still occur because the concentration of active radicals at any given time is very small. The possible routes for termination during a surface-initiated polymerization are shown in Figure 1.3. Pathway B is improbable and pathways A and C are favored on planar surfaces because of the very low concentration of radicals present. Polymerizations on high surface area substrates (i.e. particles) tend to terminate via pathway B.[7]

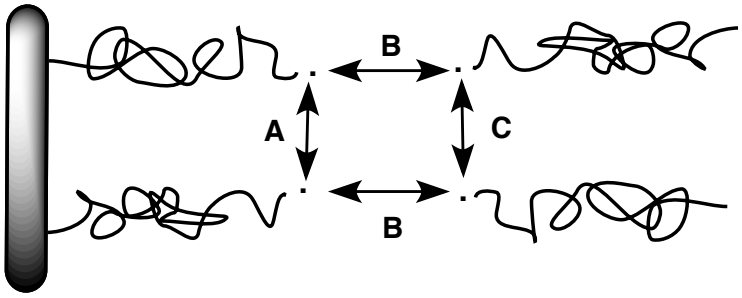

Figure 1.3. Possible termination pathways in surface-initiated free radical polymerizations. A) Coupling of two surface-bound radical centers. B) Coupling of one bound and one solution radical center. C) Coupling of two solution radical centers.

The rate of polymerization (R_p) is defined by Equation 1.3, where k_p is the rate constant for propagation, [M] is the monomer concentration, R_i is the rate of initiation, and k_t is the rate constant for termination. The rate of initiation has several parameters that should be taken into consideration (Eq. 1.4). A factor of 2 is used in front of the termination rate constant due to the loss of two radicals when coupling occurs. The steady state approximation, where the concentration of active radicals is believed to be constant, allows the polymerization rate to be determined without knowing the actual concentration of primary radicals or radical centers. The rate of polymerization is directly proportional to the concentration of monomer. However, R_p is only dependent on $(R_i)^{1/2}$. If the concentration of initiator is doubled, the R_p is only increased by a factor of $\sqrt{2}$.

$$R_p = k_p[M]\left(\frac{R_i}{2k_t}\right)^{1/2} \qquad \text{(Eq. 1.3)}$$

$$R_i = 2fk_d[I] \qquad \text{(Eq. 1.4)}$$

There are several advantages when using photoinitiation for generating polymer films. First, there are no limitations with temperature sensitive molecules and monomers because the polymerization is usually performed at room temperature. Second, turning the light source on or off can temporally control the polymerization. Also, there are several factors that can be adjusted to control the polymerization rate such as wavelength and light intensity, time of polymerization, and added temperature. Finally, the polymerization can be spatially directed through the use of various photolithography techniques, providing easy accessibility to patterned surfaces.[5] Drawbacks of using photoinitiation over thermal initiation can include absorbance of the monomer/solvent system[6] and penetration depth of the photons,[5] both of which can be adjusted for.

Postpolymerization Modification and Click Chemistry

When grafting polymers to and from surfaces, one of two strategies can be employed to incorporate specific chemical functionality along the backbone of a polymer chain: synthesizing a monomer that already contains the desired functional group, or performing multiple modification steps after polymerization. No postpolymerization modification is necessary if the functionality is already present in the monomer.[8] However, most polymerization methods are intolerant of certain functional groups, resulting in a loss of the desired functionality. For example, many polymerizations require organic solvents, UV light, or high temperatures, which can denature biomacromolecules or degrade other highly reactive functionalities. Fewer initial experiments are needed for multistep polymer modification, but often several

permutations are required to convert a polymer scaffold into the desired functionality because of both side reactions and poor yield.[9]

Designing a functional monomer that can withstand polymerization conditions but be derivatized in a single step is a simple, straightforward method for creating functional interfaces. In these cases, postpolymerization modification is utilized to generate polymers with sophisticated chemical functionality that would otherwise be difficult to produce. New and complex moieties such as nanostructures and biomolecules can rapidly be incorporated along the backbone of a polymer without degradation. With postpolymerization modification, a monomer containing a reactive group is first polymerized, followed by a second reaction to covalently attach the desired functionality.

With the advent of click chemistry by Sharpless,[10] the implementation of postpolymerization modification is an ever growing area of research. Examples of click reactions include, but are not limited to, non-aldol carbonyl chemistry such as oxime, hydrazone, and amide formation, oximes,[10-12] thiol-ene[13, 14] and thiol-yne,[15, 16] activated ester coupling,[17-23] azide-alkyne cycloaddition,[10, 24-26] and some Diels-Alder reactions.[27, 28] These reactions provide an efficient coupling strategy because of their functional group versatility, modularity, high yields with little to no side reactions, and mild reaction conditions.[10] With respect to polymer coatings, the modification of polymer interfaces using these reactions has emerged as an efficient way to control both the chemical composition and conformation of the polymer chains immobilized to a surface.

Common in peptide chemistry, activated ester reactive polymers were pioneered in 1972 by Ringsdorf and coworkers,[21] but only recently have been used for the functionalization of surfaces. Activated esters are considered click-like reactions because

they require no metal catalyst, have little to no side reactions or products, and reach quantitative conversion under mild conditions, making them suitable for biological studies. Activated ester chemistry yields amides through the covalent attachment of amines to carboxylic acid moieties.[29] This dissertation focuses on a new activated ester polymer scaffold, poly(pentafluorophenyl acrylate). This polymer was chosen as a universal platform for the generation of complex surfaces because of its high hydrolytic stability, increased solubility compared to previous active ester platforms, and high reactivity toward strong and weak nucleophiles.[30, 31]

Complex Surfaces

As thin film technology continues to advance, the demand for chemical complexity on two- and three-dimensional surfaces with well-defined spatial control has significantly increased. This is especially true for new technologies such as sensors and diagnostic arrays, microfluidic devices, membranes with selective permeability, and mediating interactions at the solid-biological interface. The ability to tune the interfacial properties such as wetting, surface energy, and adhesion allows one to control the interactions between the substrate and surrounding environment. Polymer-based thin films containing reactive functionality offer significant advantages for intricately designing complex coatings in terms of both structure and morphology.[1, 32-34] Postpolymerization modifications using a variety of click chemistries is a strategy that has gained considerable attention because of the rapid reaction rates, chemical orthogonality, and mild reaction conditions, which is of critical importance.[27, 34, 35] There are different ways to make multi-component surfaces, including the use of sequential

click reactions or functionalizing the surface in a self-sorting manner, in which multiple modifications are performed in one-pot. This provides an extra stage in which the postpolymerization functionalization can be tailored for the compatibility of the modifying molecules.

Objectives and Dissertation Outline

The objectives of this dissertation are as follows: 1) to understand the grafting from photoinitiated polymerization kinetics of pentafluorophenyl acrylate, 2) determine the kinetics of postpolymerization modification of pentafluorophenyl acrylate with various amino nucleophiles, 3) utilize photolithography in order to graft patterns of pentafluorophenyl acrylate and a second click monomer from the surface, 4) establish conditions for the one-pot functionalization of a self-sorting surface to produce complex surfaces, and 5) exploit the high reactivity of pentafluorophenyl acrylate to graft polymer films directly to oxide surfaces as a platform for complex surface generation.

The rest of this dissertation is organized into four chapters. Chapter 2 describes the photoinitiated polymerization kinetics of poly(pentafluorophenyl acrylate) from silicon substrates by varying monomer concentration and polymerization time. The kinetics for aminolysis were studied using three amines of differing nucleophilicity. These results were compared to the aminolysis kinetics of the active ester polymer platform that had been used previously by the group, poly(*N*-hydroxysuccimide 4-vinylbenzoate). It was found that the new platform not only had faster reaction kinetics, but it was also more reactive toward poor nucleophiles. This chapter is published in *Macromolecules,* **2012,** *45,* 5444-5450.

Chapter 3 uses photolithographic methods during polymerization to generate patterned surfaces on silicon oxide surfaces. Pentafluorophenyl acrylate was first polymerized from the surface in the presence of a shadow mask, preserving photoinitiators for a polymerization with a second monomer, 4-(trimethylsilyl) ethynylstyrene, which undergoes copper(I)-catalyzed azide-alkyne cycloaddition (CuAAC) with azides. The substrate was functionalized via aminolysis and dual desilylation/CuAAC in one-pot with two different dyes, 1-aminomethylpyrene and 5-azidofluorescein, respectively. Various characterization methods confirmed little to no cross contamination across the self-sorting surface. This chapter was published in *Langmuir,* **2013,** *29,* 5920-5926.

Chapter 4 describes the direct grafting of poly(pentafluorophenyl acrylate) to oxide surfaces. Thermal annealing of spincoated polymer yielded ultrathin films in which some of the active esters reacted with surface silanols of the substrate. Latent pentafluorophenyl groups were present after film attachment, allowing postpolymerization modification to be performed. Reactive microcapillary printing was used to pattern an amino-cyclooctyne molecule to the surface. A one-pot aminolysis/strain-promoted azide-alkyne cycloaddition was performed on the self-sorting surface to provide distinct areas of chemical functionality. This chapter was published in *Chemical Communications,* **2014,** *50,* 5307-5309.

Finally, Chapter 5 provides a general summary of the work completed for this dissertation, as well as the future direction for this research.

References

1. Orski, S. V., Fries, K. H., Sontag, S. K. and Locklin, J., *J. Mater. Chem.*, 2011, **21**, 14135-14149.
2. Rühe, J., in *Polymer Brushes*, Wiley-VCH Verlag GmbH & Co. KGaA, 2004, pp. 1-31.
3. Senaratne, W., Andruzzi, L. and Ober, C. K., *Biomacromolecules*, 2005, **6**, 2427-2448.
4. Liu, Y., Klep, V., Zdyrko, B. and Luzinov, I., *Langmuir*, 2004, **20**, 6710-6718.
5. Odian, G., *Principles of Polymerization*, John Wiley & Sons, Inc., Hoboken, New Jersey, 2004.
6. Turgman-Cohen, S. and Genzer, J., *J. Am. Chem. Soc.*, 2011, **133**, 17567-17569.
7. Prucker, O. and Ruhe, J., *Macromolecules*, 1998, **31**, 602-613.
8. Jain, P., Dai, J., Baker, G. L. and Bruening, M. L., *Macromolecules*, 2008, **41**, 8413-8417.
9. Huang, W., Kim, J.-B., Bruening, M. L. and Baker, G. L., *Macromolecules*, 2002, **35**, 1175-1179.
10. Kolb, H. C., Finn, M. G. and Sharpless, K. B., *Angew. Chem. Int. Ed.*, 2001, **40**, 2004-2021.
11. Jawalekar, A. M., Reubsaet, E., Rutjes, F. P. J. T. and van Delft, F. L., *Chem. Commun.*, 2011, **47**.
12. Sanders, B. C., Friscourt, F., Ledin, P. A., Mbua, N. E., Arumugam, S., Guo, J., Boltje, T. J., Popik, V. V. and Boons, G.-J., *J. Am. Chem. Soc.*, 2010, **133**, 949-957.

13. Hoyle, C. E. and Bowman, C. N., *Angew. Chem. Int. Ed.*, 2010, **49**, 1540-1573.

14. Campos, L. M., Killops, K. L., Sakai, R., Paulusse, J. M. J., Damiron, D., Drockenmuller, E., Messmore, B. W. and Hawker, C. J., *Macromolecules*, 2008, **41**, 7063-7070.

15. Hensarling, R. M., Doughty, V. A., Chan, J. W. and Patton, D. L., *J. Am. Chem. Soc.*, 2009, **131**, 14673-14675.

16. Lowe, A. B., Hoyle, C. E. and Bowman, C. N., *J. Mater. Chem.*, 2010, **20**.

17. Cullen, S. P., Liu, X., Mandel, I. C., Himpsel, F. J. and Gopalan, P., *Langmuir*, 2007, **24**, 913-920.

18. Kessler, D. and Theato, P., *Langmuir*, 2009, **25**, 14200-14206.

19. Murata, H., Prucker, O. and Rühe, J., *Macromolecules*, 2007, **40**, 5497-5503.

20. Orski, S. V., Fries, K. H., Sheppard, G. R. and Locklin, J., *Langmuir*, 2010, **26**, 2136-2143.

21. Theato, P., *J. Polym. Sci., Part A: Polym. Chem.*, 2008, **46**, 6677-6687.

22. Li, R. C., Hwang, J. and Maynard, H. D., *Chem. Commun.*, 2007, 3631-3633.

23. Subr, V. and Ulbrich, K., *React. Funct. Polym.*, 2006, **66**, 1525-1538.

24. Kuzmin, A., Poloukhtine, A., Wolfert, M. A. and Popik, V. V., *Bioconjugate Chem.*, 2010, **21**, 2076-2085.

25. Lutz, J.-F., *Angew. Chem. Int. Ed.*, 2008, **47**, 2182-2184.

26. Orski, S. V., Poloukhtine, A. A., Arumugam, S., Mao, L., Popik, V. V. and Locklin, J., *J. Am. Chem. Soc.*, 2010, **132**, 11024-11026.

27. Iha, R. K., Wooley, K. L., Nystrom, A. M., Burke, D. J., Kade, M. J. and Hawker, C. J., *Chem. Rev.*, 2009, **109**, 5620-5686.

28. Arumugam, S., Orski, S. V., Locklin, J. and Popik, V. V., *J. Am. Chem. Soc.*, 2011, **134**, 179-182.

29. Hawker, C. J. and Wooley, K. L., *Science*, 2005, **309**, 1200-1205.

30. Arnold, R. M., Sheppard, G. R. and Locklin, J., *Macromolecules*, 2012, **45**, 5444-5450.

31. Eberhardt, M., Mruk, R., Zentel, R. and Théato, P., *Eur. Polym. J.*, 2005, **41**, 1569-1575.

32. Azzaroni, O., *J. Polym. Sci., Part A: Polym. Chem.*, 2012, **50**, 3225-3258.

33. Barbey, R. l., Lavanant, L., Paripovic, D., Schüwer, N., Sugnaux, C., Tugulu, S. and Klok, H.-A., *Chem. Rev.*, 2009, **109**, 5437-5527.

34. Arnold, R. M., Huddleston, N. E. and Locklin, J., *J. Mater. Chem.*, 2012, **22**, 19357-19365.

35. Sumerlin, B. S. and Vogt, A. P., *Macromolecules*, 2009, **43**, 1-13.

CHAPTER 2

COMPARATIVE AMINOLYSIS KINETICS OF DIFFERENT ACTIVE ESTER POLYMER BRUSH PLATFORMS IN POSTPOLYMERIZATION MODIFICATION WITH PRIMARY AND AROMATIC AMINES[1]

[1] Arnold, R.M.; Sheppard, G.R.; and Locklin, J. *Macromolecules,* **2012,** *45* (13), 5444-5450. Reproduced with permission from Arnold, R.M.; Sheppard, G.R.; and Locklin, J. *Macromolecules,* **2012,** *45* (13), 5444-5450. Copyright 2012 American Chemical Society.

Abstract

The kinetics of aminolysis between two different active ester polymer brush platforms, poly(4-pentafluorophenyl acrylate) (poly(PFPA)) and poly(*N*-hydroxysuccinimide-4-vinyl benzoate) (poly(NHS4VB)), are compared using primary and aromatic amines with varying reactivity towards postpolymerization modification. UV-vis was used to monitor the aminolysis of both brush platforms with 1-aminomethylpyrene (AMP), 1-aminopyrene (AP), and $Ru(bpy)_2(phen\text{-}5\text{-}NH_2)(PF_6)$ ($Ru^{+2}A$). Using a pseudo-first order kinetics model, the pseudo-first order rate constant (k') was calculated for each system. The k' of poly(PFPA) modified with AMP, AP, and $Ru^{+2}A$ were 2.46×10^{-1} s^{-1}, 5.11×10^{-3} s^{-1}, and 2.59×10^{-3} s^{-1}, respectively, while poly(NHS4VB) can only be functionalized with the alkyl amine, albeit at a slower rate constant compared to poly(PFPA) with AMP, where k' is 3.49×10^{-3} s^{-1}. The kinetics of surface-initiated photopolymerization of PFPA from oxide surfaces was also investigated as an effective method to control grafting density and film thickness.

Introduction

With the increased interest in specialized surfaces for biotechnology and materials research, a substrate that has tunable functionalities is the most desirable.[1-7] The interfacial properties of the substrate play an important role in the development of these technologies, and can be adjusted using polymer films of various compositions and conformations, where covalent attachment ranges from the mushroom to the brush regime. Polymer brushes, which are usually created using a grafting from method, consist of macromolecular chains that are polymerized directly from a surface-bound initiator. When immobilized polymer chains are densely packed on a surface, steric crowding causes the chains to stretch away from the substrate to balance the free energy associated with chain stretching and chain-solvent interactions.[8] Because of this extended conformation, surface-bound polymer chains with high grafting density (brush regime) exhibit unique properties at an interface compared to films with low grafting density (mushroom regime), such as wettability, adhesion, and self-assembly.[5, 7]

Since not all polymerization techniques are tolerant to certain chemical functionalities, the utilization of click reactions for postpolymerization modification has recently become a rapidly growing field of interest.[9, 10] These reactions are wide in scope, quickly reach high conversion under simple reaction conditions, and generate by-products that are undisruptive to the system.[11] There are several types of click chemistries, including thiol-yne, azlactones, activated esters, copper-free azide-alkyne cycloaddition and certain Diels-Alder reactions, that exploit various reactive groups for chemical modification.[12]

Polymers synthesized from activated ester-containing monomers are a common substrate for postpolymerization modification. These polymers contain pendant leaving groups that can readily react with good nucleophiles such as thiols or amines under mild conditions. Several types of activated esters have been used previously, including *N*-hydroxysuccinimide (NHS)[13-21] and pentafluorophenol (PFP).[22-24] NHS is widely used for the surface immobilization of biological macromolecules to polymer interfaces through conjugation of the activated ester with lysine side chains or the N-terminus of the peptide backbone.[25-28] However, NHS is not ideal for coupling because of poor solubility, reduced reactivity compared to other activated esters, and susceptibility to hydrolysis and other side reactions.[25, 29-37] On the other hand, PFP as a leaving group in carbonyl substitution reactions has higher versatility in polymer synthesis and postpolymerization functionalization when compared to NHS because of a wider solubility range in organic solvents and exceptional reactivity towards amines. It has been shown that activated esters containing PFP pendant groups are less prone to hydrolysis and are more reactive towards poor nucleophiles, specifically secondary and aromatic amines.[34]

Activated ester polymers have been thoroughly studied in solution,[38-41] but not until recently have these polymers been grafted from surfaces in the brush configuration.[42-47] Utilizing active ester polymer brushes has many advantages over other polymer grafting regimes, such as the generation of a greater volume of functional groups as the polymer extends into the third dimension. The presence of accessible pendant groups for post-functionalization also has a large influence on the interfacial properties.[5] To understand the reaction scope and versatility of activated esters in the brush regime, the kinetics of postpolymerization modification with amines of various size and

reactivities must be assessed. In this chapter, the reaction kinetics of two surface-grafted activated ester polymer brushes, *N*-hydroxysuccinimide-4-vinyl benzoate (NHS4VB) and 4-pentafluorophenyl acrylate (PFPA), were investigated using alkyl and aromatic amines. Taking advantage of the different reactivities between the two leaving groups can lead to a universal surface platform that allows for the creation of complex and multifunctional interfaces.

Experimental

Materials

Solvents were distilled from sodium-ketyl (tetrahydrofuran, THF) or calcium hydride (toluene and dichloromethane, DCM), except anhydrous dimethyl sulfoxide (DMSO) and dimethylformamide (DMF), which were purchased from EMD (Drisolv, 99.8% by GC). Silicon wafers (orientation <100>, native oxide) were purchased from University Wafer. Quartz slides were purchased from Technical Glass Products. Impurities were removed from N,N,N',N'',N''-pentamethyldiethylenetriamine (PMDETA), purchased from TCI, and pentafluorophenol, purchased from Oakwood Products, through distillation. The atom transfer radical polymerization (ATRP) initiator, 11-(2-bromo-2-methyl)propionyloxyundecenyl trichlorosilane,[48] NHS4VB,[45] and PFPA[22] were all prepared according to literature procedures. PFPA was further purified by distillation, and any residual acrylic acid was removed by passing the PFPA through a plug of neutral alumina with DCM. $Ru(bpy)_2(phen\text{-}5\text{-}NH_2)(PF_6)$ ($Ru^{+2}A$) was received as a gift from the Schanze group at the University of Florida. All other chemicals were purchased from Alfa Aesar or TCI, and were used as received.

Synthesis of AIBN Initiator

The free radical initiator, **1**, was synthesized through a three-step procedure from azobis-4-cyanovaleric acid (Scheme 2.1). Briefly, two sequential Steglich esterifications were performed, followed by a hydrosilylation reaction to generate the azo-based silane initiator.

1a In a round bottom flask purged with nitrogen, 50 mL dry THF, 4-4'-azobis(4-cyanovaleric acid) (10.00 g, 35.7 mmol), 4-dimethylaminopyridine (DMAP, 0.256 g, 2.1 mmol), and n-propanol (2.13 g, 35.5 mmol) were stirred at 0 °C. N,N'-dicyclohexylcarbodiimide (DCC, 7.36 g, 35.7 mmol) was dissolved in 20 mL DCM and added dropwise to the solution overnight. The solution was vacuum filtered, concentrated under reduced pressure, and then extracted with DCM and washed with brine. The organic layer was dried with magnesium sulfate, filtered, and removed under vacuum. A waxy, off-white solid was collected (78.0 % yield). ^{1}H NMR (300 MHz, $CDCl_3$) δ 4.07 (m, 2H, 6.7 Hz), 2.69-2.26 (m, 8H), 1.74 (s, 3H), 1.69 (s, 3H), 1.64 (m, 2H), 0.95 (t, 3H, 7.2 Hz). ^{13}C NMR (300 MHz, $CDCl_3$) δ 176.53, 171.71, 117.72, 117.62, 72.18, 71.96, 66.97, 29.39, 29.31, 29.15, 29.07, 24.12, 23.91, 22.06, 10.55.

1b 8.93 g of **1a** (27.7 mmol) was dissolved in 50 mL dry DCM in a chilled round bottom flask, along with 1.60 g allyl alcohol (28.0 mmol), and 0.20 g DMAP (1.63 mmol). 5.71 g of DCC (27.7 mmol) in 15 mL DCM was added dropwise overnight. The urea salt was removed by vacuum filtration, and the resulting solution was washed with brine and saturated sodium bicarbonate. The organic layer was dried with magnesium sulfate and the solvent was removed under reduced pressure. The product collected was an oily residue, which was precipitated in cold hexane, resulting in white crystals (82.3%

yield). ^{1}H NMR (300 MHz, $CDCl_3$) δ 5.91 (m, 1H, 6.0 Hz), 5.33 (m, 1H), 5.29 (m, 1H), 4.61 (m, 2H), 4.06 (m, 2H, 6.8 Hz) 2.63-2.26 (m, 8H), 1.73 (s, 3H), 1.68 (s, 3H), 1.64 (m, 2H), 0.95 (t, 3H, 7.5 Hz). ^{13}C NMR (300 MHz, $CDCl_3$) δ 171.59, 171.17, 131.96, 119.10, 117.68, 117.64, 72.17, 72.12, 66.91, 65.91, 33.42, 33.37, 29.31, 29.27, 24.16, 23.97, 22.09, 10.55.

1 10 mL of dry DCM was added to a round bottom flask along with **1b** (1 g, 2.76 mmol), trichlorosilane (3.74 g, 27.6 mmol), and a catalytic amount of chloroplatinic acid. The reaction was allowed to stir overnight. The solvent and any residual trichlorosilane was removed under vacuum at 100 mTorr, with the resulting waxy solid being transferred into a nitrogen filled glovebox for storage. ^{1}H NMR (300 MHz, $CDCl_3$) δ 4.16 (m, 2H), 4.07 (m, 2H), 2.64-2.26 (m, 8H), 1.94 (m, 2H), 1.73 (s, 3H), 1.68 (s, 3H), 1.64 (m, 2H), 1.46 (m, 2H), 0.95 (t, 3H). ^{13}C NMR (300 MHz, $CDCl_3$) δ 171.60, 171.14, 117.68, 117.64, 72.17, 72.06, 66.86, 65.92, 29.36, 29.33, 29.25, 29.18, 24.14, 23.93, 22.06, 21.93, 20.98, 10.55.

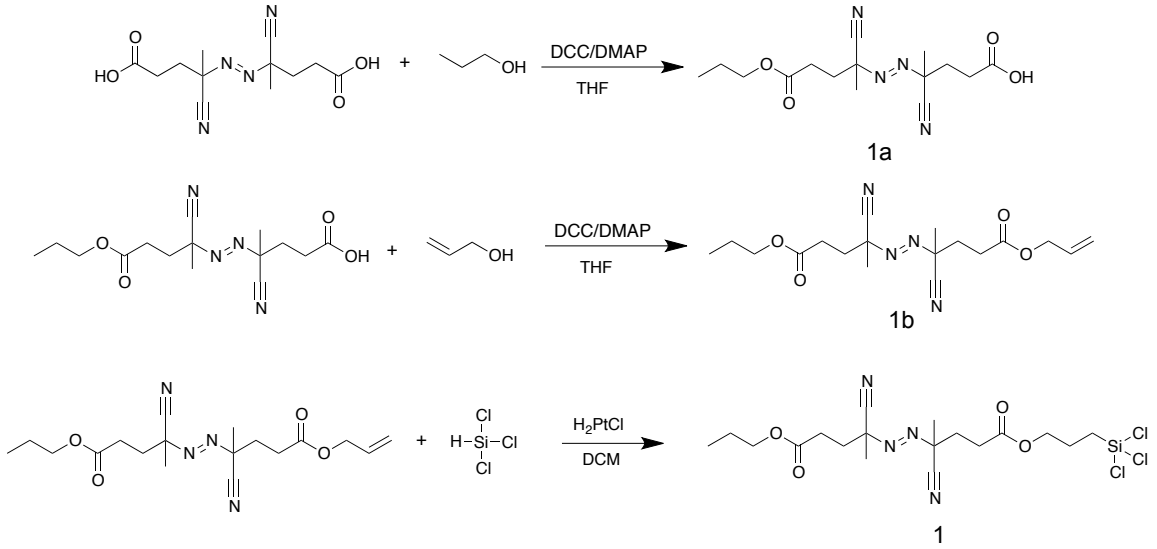

Scheme 2.1. Synthesis of azo-based surface-bound initiator, **1**.

Preparation of Initiator Layers

Silicon wafers and quartz slides cut to approximately 8 x 20 mm^2 were sonicated in hexane, IPA, acetone, and deionized water for 15 minutes each. The substrates were dried in a stream of nitrogen, and subjected to argon plasma (Harrick Plasma, PDC-32-G, 0.8 mbar, 18 W) for 5 minutes. The substrates were transferred into a nitrogen filled glovebox along with dry, degassed reagents. A 10 mM stock solution of each initiator was made using 20 mL of toluene. The initiator solution was added to two different batches of substrates and allowed to sit for 16 hrs. They were then removed from the box, rinsed with toluene, and dried with nitrogen. It is assumed the grafting density and polymerization thicknesses are the same for the silicon and quartz substrates since the two types of substrates were cleaned and treated under identical conditions.

Polymerization of NHS4VB

Substrates with the ATRP initiator and NHS4VB (0.663 g, 2.70 mmol) were placed into a flat bottom Schlenk flask with a stir bar. The glassware was transferred into a glovebox where 1.5 mL DMSO and 93 μL of an ATRP stock solution were added. The stock solution consisted of DMSO (500 μL), PMDETA (423 μL, 2.03 mmol), CuBr (39 mg, 0.27 mmol), and $CuCl_2$ (7.26 mg, 0.054 mmol). The Schlenk was sealed, transferred out of the glovebox, and placed in a 50 °C oil bath to stir overnight. When the polymerization was complete, the substrates were removed from the Schlenk flask, rinsed with DMF, and dried with nitrogen.

Polymerization of PFPA

Surface-initiated free radical polymerization substrates were cut to approximately 8 x 10 mm^2, placed into 8 mL glass vials, and transferred into the glovebox. Dry, degassed 1,4-dioxane (72.6 μL) and monomer (291.3 μL, 85 wt%) were added to the vial and stirred. The vials were removed from the glovebox and placed into a UV reactor (Rayonet RPR-600 Mini, 350 nm, 1.25 mW/cm^2) for two hours. The substrates were removed from the reactor, rinsed and sonicated in chloroform and THF for several hours, and dried under a stream of nitrogen.

The kinetics of polymerization was analyzed using five polymerization vials as described above. The polymerizations reacted for 2, 3.5, 5.5, 8, 10, 12.25, 24, and 48 hours. For each substrate, the film thickness was analyzed using spectroscopic ellipsometry. The dependence of film thickness with respect to monomer concentration was determined using two sets of five substrates. One set of substrates were reacted for two hours with monomer concentrations of 55, 65, 75, 80, 85, and 90 wt%, while the other set was reacted for 22 hours using monomer concentrations of 55, 65, 70, 80,and 90 wt%.

Control experiments were performed in which silicon substrates containing no initiator layer underwent the same photo-polymerization conditions as stated above. Spectroscopic ellipsometry showed no thickness change after the substrate was rinsed with THF, demonstrating that crosslinking of the polymer with the silicon oxide surface did not occur.

The effect of sonication time on polymer thickness was determined using an 8 x 10 cm^2 substrate that was polymerized for 2 hours at 85 wt% monomer submerged in 15

mL THF. The thickness was recorded after sonication in a Branson 3510 (100 W, 42 kHz) using spectroscopic ellipsometry. After every hour, the substrate was removed, rinsed with chloroform, and dried. The thickness was recorded, and the process was repeated.

Kinetics of Functionalization with Aromatic and Alkyl Amines

The postpolymerization functionalization of the poly(NHS4VB) and poly(PFPA) kinetics were monitored by taking *ex situ* UV-vis spectra using a spectrometer equipped with a slide holder accessory. Quartz substrates were used for UV-vis experiments because the three amines, AMP, AP, and $Ru^{+2}A$, have absorbance maxima at 345, 289, and 290 nm, respectively. Silicon substrates were used to determine thickness changes of the brushes and for FTIR analysis. A quartz substrate was placed into a 55 mM solution of 1-aminopyrene, 1-aminomethylpyrene, or $Ru(bpy)_2(phen\text{-}5\text{-}NH_2)(PF_6)$ with triethylamine (2 mmol triethylamine:1 mmol amine) in anhydrous DMF at 40 °C for various time intervals. The substrate was then removed, rinsed with anhydrous DMF, dried with nitrogen, and the UV-vis spectrum from 200 to 800 nm was recorded. This process was repeated until the absorbance value reached a maximum and remained consistent for several data points. Spectra were baseline corrected and the absorbance maximum was used to monitor the rate of functionalization. The kinetic data was fit to a linear form of the pseudo-first order model using a linear regression algorithm in MATLAB (v. 7.1, MathWorks). The kinetic curves and UV-vis data for each aminolysis reaction can be found in Appendix A.

Characterization

Film thickness was determined on a J. A. Woollam M-2000V spectroscopic ellipsometer with a white light source at three angles of incidence (65°, 70°, and 75°) to the silicon wafer normal. A Cauchy model was used to fit the film thickness, extinction coefficient, and refractive index of the polymer brush layer. Static contact angle measurements were taken on a Krüss DSA 100 using a 1 μL drop of 18 MΩ water (pH 7). For each trial, three drops were recorded for the substrate and the values were averaged. UV-vis spectroscopy was taken on a Varian 50 Bio spectrometer. FTIR measurements were taken with a Nicolet Model 6700 with a grazing angle attenuated total reflectance accessory (GATR) at 256 scans with a 4 cm^{-1} resolution.

Results and Discussion

Synthesis of PFPA Polymer Brushes

The synthesis of poly(PFPA) brushes was carried out using photoinitiated free radical polymerization from silicon and quartz substrates (Scheme 2.2b). An asymmetric azo-based silane initiator was attached to the surface through self-assembled monolayer formation. The propyl ester was used instead of the previously reported butyl ester,[49] which allowed for easier purification. Although azo-based initiators are typically used for thermal initiation at temperatures above 60 °C, they also are effective photo-initiators when irradiated with UV light (300-360 nm). Initiation is known to be slow in both methods, with the half-life of AIBN being 10 hours at 65 °C, and a photochemical quantum yield of approximately 0.48 in benzene as a solvent.[1, 50]

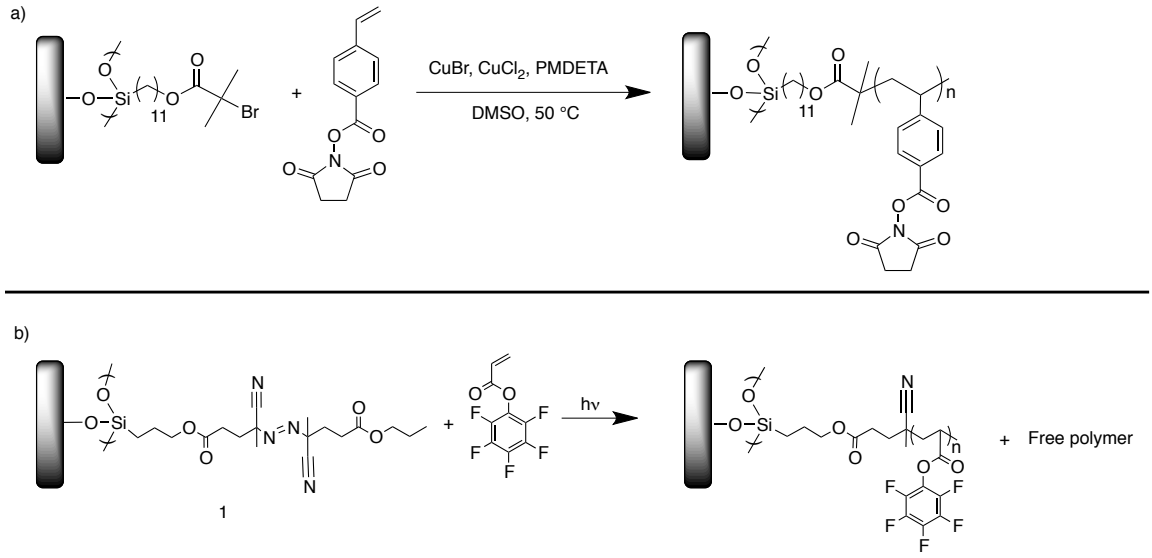

Scheme 2.2. a) Surface-initiated ATRP of NHS4VB[45] and b) surface-initiated free radical polymerization of PFPA from oxide substrates.

It is important to note that we also attempted polymerizations with PFPA using surface-initiated ATRP, but the technique was not reproducible and typically resulted in polymer films with a thickness of less than 5 nm. It is speculated that the monomer degrades or hydrolyzes under the polymerization conditions, yielding acidic functionality. Acidic monomers have been known to poison ATRP due to the ability of the protonated monomer to interact with the catalyst, resulting in a complete loss of activity.[51] For this reason, the more robust method of free radical polymerization was used to graft PFPA from surfaces. The silicon and quartz initiator substrates were placed in an 85 wt% monomer solution of dry, degassed PFPA and 1,4-dioxane. After 2 hours in a UV reactor (350 nm, 1.25 mW/cm^2), a film of approximately 50 nm was obtained.

One of the benefits of using pentafluorophenol as the pendant group of the active ester compared to other leaving groups, such as *N*-hydroxysuccinimide, is the increase in

reactivity towards carbonyl substitution reactions.[23, 34] Since activated esters are known to be susceptible to hydrolysis,[25] the contact angle of the poly(PFPA) film was monitored over an extended period of time to determine if the increased reactivity had an effect on the hydrolytic stability of the brush-coated substrate. The contact angle of a poly(PFPA) film that was stored in a petri dish in ambient laboratory conditions was recorded (Figure 2.1). The average contact angle of the substrate was 93.1° ± 1.1° over a 129 day period. The stability of the contact angle implies that hydrolysis of the leaving group does not occur during storage under atmospheric conditions, even with high relative humidity (Athens, GA in the summertime). It is speculated that the hydrophobic nature of the densely packed pentafluorophenyl groups about the polymer backbone protect against hydrolysis because of their low surface energy.

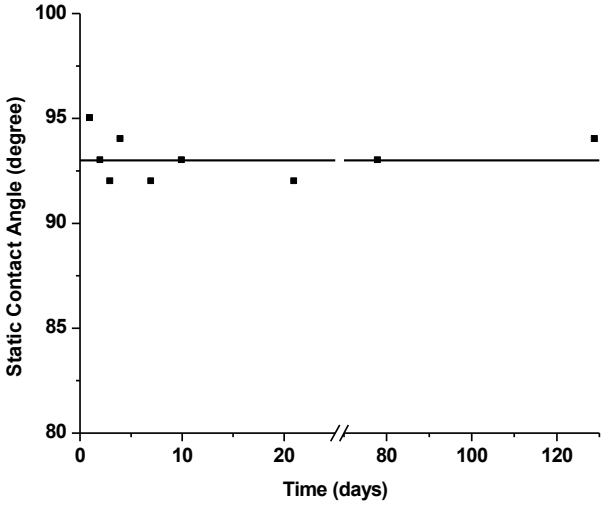

Figure 2.1. Contact angle stability of poly(PFPA) in ambient conditions.

Polymerization Kinetics

Figure 2.2 shows the poly(PFPA) brush thickness versus reaction time as measured by spectroscopic ellipsometry. As observed for other surface-initiated free radical polymerizations, a linear increase in poly(PFPA) film thickness is obtained with short polymerization times (up to ~12 hours), followed by a gradual plateau in thickness as time increases up to 48 hours.[52, 53] In free radical polymerization from planar substrates, high molecular weight polymer is formed very rapidly after initiation, and the molecular weight of the polymer remains approximately unchanged throughout the polymerization.[53-56] Because of the long half-life of the AIBN photo-initiator and the small concentration of initiators bound to a low surface area (planar) substrate, the low concentration of radicals generated in solution reduce the probability of termination by bimolecular coupling of a propagating polymer chain on the surface with a growing polymer in solution. At low initiator conversion, the increase in thickness is attributed to the constant increase in grafting density (σ, Eq. 2.1),

$$\sigma = \frac{h\rho N_A}{M_n} \quad (2.1)$$

where h is thickness, ρ is the bulk density of the polymer, N_A is Avogadro's number, and M_n is the number average molecular weight of the polymer.[44] As polymerization time is increased, more immobilized AIBN molecules decompose and initiate a growing polymer chain. With increasing time, the grafting distance between chains decreases, which results in an increased grafting density of the polymers bound to the surface. If the concentration of radicals in the solution is high, the linear relationship between grafting density and thickness is no longer valid. An increase in molecular weight is observed with reaction time due to the increased probability of bimolecular coupling between surface bound and

freely propagating polymer chains. This is the case when polymerization is performed from high surface area substrates (i.e. spherical particles), where the non-attached initiator fragment that goes on to initiate polymerization in solution is typically several orders of magnitude higher compared to surface-initiated reactions on planar substrates.[52]

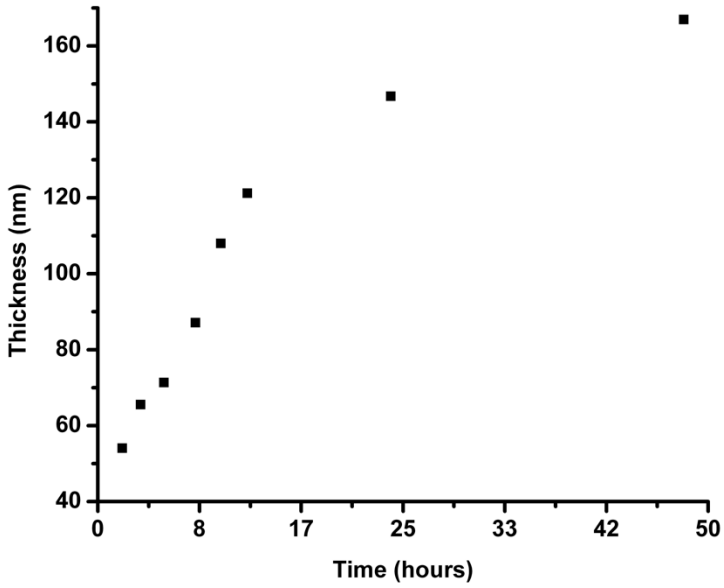

Figure 2.2. Thickness increase of poly(PFPA) with polymerization time. Reaction conditions: 80 wt% PFPA in dioxane, 1.25 mW/cm^2, 350 nm light.

Figure 2.3 shows the effect of monomer concentration (ranging from 55 to 90 wt% PFPA in dioxane) on polymer film thickness for two different reaction times: (a) 2 hours and (b) 22 hours of photo-polymerization. A linear increase in thickness is observed with increasing monomer concentration (Figure 2.3a) after 2 hours of polymerization. The viscosity of each solution increases with increasing monomer concentration, but even at 90 wt% PFPA, the reaction mixture still flows. Figure 2.3b

shows an exponential increase in thickness after 22 hours of polymerization, when the reaction reaches high monomer conversion. The reaction mixture changes from gel-like to a glassy solid as the concentration of monomer is increased from 55 to 90 wt%. The exponential increase is attributed to autoacceleration of the polymerization, also known as the Trommsdorff effect.[57] With free radical polymerization at high monomer conversion, the polymerization solution gels due to entanglements and an increased viscosity. The diffusion rate of the radical polymer chain ends in the mixture slows, causing a reduction in the rate of termination of the chains. While the diffusion rate of the monomer is relatively unchanged, this has the effect of increasing the rate of propagation, resulting in a rapid increase in thickness.[57] No two-dimensional Trommsdorff effect is observed with this system because the concentration of radicals in the polymerization is low as the reaction proceeds from a planar substrate.[52] This reduces the probability of bimolecular coupling between a surface-attached radical and a propagating radical chain in solution, minimizing any two-dimensional viscosity increase that can occur due to diffusion of the free, non-bonded chain into the polymer brush as a termination pathway. A thickness of 200 nm was reached after 22 hours of polymerization at 90 wt% monomer, which is approximately 3 times greater than the same reaction after 2 hours.

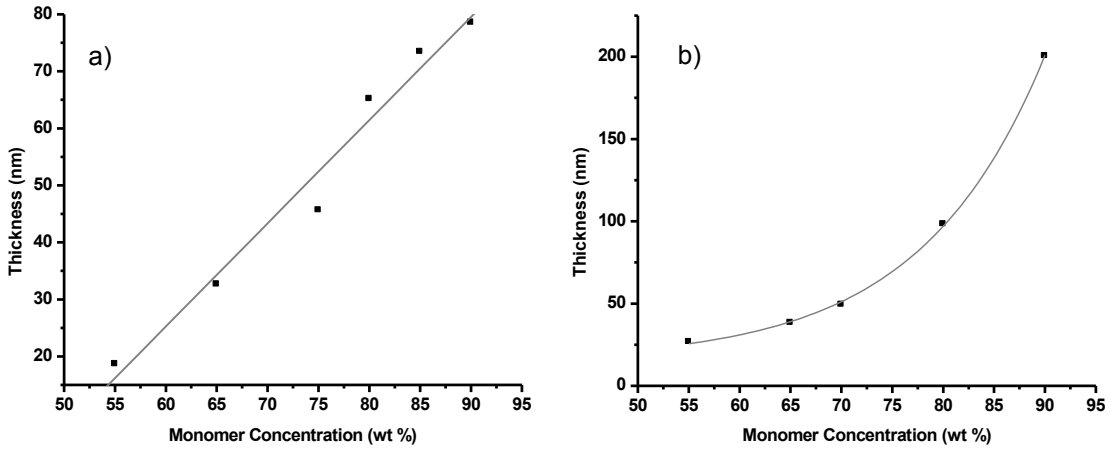

Figure 2.3. Polymerization of PFPA with varying monomer concentration after a) 2 hours and b) 22 hours.

At high monomer conversion, long sonication times were necessary to remove the substrate from the reaction vessel and dissolve the glassy solid reaction mixture. For these reasons, we investigated the effect of sonication time on film thickness to determine if sonication caused damage to the surface-attached polymer in the form of chain scission or degrafting (Figure 2.4). The thickness of the polymer was recorded after every hour of sonication up to a total of 9 hours. Initially, a steady decrease in film thickness is observed due to the removal of entangled, physisorbed polymer but after approximately 4 hours, the film thickness remained constant. This is good evidence that no chain scission or degrafting occurs under these sonication conditions (100 W, 42 kHz).

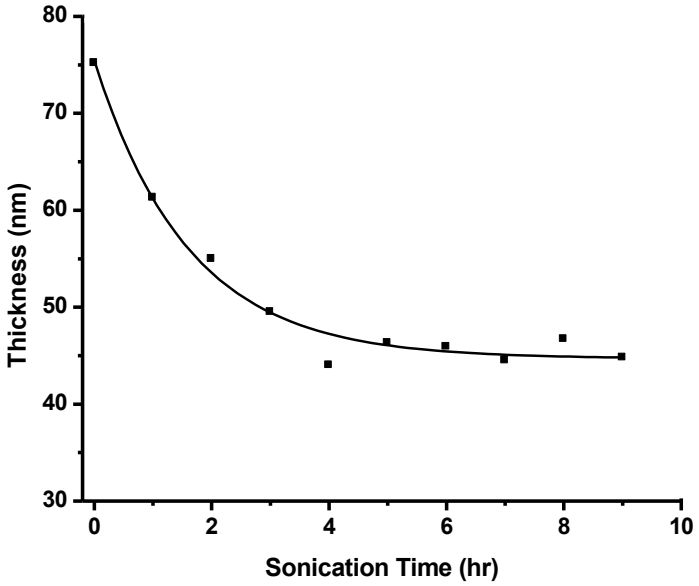

Figure 2.4. Thickness of poly(PFPA) on silicon vs. sonication time.

Aminolysis Kinetics

To investigate the kinetics of the aminolysis reaction, poly(NHS4VB) and poly(PFPA) brushes on silicon and quartz were post-functionalized with three amines: 1-aminopyrene (AP), 1-aminomethylpyrene (AMP), and $Ru(bpy)_2(phen\text{-}5\text{-}NH_2)(PF_6)$ ($Ru^{+2}A$), where the expected order of nucleophilicity is AMP > AP > $Ru^{+2}A$. The UV-vis kinetics of the reaction between poly(PFPA) and AMP reached a final absorbance plateau in approximately 15 seconds, while the reaction kinetics with the two aromatic amines, $Ru^{+2}A$ and AP, were complete after approximately 1 hour. The second order aminolysis reaction can be reduced to a pseudo-first order by using an amine concentration several orders of magnitude greater than that of the reactive groups in the polymer brush.[58] As the reaction proceeds, the change in amine concentration (55 mM) in solution is negligible. The rate equation can be simplified to a pseudo-first order model (Equation

2.2), where k' is the pseudo-first order rate constant, and A_o, A_∞, and A_t correlate to the initial absorbance, the final absorbance, and absorbance at time t, respectively. The pseudo-first order rate constant for amide formation of each substrate was determined from a regression analysis to be 2.46 x 10^{-1} s^{-1}, 2.59 x 10^{-3} s^{-1}, and 5.11 x 10^{-3} s^{-1}, respectively (Figure 2.5a).

$$\ln\left(\frac{A_0 - A_\infty}{A_t - A_\infty}\right) = k't \quad (2.2)$$

The same postpolymerization functionalization experiments were performed with poly(NHS4VB) in order to compare the aminolysis kinetics to that of poly(PFPA). Poly(NHS4VB) reached an absorbance plateau after approximately 1 hour during functionalization with AMP. A k' of 3.49 x 10^{-3} s^{-1} was calculated using a pseudo-first order kinetics model (Figure 2.5b). No conversion of poly(NHS4VB) with the aromatic amine AP was observed through UV-vis or FTIR. Eberhardt, *et al*. reported the same findings for homopolymers containing *N*-hydroxysuccinimide and pentafluorophenol pendant groups in solution.[22] No reaction was observed between poly(NHS4VB) and Ru^{+2}A, which also has reduced reactivity towards carbonyl substitution reactions.

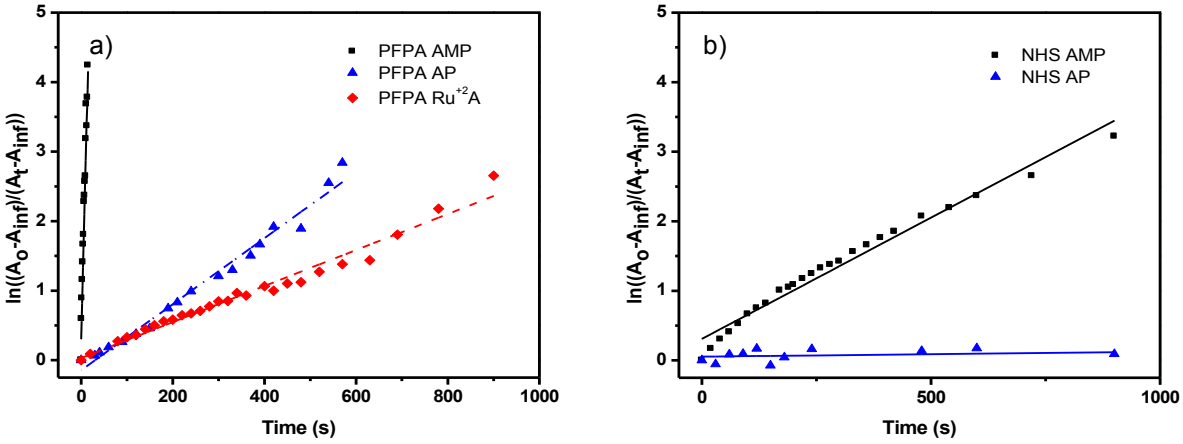

Figure 2.5. a) Aminolysis kinetics of poly(PFPA) using a pseudo-first order model with three amines: an alkyl amine (AMP, black squares), and two aromatic amines (AP, blue triangles and $Ru^{+2}A$, red diamonds). b) Aminolysis kinetics of poly(NHS4VB) with an alkyl amine (AMP, black squares) and an aromatic amine (AP, blue triangles). Lines represent the pseudo-first order regression analysis.

In comparing the two polymer brush platforms (Table 2.1), poly(PFPA) modified with AMP exhibited the fastest kinetics with a pseudo-first order rate constant of 2.46 x 10^{-1} $s^{-1.}$ This was two orders of magnitude faster than the reaction of AMP with poly(NHS4VB) substrates under identical conditions, which had a k' of 3.49 x 10^{-3} s^{-1}. Poly(PFPA) functionalized with AP had a pseudo-first order rate constant of 5.11 x 10^{-3} s^{-1}, which was approximately twice as large as poly(NHS4VB) modified with AMP and poly(PFPA) functionalized with $Ru^{+2}A$ (2.59 x 10^{-3} s^{-1}).

Table 2.1. Pseudo-first order rate constants, film thickness, and amide concentration in the polymer brush for poly(NHS4VB) and poly(PFPA) functionalized with AMP, AP, and $Ru^{+2}A$.

Brush	Amine	k' (s^{-1})	Thickness before (nm)	Thickness after (nm)	Extinction Coefficient ($cm^{-1}M^{-1}$)	Concentration of Amine ($molecules/cm^2$)
Poly(NHS4VB)	AMP	3.49×10^{-3}	48.6	75.4	32,204 [b]	1.20×10^{16}
Poly(NHS4VB)	AP	NR[a]	57.2	56.7	23,465 [c]	-
Poly(PFPA)	AMP	2.46×10^{-1}	54.4	94.3	32,204 [b]	1.94×10^{16}
Poly(PFPA)	AP	5.11×10^{-3}	46.3	41.6	23,465 [c]	8.51×10^{15}
Poly(PFPA)	$Ru^{+2}A$	2.59×10^{-3}	47.8	57.3	47,000 [d]	3.60×10^{15}

[a] NR = no reaction. [b] At 345 nm. [c] At 289 nm. [d] At 290 nm.

FTIR data of the brushes before and after postpolymerization modification was recorded in order to examine the extent of reaction in each reactive ester platform. In the reaction of poly(NHS4VB) with AMP, a reduction of the active ester stretches of NHS at 1802 and 1739 cm^{-1} is observed, along with the appearance of amide I and amide II bands at 1651 and 1536 cm^{-1}, respectively (Figure 2.6). It is important to note that some residual NHS is still present in the brush after functionalization. This could be explained by two different situations: 1) the reaction did not achieve full conversion, or 2) *N*-substituted glutarimides were formed by a ring-closing reaction of adjacent amides on neighboring active esters.[59] Poly(PFPA) has two strong bands at 1785 and 1523 cm^{-1} corresponding to the C=O stretch of the ester and the aromatic ring stretch of the pendant group (Figure 2.7). In all three postpolymerization modifications, complete disappearance of these bands is observed, implying that the reaction reached completion or that there was a combination of aminolysis and a side reaction, such as hydrolysis. After functionalization with the alkyl amine, AMP, amide I and amide II bands appear at 1656 and 1529 cm^{-1} with a small peak at 1728 cm^{-1} which is likely the carbonyl stretch of the

carboxylic acid. It is speculated that a small amount of PFPA left unreacted near the surface of the substrate hydrolyzed due to unavoidable water present on all surfaces. The two aromatic amines, AP and $Ru^{+2}A$, display an amide I peak present at 1626 and 1623 cm^{-1}, respectively, and a carboxylic acid carbonyl stretch at 1724 and 1716, cm^{-1}, respectively. The intensity of the carboxylic acid carbonyl stretch is most dominant in the sample with $Ru^{+2}A$ relative to the silicon oxide stretch (broad peak ~ 880 cm^{-1}), which is most likely due to hydrolysis of the underlying active ester sites. We speculate that the formation of a blocking layer results between the charged, bulky $Ru^{+2}A$ and the outermost layer of the brush. As functionalization occurs, the reactive sites at the top of the brush are modified first, and both sterics along with charge repulsion of the $Ru^{+2}A$ group essentially blocks the lower reactive ester groups in the brush layer. It becomes difficult for other $Ru^{+2}A$ to diffuse down into the brush to react once the top layers are functionalized.

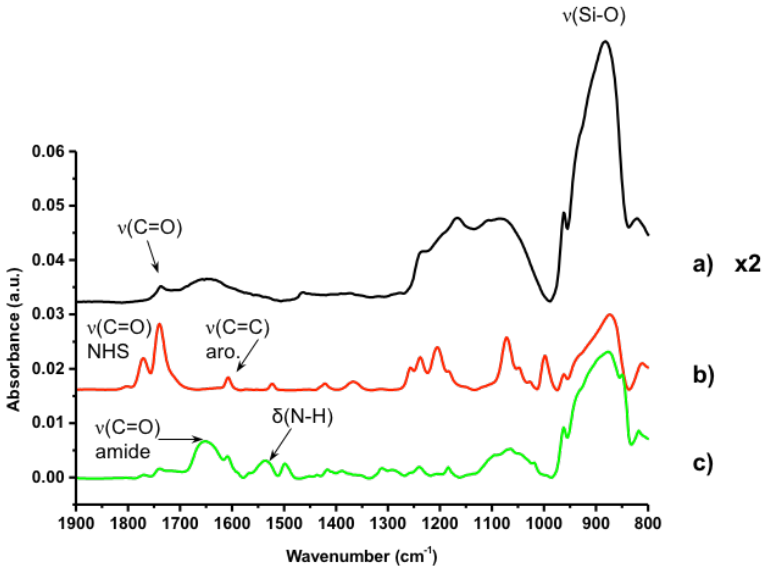

Figure 2.6. a) ATRP initiator on silicon. b) Poly(NHS4VB) brush. c) Postpolymerization functionalization of poly(NHS4VB) with AMP.

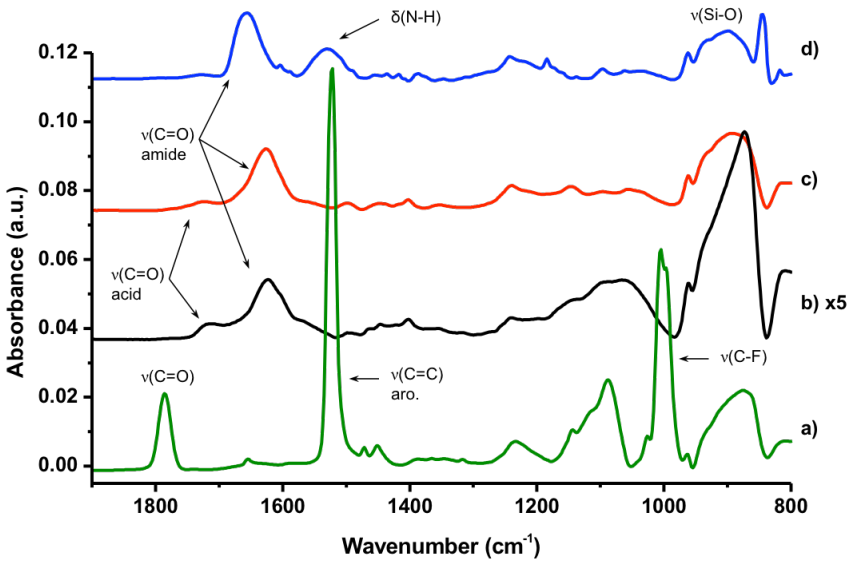

Figure 2.7. FTIR spectra on silicon substrates of a) poly(PFPA) brush and postpolymerization modifications with b) $Ru^{+2}A$, c) AP, and d) AMP.

To confirm the bands observed around 1720 cm^{-1} were carboxylic acid carbonyl stretches, and not from side reactions such as glutarimide formation,[59] the substrates were placed into a solution of EDC/NHS in order to generate NHS on any hydrolyzed areas of the PFPA brush (Figure 2.8). While the substrate functionalized with AMP showed no appearance of the characteristic NHS peaks at 1801, 1769, and 1738 cm^{-1}, these bands were observed in the substrates modified with AP and $Ru^{+2}A$, indicating hydrolysis had most likely occurred during amine functionalization, although care was taken to exclude water from the reaction conditions. Comparing the relative intensities of the NHS peaks to the amide I and silicon oxide stretches within each sample, the substrate with $Ru^{+2}A$ had more NHS generation relative to the amount of amide I present compared to the AP surface. These results suggest that poly(PFPA) reached complete conversion with the

alkyl amine, while modification with AP had a higher conversion than that of $Ru^{+2}A$, as expected based on the relative nucleophilicities of the amines.

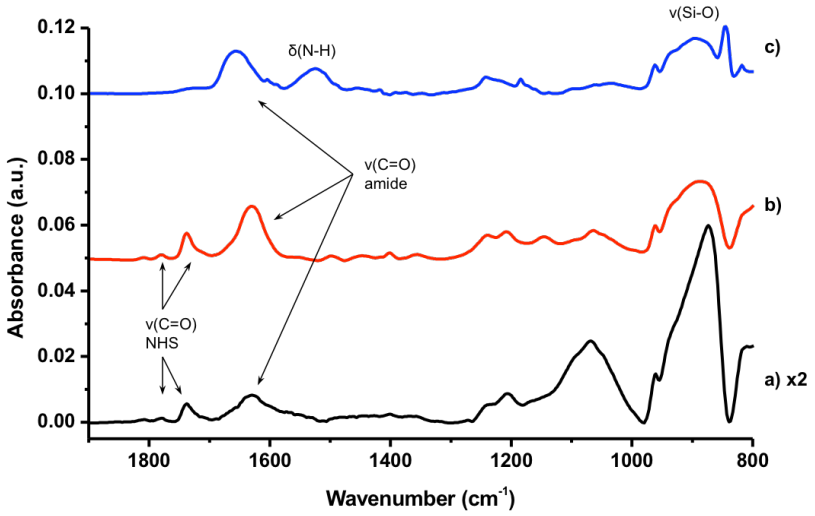

Figure 2.8. FTIR spectra of poly(PFPA) silicon substrates with a) $Ru^{+2}A$, b) AP, and c) AMP after generation of NHS.

Because the grafting density of the polymer covalently immobilized to the substrate does not change after the postpolymerization modification, Murata *et al.* previously determined the relationship between the molecular weight of the surface-bound polymer and polymer brush thickness.[44] If the attacking nucleophile is greater in molar mass than the pendant group, a thickness increase will occur due to an increase in molecular weight. Likewise, if the attacking nucleophile has a smaller molar mass than the leaving group, a thickness decrease will be observed. The thickness of each brush platform on silicon/silicon oxide was measured before and after aminolysis using spectroscopic ellipsometry (Table 2.1). As expected, each reactive ester coating showed an increase in thickness after functionalization, except for the functionalization of

poly(PFPA) with AP, where a 10% decrease in thickness was observed (46.3 to 41.6 nm). The pentafluorophenol leaving group has a molecular weight of 184.06 g/mol, which is similar to AP, with a molecular weight of 217.26 g/mol. Even though there is only a small difference in the molecular weight of leaving group compared to AP, a slight increase in thickness should still be observed in the case of full conversion. The appearance of carboxylic acid carbonyl stretches in the FTIR spectra indicate that hydrolysis occurred within the brush, which causes a loss in molecular weight. We speculate that the net sum of these two reactions give rise to the slight decrease in film thickness.

The concentration of amine within the brush was calculated using the UV-vis and thickness data (Table 2.1), assuming that all amines reacted with the activated esters in a 1:1 molar ratio. Using the molar extinction coefficient of each amine, along with the maximum absorbance recorded for each brush, the concentration of amide functional groups was determined. The extinction coefficient for AMP (32,204 cm^{-1} M^{-1} at 345 nm) was taken from a previous publication[45] and that of $Ru^{+2}A$ at 290 nm (47,000 cm^{-1} M^{-1}) was provided by the Schanze group. The extinction coefficient for AP was determined using five UV-vis spectra of AP in dry DMF ranging in concentration from 0.081 to 0.705 μM. The absorbance at 289 nm was plotted against the concentration of the solution to obtain a linear line (Figure 2.9). The slope of the line corresponds to the extinction coefficient, which was determined to be 23,465 cm^{-1} M^{-1}. Poly(PFPA) with AMP showed the highest concentration of amide present at 1.9 x 10^{16} molecules/cm^2, followed by AP with 8.5 x 10^{15} molecules/cm^2, and $Ru^{+2}A$ with the least at 3.6 x 10^{15} molecules/cm^2. For comparison, the poly(NHS4VB) with AMP had a concentration of

1.2 x 10^{16} molecules/cm^2. The density of functional groups in these reactive ester brush platforms is several orders of magnitude higher than that observed in SAMs based on NHS esters[60, 61] and far outnumbers the total functional sites in polymer matrices prepared through a grafting to approach.[62]

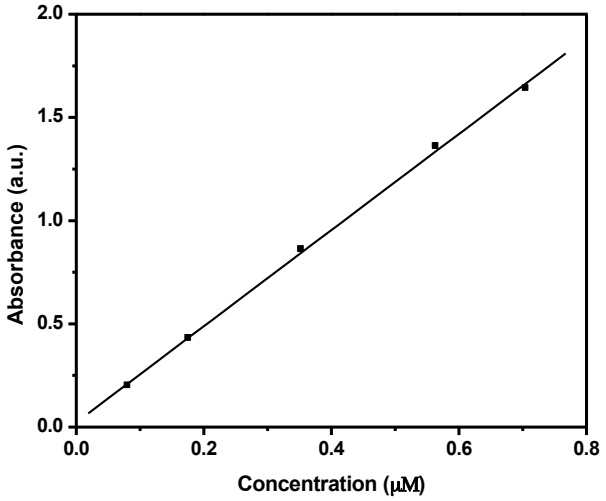

Figure 2.9. Absorbance vs. concentration of AMP in DMF.

Conclusions

In this work, the photoinitiated polymerization of PFPA from a surface bound, free radical azo-initiator was studied. A linear relationship between the change in thickness with polymerization time and monomer concentration (at low monomer conversion) was observed, leading to reactive ester brush platforms with excellent control over film thickness. At high monomer conversions and long polymerization times, the polymer film thickness increased exponentially due to autoacceleration. The kinetics of postpolymerization aminolysis was also studied for five different systems. Unlike

poly(PFPA), poly(NHS4VB) reacted with only primary alkyl amine nucleophiles, and no conversion was observed when subjected to aromatic amines under the same reaction conditions. As expected, the fastest reaction time was observed between poly(PFPA) and primary alkyl amines, which was completed after approximately 15 seconds, with a pseudo-first order rate constant of 2.46×10^{-1} s^{-1}. The reactions between poly(PFPA) with aromatic amines AP and $Ru^{+2}A$, along with poly(NHS4VB) and the primary amine AMP all took approximately 1 hour to reach completion, with a k' of 5.11×10^{-3} s^{-1}, 2.59×10^{-3} s^{-1}, and 3.49×10^{-3} s^{-1}, respectively. This poly(PFPA) reactive ester platform that has high hydrolytic stability and excellent reactivity to both aromatic and aliphatic amines will allow for a straightforward method to create new and complex functional interfaces.

References

1. Ayres, N., *Polym. Chem.*, 2010, **1**, 769-777.
2. Barbey, R. l., Lavanant, L., Paripovic, D., Schüwer, N., Sugnaux, C., Tugulu, S. and Klok, H.-A., *Chem. Rev.*, 2009, **109**, 5437-5527.
3. Grest, G. S., *Polymers in Confined Environments*, 1999.
4. Klein, J., Kumacheva, E., Mahalu, D., Perahia, D. and Fetters, L. J., *Nature*, 1994, **370**, 634-636.
5. Orski, S. V., Fries, K. H., Sontag, S. K. and Locklin, J., *J. Mater. Chem.*, 2011, **21**, 14135-14149.
6. Ratner, B. D., Hoffmann, F. J. and Lemons, J. E., *Biomaterials Science, An Introduction to Materials in Medicine*, Academic Press, San Diego, 1996.
7. Senaratne, W., Andruzzi, L. and Ober, C. K., *Biomacromolecules*, 2005, **6**, 2427-2448.
8. Milner, S. T., *Science*, 1991, **251**, 905-914.
9. Sumerlin, B. S. and Vogt, A. P., *Macromolecules*, 2009, **43**, 1-13.
10. Iha, R. K., Wooley, K. L., Nystrom, A. M., Burke, D. J., Kade, M. J. and Hawker, C. J., *Chem. Rev.*, 2009, **109**, 5620-5686.
11. Galvin, C. J. and Genzer, J., *Prog. Polym. Sci.*, 2012, **37**, 871-906.
12. Arnold, R. M., Huddleston, N. E. and Locklin, J., *J. Mater. Chem.*, 2012.
13. Arisumi, K., Feng, F., Miyashita, T. and Ninomiya, H., *Langmuir*, 1998, **14**, 5555-5558.
14. Desai, A., Atkinson, N., Rivera, F., Devonport, W., Rees, I., Branz, S. E. and Hawker, C. J., *J. Polym. Sci., Part A: Polym. Chem.*, 2000, **38**, 1033-1044.

15. Favier, A., D'Agosto, F., Charreyre, M. T. and Pichot, C., *Polymer*, 2004, **45**, 7821-7830.

16. Ghosh, S., Basu, S. and Thayumanavan, S., *Macromolecules*, 2006, **39**, 5595-5597.

17. Hu, Z., Liu, Y., Hong, C. and Pan, C., *J. Appl. Polym. Sci.*, 2005, **98**, 189-194.

18. Mammen, M., Dahmann, G. and Whitesides, G. M., *J. Med. Chem.*, 1995, **38**, 4179-4190.

19. Pedone, E., Li, X., Koseva, N., Alpar, O. and Brocchini, S., *J. Mater. Chem.*, 2003, **13**, 2825-2837.

20. Vosloo, J. J., Tonge, M. P., Fellows, C. M., D'Agosto, F., Sanderson, R. D. and Gilbert, R. G., *Macromolecules*, 2004, **37**, 2371-2382.

21. Wong, S. Y. and Putnam, D., *Bioconjugate Chem.*, 2007, **18**, 970-982.

22. Eberhardt, M., Mruk, R., Zentel, R. and Théato, P., *Eur. Polym. J.*, 2005, **41**, 1569-1575.

23. Nilles, K. and Theato, P., *Eur. Polym. J.*, 2007, **43**, 2901-2912.

24. Vogel, N. and Théato, P., *Macromolecular Symposia*, 2007, **249-250**, 383-391.

25. Hermanson, G. T., *Bioconjugate Techniques*, second edn., Academic Press, New York, New York, 2008.

26. Jain, P., Dai, J., Baker, G. L. and Bruening, M. L., *Macromolecules*, 2008, **41**, 8413-8417.

27. Lofas, S. and Johnsson, B., *J. Chem. Soc., Chem. Commun.*, 1990, 1526-1528.

28. Tsujii, Y., Ohno, K., Yamamoto, S., Goto, A. and Fukuda, T., ed. R. Jordan, Springer Berlin / Heidelberg, 2006, vol. 197, pp. 1-45.

29. Barringer, J. E., Messman, J. M., Banaszek, A. L., Meyer, H. M. and Kilbey, S. M., *Langmuir*, 2008, **25**, 262-268.

30. Buck, M. E., Breitbach, A. S., Belgrade, S. K., Blackwell, H. E. and Lynn, D. M., *Biomacromolecules*, 2009, **10**, 1564-1574.

31. Buck, M. E., Zhang, J. and Lynn, D. M., *Adv. Mater.*, 2007, **19**, 3951-3955.

32. Chen, G., Huynh, D., Felgner, P. L. and Guan, Z., *J. Am. Chem. Soc.*, 2006, **128**, 4298-4302.

33. Pasut, G., Mero, A., Caboi, F., Scaramuzza, S., Sollai, L. and Veronese, F. M., *Bioconjugate Chem.*, 2008, **19**, 2427-2431.

34. Theato, P., *J. Polym. Sci. Pol. Chem.*, 2008, **46**, 6677-6687.

35. Theato, P. and Zentel, R., *Langmuir*, 1999, **16**, 1801-1805.

36. Wood, K. C., Azarin, S. M., Arap, W., Pasqualini, R., Langer, R. and Hammond, P. T., *Bioconjugate Chem.*, 2008, **19**, 403-405.

37. Hausch, M., Zentel, R. and Knoll, W., *Macromol. Chem. Phys.*, 1999, **200**, 174-179.

38. Batz, H.-G., Franzmann, G. and Ringsdorf, H., *Angew. Chem. Int. Edit.*, 1972, **11**, 1103-1104.

39. Cline, G. W. and Hanna, S. B., *J. Am. Chem. Soc.*, 1987, **109**, 3087-3091.

40. Cline, G. W. and Hanna, S. B., *J. Org. Chem.*, 1988, **53**, 3583-3586.

41. Ferruti, P., Bettelli, A. and Feré, A., *Polymer*, 1972, **13**, 462-464.

42. Arumugam, S., Orski, S. V., Locklin, J. and Popik, V. V., *J. Am. Chem. Soc.*, 2011, **134**, 179-182.

43. Gunay, K. A., Schuwer, N. and Klok, H.-A., *Polym. Chem.*, 2012.

44. Murata, H., Prucker, O. and Ruhe, J., *Macromolecules*, 2007, **40**, 5497-5503.

45. Orski, S. V., Fries, K. H., Sheppard, G. R. and Locklin, J., *Langmuir*, 2009, **26**, 2136-2143.

46. Orski, S. V., Poloukhtine, A. A., Arumugam, S., Mao, L., Popik, V. V. and Locklin, J., *J. Am. Chem. Soc.*, 2010, **132**, 11024-11026.

47. Schuh, C. and Rühe, J. r., *Macromolecules*, 2011, **44**, 3502-3510.

48. Matyjaszewski, K., Miller, P. J., Shukla, N., Immaraporn, B., Gelman, A., Luokala, B. B., Siclovan, T. M., Kickelbick, G., Vallant, T., Hoffmann, H. and Pakula, T., *Macromolecules*, 1999, **32**, 8716-8724.

49. Fan, X., Xia, C., Fulghum, T., Park, M.-K., Locklin, J. and Advincula, R. C., *Langmuir*, 2002, **19**, 916-923.

50. Alvarez, J., Encinas, M. V. and Lissi, E. A., *Macromol. Chem. Phys.*, 1999, **200**, 2411-2415.

51. Beers, K. L., Boo, S., Gaynor, S. G. and Matyjaszewski, K., *Macromolecules*, 1999, **32**, 5772-5776.

52. Prucker, O. and Ruhe, J., *Macromolecules*, 1998, **31**, 602-613.

53. Dyer, D., ed. R. Jordan, Springer Berlin / Heidelberg, 2006, vol. 197, pp. 47-65.

54. Konradi, R. and Rühe, J., *Macromolecules*, 2005, **38**, 4345-4354.

55. Konradi, R. and Rühe, J., *Macromolecules*, 2005, **38**, 6140-6151.

56. Konradi, R. and Rühe, J., *Langmuir*, 2006, **22**, 8571-8575.

57. Tulig, T. J. and Tirrell, M., *Macromolecules*, 1981, **14**, 1501-1511.

58. Levenspiel, O., *Chemical Reaction Engineering*, 3rd edn., John Wiley & Sons, Inc,, Hoboken, 1999.

59. Devenish, S. R. A., Hill, J. B., Blunt, J. W., Morris, J. C. and Munro, M. H. G., *Tetrahedron Lett.*, 2006, **47**, 2875-2878.

60. Gooding, J. J. and Hibbert, D. B., *TrAC, Trends Anal. Chem.*, 1999, **18**, 525-533.

61. Lockett, M. R., Phillips, M. F., Jarecki, J. L., Peelen, D. and Smith, L. M., *Langmuir*, 2007, **24**, 69-75.

62. Xu, F., Persson, B., Löfås, S. and Knoll, W., *Langmuir*, 2006, **22**, 3352-3357.

CHAPTER 3

SELF-SORTING CLICK REACTIONS THAT GENERATE SPATIALLY CONTROLLED CHEMICAL FUNCTIONALITY ON SURFACES[1]

[1] Arnold, R.M. and Locklin, J. *Langmuir,* **2013,** *29* (19), 5920-5926. Reproduced with permission from Arnold, R.M. and Locklin, J. *Langmuir,* **2013,** *29* (19), 5920-5926.

Abstract

This chapter describes the generation of a patterned surface that can be postpolymerization modified to incorporate fragile macromolecules or delicate biomolecules without the need for special equipment. Two monomers that undergo different click reactions, pentafluorophenyl acrylate (PFPA) and 4-(trimethylsilyl) ethynylstyrene (TMSES), were sequentially polymerized from a silicon surface in the presence of a shadow mask with UV light, generating 12.5 and 62 micron pitch patterns. Two different dyes, 1-aminomethylpyrene (AMP) and 5-azidofluorescein (AF), were covalently attached to the polymer brushes through aminolysis and dual desilylation/Copper(I)-catalyzed azide-alkyne cycloaddition (CuAAC) in one pot. Unlike most CuAAC reactions, the terminal alkyne of TMSES was not deprotected prior to functionalization. Although a 2 nm thickness increase was observed for poly(PFPA) brushes after polymerization of TMSES, cross-contamination was not observed through fluorescence microscopy after functionalization.

Introduction

Self-sorting, the efficient recognition and assembly of corresponding components within a mixture,[1-4] is commonplace in biology, generating some of the most complex and important architectures in nature. Specific examples include formation of the DNA double helix, the assembly of protein subunits to establish quaternary structure, and the compartmentalization of molecular components to form the cell.[1, 4, 5] The sorting process can be thermodynamically or kinetically driven,[4] and can occur in two different manners, either through a homomeric or a heteromeric recognition process.[3] Homomeric processing, or narcissistic association, occurs when molecules in the system are highly attracted to themselves, much like schools of fish that group by species.[2, 4] The complementary pairing of adenine with tyrosine and cytosine with guanine are examples of heteromeric, or social, recognition, which involves host-guest relationships where molecules have a high affinity for specific partners.[2, 4]

While self-sorting processes have been widely studied in solution with proteins and peptides,[6, 7] metal-ligand complexes,[8, 9] and small molecule mixtures,[10, 11] self-sorting in polymer systems has been less prevalent,[1, 12] especially on surfaces. The earliest form of a self-sorting surface is seen in the formation of self-assembled monolayers on two different metals or metal oxide combinations.[13-15] Even though patterned polymer brushes[16-18] and postpolymerization modification has been studied for several years,[19-21] not until recently have polymer coatings and other thin films utilized self-sorting processes to add functionality to the system.[22-24]

The ability to design a system that contains components capable of simultaneous and orthogonal functionalization within a complex mixture is a critical factor in

advancing the generation of multifunctional substrates. While engineering disciplines have depended on surface microstructures to add complexity to devices, analytical techniques in materials science,[25] chemistry,[26, 27] and biology[28, 29] are beginning to explore similar strategies. Currently, there are several techniques that can be used to fabricate surface patterns,[30-32] each of which is application dependent. For example, various types of lithography can be used to create patterned surfaces in two dimensions, including photo-, electron or ion beam, and nanoimprint lithography.[30, 32] Other methods for generating patterns include plasma enhanced chemical vapor deposition (PECVD), microcontact printing (μCP), and nanoparticle self-assembly.[22, 23, 30, 32] However, many of these systems have limitations, such as complicated and lengthy processes, limited replication fidelity, low resolution and defects, distortion and broadening of the pattern, abrasive or harsh conditions, and high operating costs with limited access.[30, 32, 33] For devices that contain patterns of surface-immobilized biomolecules, photolithography is not desirable because it requires organic solvents and UV light,[33, 34] which can dehydrate and degrade biofunctionality.[35] Delicate nanostructures can also be damaged by corrosive etching processes, high baking temperatures, and stamp deformations.[30] Developing a universal platform that contains two different, orthogonal chemistries with self-sorting capabilities allows the addition of sensitive nanostructures or biomacromolecules to the surface with control over spatial selectivity.

In this chapter, a method enabling the fabrication of self-sorting surfaces without the need for expensive or specialized equipment and procedures is introduced. Photopatterning of surface-initiated polymer brushes containing reactive monomers with different recognition elements is utilized. A shadow mask placed in contact with the

substrate during the first polymerization preserves initiators for a subsequent polymerization, resulting in micron-sized patterns that are generated without the need of sophisticated equipment or harsh conditions. Functionalizing the surface with molecules that ordinarily would not survive polymerization is easily completed through the postpolymerization modification of poly(pentafluorophenyl acrylate) (PFPA) and poly(4-(trimethylsilyl) ethynylstyrene) (TMSES) brushes.

Experimental Section

Materials

Solvents were distilled from calcium hydride (toluene and DCM), except anhydrous dimethylformamide (DMF) and diethyl ether, which were purchased from EMD (Drisolv, 99.8% by GC), and 1,4-dioxane, which was dried over molecular sieves (0.4 nm). Silicon wafers (orientation <100>, native oxide) were purchased from University Wafer. TEM grids (copper, 400 mesh and 2000 mesh) were purchased from Ted Pella. Pentafluorophenyl acrylate (PFPA),[36] 4-(trimethylsilyl) ethynylstyrene (TMSES),[37] 5-azidofluorescein,[38] and the azo-silane initiator[39] were all prepared according to literature procedures. PFPA was further purified by distillation, and any residual acrylic acid was removed by passing the PFPA through a plug of neutral alumina with DCM. All other chemicals were purchased from Alfa Aesar, Sigma Aldrich, or TCI, and were used as received.

Preparation of Initiator Layers

Silicon wafers cut to approximately 10 x 20 mm^2 were sonicated in hexane, isopropanol, acetone, and deionized water for 15 minutes each. The substrates were dried

in a stream of nitrogen, subjected to argon plasma (Harrick Plasma, PDC-32-G, 0.8 mbar, 18 W) for 5 minutes, and transferred into a nitrogen-filled glovebox along with dry, degassed reagents. A 10 mM stock solution of the azo-initiator was made using 20 mL of toluene. The initiator solution was added to the substrates and allowed to sit for 16 hours. They were then removed from the glovebox, rinsed with toluene, and dried with nitrogen.

Surface-Initiated Free Radical Copolymerization of PFPA and TMSES

Silicon initiator substrates in 8 mL glass vials, along with dry, degassed TMSES, PFPA, and dioxane were transferred into a glovebox. A solution of 85 wt% monomer (70 wt% TMSES: 30 wt% PFPA) in dioxane was mixed and added to the vial. The polymerization vessel was removed from the box and placed into a UV reactor (350 nm, 1.25 mW/cm^2) for 4 hours. The substrates were then removed, rinsed and sonicated in tetrahydrofuran (THF), chloroform, and DMF, and dried in a stream of nitrogen.

Development of Photo-patterned Substrate

Silicon substrates with an initiator monolayer were transferred into a glovebox. A handheld UV lamp fitted with a Rayonet UV bulb (350 nm) was used to photopattern the PFPA polymer brushes. The irradiation was carried out at 4.20 mW/cm^2 for 3 hours at a distance of 1 mm from the substrate. Copper TEM grids (400 mesh and 2000 mesh) were used as shadow masks and placed in intimate contact with the initiator substrate. Dry, degassed 1,4-dioxane (36.2 μL) and monomer (145.7 μL, 85 wt%) were added to a vial and stirred. A 50 μL aliquot of the 85 wt% PFPA solution was added on top of the TEM grids, and two pieces of quartz were placed on the top and bottom of the substrate. By clamping together the quartz and silicon pieces, no space exists between the grid and the initiator surface, giving clean pattern lines and saving initiators for a second

polymerization. See Figure 3.1 for a representation of the setup. After the polymerization, the substrate was removed from the glovebox, rinsed and sonicated in chloroform and THF for several hours, and dried with nitrogen. The PFPA patterned substrate was transferred into the glovebox and placed in a quartz cuvette containing neat TMSES. A handheld UV lamp fitted with a Rayonet UV bulb (350 nm) was used polymerize TMSES from the substrate. The irradiation was carried out at 4.50 mW/cm^2 at a distance of 1 mm from the substrate. After 5 hours of polymerization time, the substrate was removed from the glovebox, rinsed and sonicated in DMF, and dried in a stream of nitrogen.

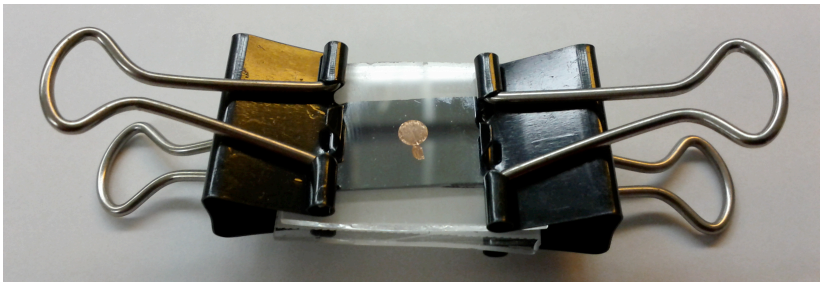

Figure 3.1. Polymerization setup for patterning of PFPA on silicon. Setup was placed under handheld UV lamp containing a 350 nm Rayonet UV bulb.

One-pot Deprotection and Click in Solution

In a flat bottom Schlenk flask, a stirbar and CuBr (27 mg, 0.1875 equiv.) were purged with nitrogen three times. Dry DMF (5 mL), TMSES (250 mg, 1.25 equiv.), benzyl azide (166 µL, 1.25 equiv.), and triethylamine (174 µL, 1.25 equiv.) were mixed together and degassed with argon for 1 hour before being added to the Schlenk flask. The flask was submerged into a 100 °C oil bath and stirred for 2 hours. The solution was then

allowed to cool to room temperature, extracted with ethyl acetate, and washed with saturated ammonium chloride and water. The organic layer was dried with sodium sulfate, and the solvent was removed under reduced pressure. A pure, white-yellow solid was collected in 72.3% yield. ^{1}H NMR (300 MHz, $CDCl_3$) δ 7.75 (d, 2H), 7.67 (s, 1H), 7.42 (d, 2H), 7.36 (m, 5H), 6.70 (dd, 1H), 5.75 (d, 1H), 5.56 (s, 2H), 5.24 (d, 1H). ^{13}C NMR (300 MHz, $CDCl_3$) δ 147.08, 137.29, 136.89, 136.65, 130.82, 129.48, 128.84, 128.58, 127.35, 126.01, 122.29, 115.06, 53.72.

One-pot Deprotection and Click on the Surface

A photopatterned poly(PFPA)/poly(TMSES) substrate was placed in a flat bottom Schlenk flask, along with a micro stirbar and CuBr (3 mg, 0.15 equiv). The flask was purged and backfilled with nitrogen 3 times. Dry DMF (3 mL), triethylamine (60 μL, 3.3 equiv.), 1-aminomethylpyrene (AMP, 40.2 mg, 1 equiv.), and 5-azidofluorescein (AF, 50 mg, 1 equiv.) were combined, degassed with argon for 1 hour, and added to the flat bottom Schlenk containing the substrate. The flask was submerged into a 100 °C oil bath and stirred for 3 hours. After the solution cooled to room temperature, the substrate was removed, rinsed with DMF, and dried with nitrogen.

Characterization

Null ellipsometry was performed on a Multiskop (Optrel GbR) instrument with a HeNe laser (632.8 nm) at 70°. Film thicknesses were determined using integrated specific software. At least three spots on each wafer were measured, and the thickness was averaged. To obtain thickness values of the samples, a simple box model was employed and a refractive index of n = 1.50 was assumed for all polymer brush layers. FTIR measurements were taken with a Nicolet Model 6700 with a grazing angle attenuated

total reflectance accessory (GATR) at 256 scans with a 4 cm^{-1} resolution. Fluorescence microscopy pictures were taken using a Zeiss AX10 Observer inverted microscope with an X-cite Series 120 fluorescent light source and Chroma Technology filters: model 61000 (395, 487, and 555 nm excitation, 450, 517, and 607 nm emission), 41000 FITC blue filter (480 nm excitation, 535 emission) and model 11000 FITC UV filter (350 nm excitation, > 430 nm emission).

Results and Discussion

Photo-initiated Polymerization of Poly(PFPA-co-TMSES)

Initially, two reactive monomers, PFPA and TMSES, with orthogonal chemistries were synthesized. Both monomers undergo what are considered "click" reactions because they reach high conversion, require simple reaction conditions, and most importantly, are modular, allowing for a one-pot, self-sorting functionalization solution.[40] PFPA, an activated ester, can easily react with primary, secondary, and aromatic amines to generate acrylamide derivatives. The presence of electron withdrawing fluorine atoms on the aromatic pendant group of PFPA leads to an increased reactivity towards nucleophiles compared to other activated esters, resulting in rapid, high conversion. Also, the hydrophobic nature of the PFPA monomer provides extra stability towards hydrolysis under ambient or even aqueous conditions. The protected alkyne of TMSES can undergo copper(I)-catalyzed azide-alkyne cycloaddition (CuAAC) with an azide in solution to generate a triazole linkage using moderate conditions. In this work, these monomers were polymerized using surface-initiated free radical polymerization (SI-FRP) both as random copolymers and patterned homopolymer brushes.

Poly(TMSES)-*co*-poly(PFPA) brushes were generated through SI-FRP to investigate the chemoselectivity of the copolymer (Scheme 3.1). An azobisisobutyronitrile-based (AIBN) silane initiator was synthesized and used to form self-assembled monolayers on silicon/silicon oxide substrates.[41, 42] Although initiators containing AIBN derivatives are usually activated thermally, they can be photoinitiated using UV light between 300 – 360 nm. Photoinitiation has the advantage of lithographic patterning, where masked initiators can be preserved for a second polymerization with subsequent monomer. For copolymerization, an 85 wt% monomer concentration in dioxane (with a feed ratio of 70:30 (w/w) TMSES:PFPA) was used for the polymerization due to the higher reactivity exhibited by acrylates compared to styrenic monomers.[43] Thicknesses of approximately 60 nm were achieved after 4 hours of polymerization in a UV reactor (350 nm, 1.25 mW/cm^2), which is slightly less than the 65 nm poly(PFPA) homopolymer brush generated after 4 hours under similar conditions (80 wt% PFPA in dioxane).[39] This is likely due to the small absorbance tail of the TMSES monomer at 350 nm (Figure 3.2, ε_{350} = 14.98 $M^{-1}cm^{-1}$), which reduces the number of photons that reach the surface, lowering the rate of initiation and resulting in an overall decrease in the rate of polymerization.

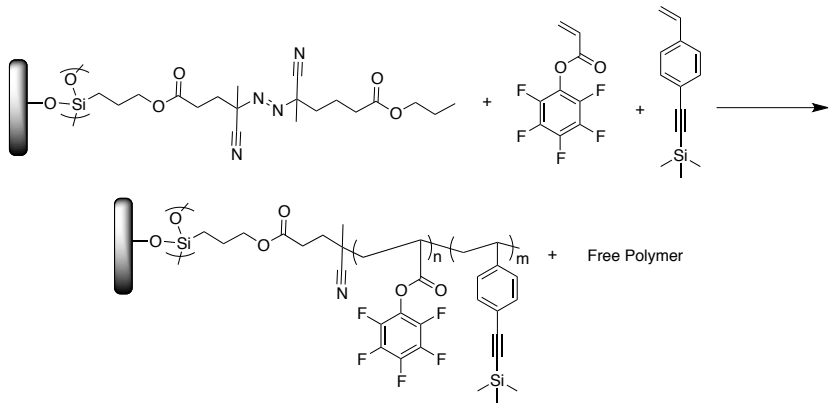

Scheme 3.1. Surface-initiated free radical polymerization of a poly(TMSES)-*co*-poly(PFPA) brush from a silicon/silicon oxide substrate using UV light.

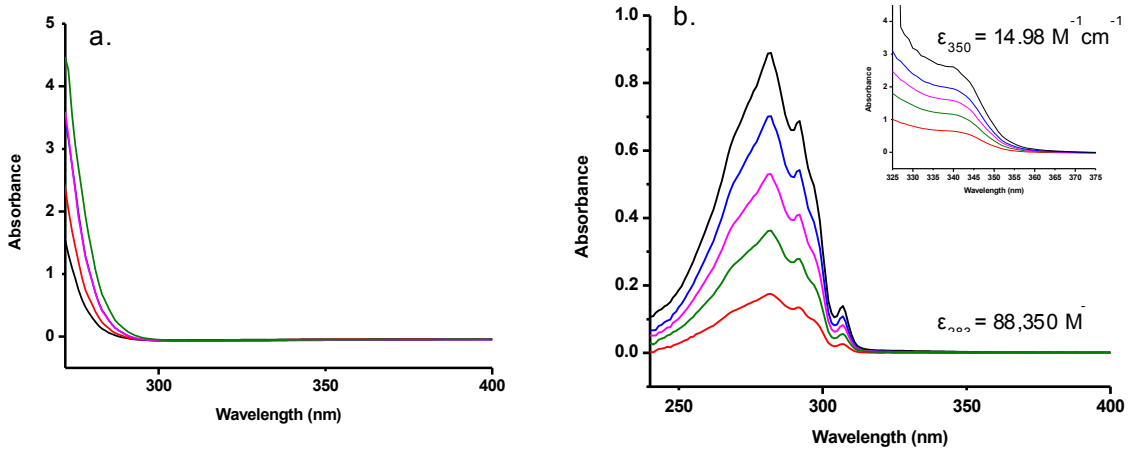

Figure 3.2. a) UV-vis spectra of five different monomer concentrations of PFPA. No absorbance is observed at the 350 nm photopolymerization. b) UV-vis spectra of five different monomer concentrations of TMSES. (Black = 1 μM, Blue = 0.8 μM, Magenta = 0.6 μM, Green = 0.4 μM, Red = 0.2 μM). Inset is a zoomed in to 350 nm.

Generation of Patterned Poly(PFPA)/Poly(TMSES) Surfaces

In order to generate patterned homopolymer surfaces, two sequential SI-FRPs were used in combination with a shadow mask as shown in Scheme 3.2. The shadow mask was placed in physical contact with the substrate and irradiation was used to first polymerize PFPA in the exposed areas. Once the substrate was rinsed and sonicated, TMSES was polymerized by flood irradiation from the initiators previously shielded by the shadow mask. Homopolymer thin films of poly(TMSES) were limited to thicknesses of 30 nm, likely due to the absorbance tail of the monomer at 350 nm as described above.

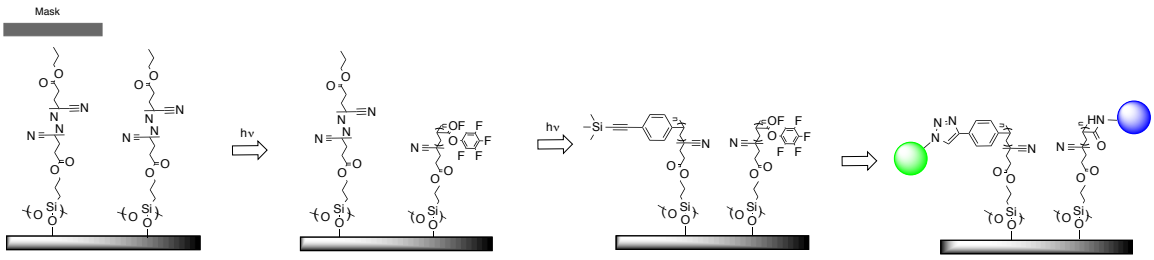

Scheme 3.2. Two step, sequential photo-initiated free radical polymerizations to generate patterned polymer brushes on silicon/silicon oxide. Green ball represents 5-azidofluorescein. Blue ball represents AMP.

Desilylation/CuAAC Studies for Poly(TMSES)

Deprotection of alkynes, while facile in solution,[44] pose many difficulties on oxide surfaces. A common method for the removal of the TMS protecting group from a terminal alkyne is through the use of fluoride anions, such as tetra-n-butylammonium fluoride.[45-47] However, fluoride ions etch silicon oxide and silicon, resulting in cleavage

of the polymer brush from the surface. Basic deprotection conditions are more reliable for surfaces,[48] but are not compatible with activated ester monomers, where hydrolysis can occur, or even complete loss of the surface-bound macromolecule because of the ester-linkage contained in the silane initiator.[49] Silver salts have been used to deprotect alkynes in the presence of esters, but are not reactive enough to completely deprotect the TMS moiety with quantitative conversion.[46, 50, 51] Recently, CuAAC has been preformed without the need to deprotect the alkyne.[52] More vigorous conditions are required, but the reaction still reaches high conversion without generating poisonous byproducts.

The tandem desilylation/CuAAC was first performed in solution to screen reaction conditions that ensured complete conversion (Scheme 3.3). TMSES was reacted with benzyl azide in the presence of copper(I) bromide at 100 °C to generate the triazole adduct. In comparing the NMR spectra of the starting materials and the product, the singlet corresponding to the methylene protons shifts from 4.34 ppm to 5.56 ppm, as well as the appearance of a singlet at 7.67 ppm, signifying generation of the triazole (Figure 3.3). A band at 1627 cm^{-1}, which correlates to the N=N triazole stretch, was observed in the FTIR spectra with complete disappearance of the protected C≡C stretch at 2158 cm^{-1} (Figure 3.4). No evidence of TMS was observed in the triazole product, which supports the hypothesis for copper acetylides in the CuAAC reaction.[53-55]

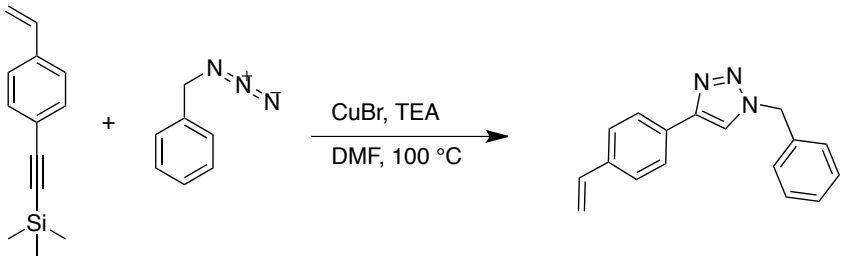

Scheme 3.3. Solution CuAAC without deprotection of the TMSES moiety.

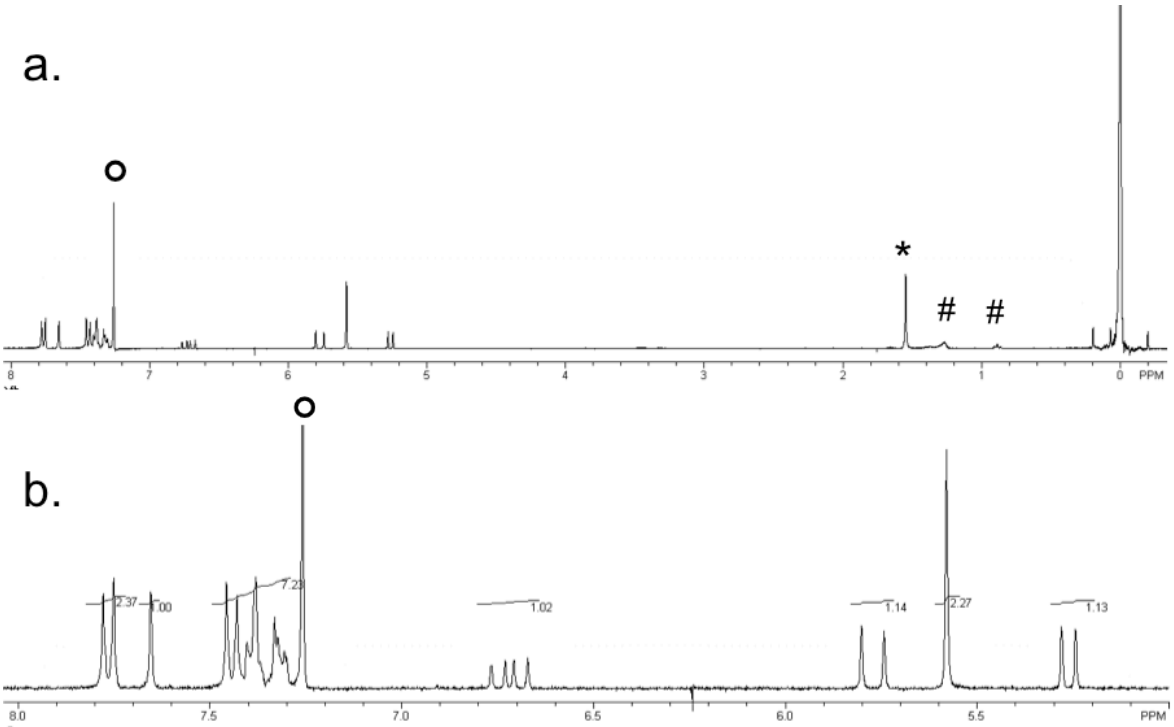

Figure 3.3. a) ^{1}H NMR spectra of 1-benzyl-4-(4-vinylphenyl)-1*H*-1,2,3-triazole. b) Zoom of 4.0-8.0 ppm region. ^{1}H NMR (300 MHz, $CDCl_3$) δ 7.75 (d, 2H), 7.67 (s, 1H), 7.42 (d, 2H), 7.36 (m, 5H), 6.70 (dd, 1H), 5.75 (d, 1H), 5.56 (s, 2H), 5.24 (d, 1H). *Residual water. #Impurities from commercially bought benzylazide. **O**NMR solvent peak.

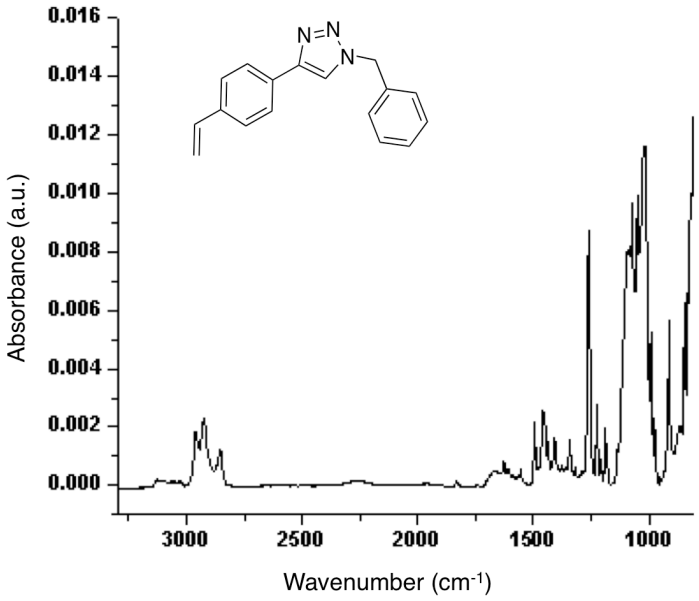

Figure 3.4. FTIR spectrum of the solution one-pot deprotection/click product.

One-pot Desilylation/CuAAC, Aminolysis Postpolymerization Modification

With the appropriate conditions for quantitative conversion optimized in solution, the one-pot desilylation/CuAAC/aminolysis reaction was performed on the copolymer brush using a combination of benzyl azide and 1-aminomethylpyrene (AMP). The grazing angle attenuated total reflectance (GATR) FTIR spectra for each step of the polymerization and functionalization of the copolymer brush are shown in Figure 3.5. The AIBN-based surface-bound initiator has three characteristic peaks: a distinct C-H stretch from the methyl groups at 2964 cm^{-1}, a C≡N stretch at 2250 cm^{-1}, and a C=O stretch at 1736 cm^{-1}. The red spectrum in Figure 3.5 corresponds to the surface after the free radical copolymerization of PFPA and TMSES. All three bands of the initiator completely disappear, while new bands from the PFPA-TMSES comonomers emerge. PFPA exhibits bands at 1785 cm^{-1} (C=O stretch) and at 1522 cm^{-1} (aromatic C=C bend). The methyl C-H stretch shifts from 2964 cm^{-1} for the initiator to 2959 cm^{-1} for the

trimethylsilyl protecting group. The protected acetylene C≡C stretch at 2158 cm^{-1} also becomes apparent after polymerization. One-pot desilylation, dual-click with AMP and benzyl azide results in a drastic change in the GATR-FTIR spectrum (Figure 3.5, Green spectrum). All stretches from the activated ester and protected alkyne pendant groups disappear completely, suggesting complete conversion of both the CuAAC and aminolysis reactions. An aromatic C-H stretch is observed at 3020 cm^{-1}, while amide I and amide II peaks emerge at 1664 cm^{-1} and 1583 cm^{-1}, respectively. While no stretch can be directly assigned to the triazole adduct formed with benzyl azide because of overlapping spectra with AMP and the weak absorbance of the triazole ring, we assume that complete functionalization occurred because of the disappearance of both the methyl C-H stretch and the protected C≡C, along with no observed bands corresponding to residual deprotected alkyne apparent in the spectrum.

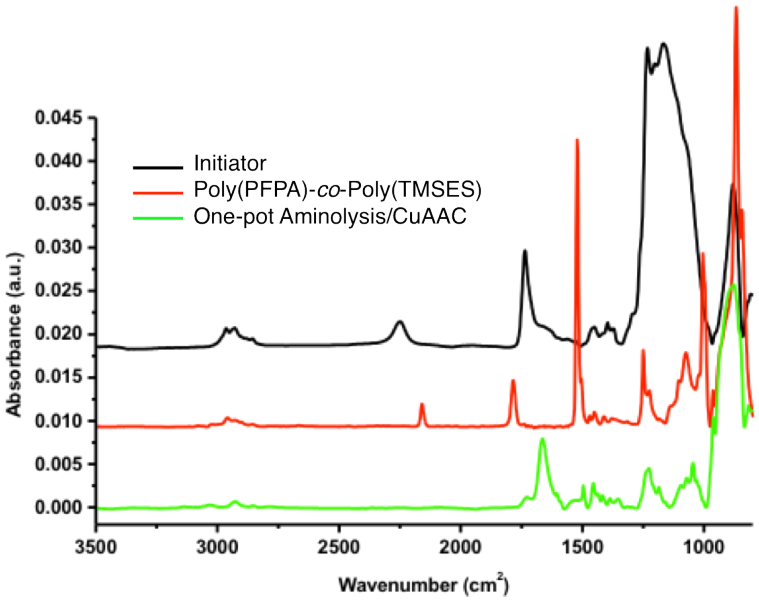

Figure 3.5. FTIR spectra for poly(TMSES)-co-poly(PFPA) functionalization on silicon/silicon oxide surfaces.

The FTIR spectra of the patterned brush, shown in Figure 3.6, display similar absorbance bands to that of the copolymer brush described above. After patterning with PFPA, the carbonyl and aromatic C=C stretches appear, while the peaks corresponding to the initiator decrease in intensity but do not completely disappear. The second polymerization with TMSES results in the complete disappearance of the initiator bands, and the appearance of the protected acetylene. Functionalization of the patterned brushes with 5-AF and AMP demonstrates complete conversion, as observed with the copolymer brush. An aromatic C-H stretch appears at 3042 cm^{-1}, amide I and amide II peaks at 1658 cm^{-1} and 1604 cm^{-1}, respectively, while the fluorescein moiety is observed through the broad peak at 3420 cm^{-1}, C=O stretch at 1732 cm^{-1}, and broad C-O-H bend at 1239 cm^{-1}. As with the copolymer film, it is assumed complete functionalization occurred on the poly(TMSES) brush due to the disappearance of the correlating prefunctionalization stretches. Since PFPA is susceptible to hydrolysis, conversion of the poly(PFPA) brush was determined by using an EDC/NHS solution to generate NHS on any part of the brush that may have hydrolyzed. No peaks corresponding to the NHS stretches (1801, 1769, and 1738 cm^{-1}) appeared in the FTIR spectra, implying no hydrolysis occurred and full conversion was reached (Data not shown). This is consistent with past studies in which modification of PFPA with an alkyl amine produced no such side reactions.[39] (Complete band assignments for all spectra are found in Table 3.1).

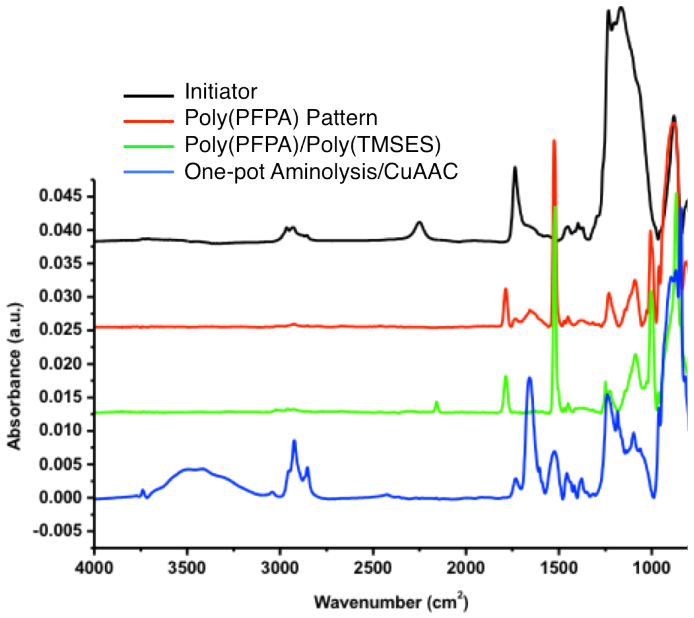

Figure 3.6. FTIR spectra of the poly(PFPA)/poly(TMSES) patterned brush with one-pot postpolymerization desilylation/dual functionalization with 1-aminomethylpyrene and azidofluorescein.

Table 3.1. List of important vibration modes and mode assignments for ATR-FTIR spectra of 3.4-3.6.

Surface	Wavenumber (cm^{-1})	Assignment	Fig.
AIBN initiator	2964	ν(CH_3)	3.4
	2929	ν(CH) sp^3	
	2250	ν(-C=N)	
	1736	ν(C=O) ester	
	1233	ν(C-O) asym.	
	1166	ν(C-O) sym.	
Poly(TMSES-*co*-PFPA)	2959	ν(CH) sp^3	3.4
	2159	ν(C≡C-Si)	
	1785	ν(C=O) PFPA	
	1521	ν(C=C) arom.	
	1250	ν(C-O) asym.	
	1005	ν(C-O) sym.	

Poly(TMSES-*co*-PFPA) One-pot deprotection/click	3030 2929 1728 1664 1496 1455 1227 1046 878 723	ν(CH) sp^2 ν(CH) sp^3 ν(C=O) carb. acid. Amide I ν(C=C) arom. ν(C=C) arom. ν(C-O) asym. ν(C-O) sym. oop oop	3.4
Poly(PFPA)/AIBN initiator	2925 1786 1737 1525 1230 1090	ν(CH) sp^3 ν(C=O) PFPA ν(C=O) init. ν(C=C) arom. ν(C-O) asym. ν(C-O) sym.	3.5
Poly(PFPA) Poly(TMSES) Patterned	3025 2959 2158 1785 1522 1250 1005	ν(CH) sp^2 ν(CH^3) ν(C≡C-SI) ν(C=O) PFPA ν(C=C) arom. ν(C-O) asym. ν(C-O) sym.	3.5
Poly(PFPA) Poly(TMSES) Dual deprotection/click	~3420 3042 2923 2853 1732 1658 1604 1524 1239	ν(-OH) ν(CH) sp^2 ν(CH) sp^3 ν(CH) sp^3 ν(C=O) fluor. Amide I Amide II ν(C=C) arom. ρ(C-O-H)	3.5
Solution one-pot deprotection/click product	3125 ~3066 2925 2855 1627	ν(CH) triazole ν(CH) sp^2 ν(CH) sp^3 ν(CH) sp^3 (C=N) triazole	3.3

5-Azidofluorescein	3431	ν(-OH)	--
	3069	ν(CH) sp^2	
	2923	ν(CH) sp^3	
	2854	ν(CH) sp^3	
	2117	N_3	
	1737	ν(C=O) ester	

Scheme 3.2 also represents the patterned polymer brush before and after postpolymerization modification. Thickness changes within the polymer brush before and after functionalization can aid in determining the conversion of the click reactions. Rühe has previously determined the relationship between polymer brush thickness and the molecular weight of the surface-bound polymer.[56] The molar mass of the attacking nucleophile compared to that of the pendant-leaving group governs whether a thickness increase (greater molar mass) or thickness decrease (smaller molar mass) will occur after functionalization, assuming no change in polymer grafting density. The thicknesses of the patterned polymer brushes on silicon/silicon oxide were measured for each polymerization, as well as before and after the desilylation/dual click using null ellipsometry (Table 3.2). Before photopolymerization, the monolayer was approximately 6 nm, which implies some unavoidable oligomerization of the trichlorosilane occurred, even under strict anhydrous conditions.[57] Photo-initiated free radical polymerization resulted in a film thickness of approximately 24 nm for the poly(PFPA) brush, while the areas covered by the shadow mask with features large enough to contain the laser spot increased by less than 1 Å. This suggests that the protected initiators are not activated during the first polymerization, and the radicals generated during polymerization of poly(PFPA) do not react with the masked initiators. The flood irradiation used to

polymerize TMSES and backfill the pattern does cause a 8% increase in the thickness of the poly(PFPA) layer, most likely due cross contamination. After postpolymerization functionalization with AMP and 5-azidofluorescein (AF), the poly(PFPA) brushes doubled in thickness while the poly (TMSES) brushes nearly tripled, as expected, because of the greater molecular weight of the functionalizing species.[48, 56, 58, 59] Theoretical thickness values for the polymer brushes after functionalization were attempted, but the estimated molar volumes based on the van der Waal radii of molecular fragments outlined by Van Krevelen gave unphysical results for the polymer backbones containing the conjugated dyes.[60]

Table 3.2. Thickness of each layer for 1) monolayer, 2) PFPA polymerization, 3) TMSES backfill polymerization, and 4) one-pot deprotection/dual click.

Layer	**Step 1**	**Step 2**	**Step 3**	**Step 4**
Initiator	6.5 nm	6.6 nm	--	--
PFPA	--	23.7	25.7 nm	52.3 nm
TMSES	--	--	32.5 nm	88.5 nm

The fidelity of the patterns generated from the self-sorting solution could be observed using two different dyes and fluorescence microscopy. The active ester moieties of poly(PFPA) underwent aminolysis with AMP (blue fluorescence), while traditional copper click chemistry was utilized for the functionalization of poly(TMSES) with AF (green fluorescence). The fluorescence images shown in Figure 3.7 demonstrate little to no cross-contamination between sequential polymerizations and orthogonal functionalization. Although we observed a 2 nm increase in the PFPA layer after

polymerization of TMSES with flood irradiation, no cross-contamination was observed with either fluorescence microscopy or GATR-FTIR. With shorter polymerization times, this is a likely issue because of the remaining active initiators in the poly(PFPA) layer that are still present after the first polymerization. Cross-contamination can be reduced and/or eliminated by reaching high conversion during the first polymerization through longer irradiation times.

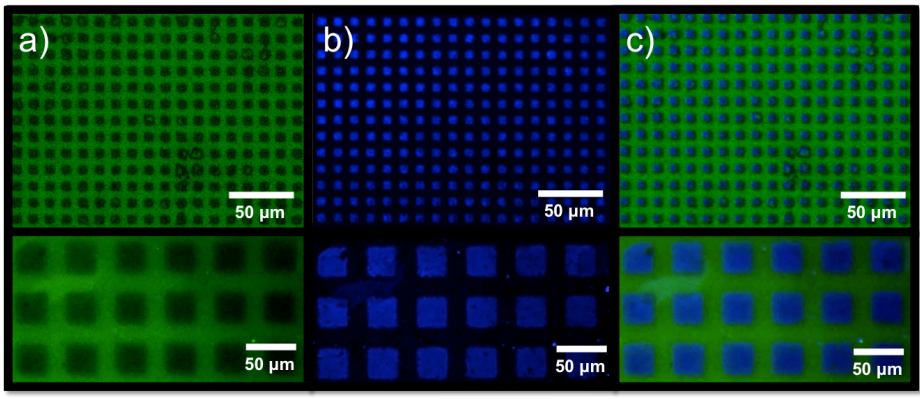

Figure 3.7. Fluorescence microscope images of patterned surfaces fabricated through sequential free radical polymerizations and self-sorting postpolymerization modification. Top row: Square grids with a 12.5 micron pitch. Bottom row: Square grids with a 62 micron pitch. a) PFPA functionalized through aminolysis with AMP excited at 350 nm. b) TMSES functionalized through CuAAC with AF excited at 480 nm. c) Excitation of both dyes with a triple filter (395, 487, and 555 nm excitation).

Conclusion

In conclusion, spatially resolved, patterned surfaces have been generated using the orthogonal postpolymerization modification of two reactive polymer brushes. Poly(PFPA) and poly(TMSES) patterns were generated using a combination of SI-FRP and photolithography. Each polymer was selectively derivatized using a mixture of amines and azides in one-pot aminolysis and desilylation/CuAAC reactions. Little to no cross contamination was observed in both the polymerization and functionalization steps based on ellipsometric thickness data and fluorescence imaging. The combination of SI-FRP and other reactive monomers can be extended to include even more chemical complexity to surfaces, as well as other materials and biological applications.

References

1. Burd, C. and Weck, M., *Macromolecules*, 2005, **38**, 7225-7230.
2. Mukhopadhyay, P., Wu, A. and Isaacs, L., *J. Org. Chem.*, 2004, **69**, 6157-6164.
3. Safont-Sempere, M. M., Fernández, G. and Würthner, F., *Chem. Rev.*, 2011, **111**, 5784-5814.
4. Wu, A. and Isaacs, L., *J. Am. Chem. Soc.*, 2003, **125**, 4831-4835.
5. Lehn, J.-M., *Science*, 2002, **295**, 2400-2403.
6. Bilgiçer, B., Xing, X. and Kumar, K., *J. Am. Chem. Soc.*, 2001, **123**, 11815-11816.
7. Schnarr, N. A. and Kennan, A. J., *J. Am. Chem. Soc.*, 2002, **125**, 667-671.
8. Enemark, E. J. and Stack, T. D. P., *Angew. Chem. Int. Ed.*, 1998, **37**, 932-935.
9. Kondo, T., Oyama, K.-i. and Yoshida, K., *Angew. Chem. Int. Ed.*, 2001, **40**, 894-897.
10. Rowan, S. J., Hamilton, D. G., Brady, P. A. and Sanders, J. K. M., *J. Am. Chem. Soc.*, 1997, **119**, 2578-2579.
11. Wu, A., Chakraborty, A., Fettinger, J. C., Flowers Ii, R. A. and Isaacs, L., *Angew. Chem. Int. Ed.*, 2002, **41**, 4028-4031.
12. Ma, Y., Kolotuchin, S. V. and Zimmerman, S. C., *J. Am. Chem. Soc.*, 2002, **124**, 13757-13769.
13. Gardner, T. J., Frisbie, C. D. and Wrighton, M. S., *J. Am. Chem. Soc.*, 1995, **117**, 6927-6933.
14. Hickman, J. J., Laibinis, P. E., Auerbach, D. I., Zou, C., Gardner, T. J., Whitesides, G. M. and Wrighton, M. S., *Langmuir*, 1992, **8**, 357-359.

15. Laibinis, P. E., Hickman, J. J., Wrighton, M. S. and Whitesides, G. M., *Science*, 1989, **245**, 845-847.

16. Farhan, T. and Huck, W. T. S., *Eur. Polym. J.*, 2004, **40**, 1599-1604.

17. Konradi, R. and Rühe, J., *Langmuir*, 2006, **22**, 8571-8575.

18. Zhao, B. and Brittain, W. J., *Prog. Polym. Sci.*, 2000, **25**, 677-710.

19. Arnold, R. M., Huddleston, N. E. and Locklin, J., *J. Mater. Chem.*, 2012, **22**, 19357-19365.

20. Galvin, C. J. and Genzer, J., *Prog. Polym. Sci.*, 2012, **37**, 871-906.

21. Gauthier, M. A., Gibson, M. I. and Klok, H.-A., *Angew. Chem. Int. Ed.*, 2009, **48**, 48-58.

22. Spruell, J. M., Wolffs, M., Leibfarth, F. A., Stahl, B. C., Heo, J., Connal, L. A., Hu, J. and Hawker, C. J., *J. Am. Chem. Soc.*, 2011, **133**, 16698-16706.

23. Im, S. G., Bong, K. W., Kim, B.-S., Baxamusa, S. H., Hammond, P. T., Doyle, P. S. and Gleason, K. K., *J. Am. Chem. Soc.*, 2008, **130**, 14424-14425.

24. Xu, H., Hong, R., Lu, T., Uzun, O. and Rotello, V. M., *J. Am. Chem. Soc.*, 2006, **128**, 3162-3163.

25. Meng, X., Lu, Y., Yang, B., Yi, G. and Jia, J., *ACS Appl. Mater. Interfaces*, 2010, **2**, 3467-3472.

26. Dunderdale, G., Howse, J. and Fairclough, P., *Langmuir*, 2012, **28**, 12955-12961.

27. Liu, G., Detcheverry, F., Ramírez-Hernández, A., Yoshida, H., Tada, Y., de Pablo, J. J. and Nealey, P. F., *Macromolecules*, 2012, **45**, 3986-3992.

28. Chiang, E. N., Dong, R., Ober, C. K. and Baird, B. A., *Langmuir*, 2011, **27**, 7016-7023.

29. Henley, W. H., Dennis, P. J. and Ramsey, J. M., *Anal. Chem.*, 2011, **84**, 1776-1780.

30. Gates, B. D., Xu, Q., Stewart, M., Ryan, D., Willson, C. G. and Whitesides, G. M., *Chem. Rev.*, 2005, **105**, 1171-1196.

31. Geissler, M. and Xia, Y., *Adv. Mater.*, 2004, **16**, 1249-1269.

32. Barbey, R., Lavanant, L., Paripovic, D., Schuwer, N., Sugnaux, C., Tugulu, S. and Klok, H. A., *Chem Rev*, 2009, **109**, 5437-5527.

33. Katz, J. S., Doh, J. and Irvine, D. J., *Langmuir*, 2005, **22**, 353-359.

34. Sorribas, H., Padeste, C. and Tiefenauer, L., *Biomaterials*, 2002, **23**, 893-900.

35. Orth, R. N., Clark, T. G. and Craighead, H. G., *Biomed. Microdevices*, 2003, **5**, 29-34.

36. Eberhardt, M., Mruk, R., Zentel, R. and Théato, P., *Eur. Polym. J.*, 2005, **41**, 1569-1575.

37. Malkoch, M., Thibault, R. J., Drockenmuller, E., Messerschmidt, M., Voit, B., Russell, T. P. and Hawker, C. J., *J. Am. Chem. Soc.*, 2005, **127**, 14942-14949.

38. Salic, A. and Mitchison, T. J., *Proceedings of the National Academy of Sciences*, 2008, **105**, 2415-2420.

39. Arnold, R. M., Sheppard, G. R. and Locklin, J., *Macromolecules*, 2012, **45**, 5444-5450.

40. Kolb, H. C., Finn, M. G. and Sharpless, K. B., *Angew. Chem. Int. Ed.*, 2001, **40**, 2004-2021.

41. Ayres, N., *Polym. Chem.*, 2010, **1**, 769-777.

42. Habicht, J., Schmidt, M., Rühe, J. and Johannsmann, D., *Langmuir*, 1999, **15**, 2460-2465.

43. Odian, G., *Principles of Polymerization*, John Wiley & Sons, Inc., Hoboken, New Jersey, 2004.

44. Valverde, I. E., Delmas, A. F. and Aucagne, V., *Tetrahedron*, 2009, **65**, 7597-7602.

45. Cooper, B. M. and Emrick, T., *J. Polym. Sci., Part A: Polym. Chem.*, 2009, **47**, 7054-7065.

46. Friscourt, F. d. r. and Boons, G.-J., *Org. Lett.*, 2010, **12**, 4936-4939.

47. Hasneen, A., Han, H. S. and Paik, H.-J., *React. Funct. Polym.*, 2009, **69**, 681-687.

48. Hensarling, R. M., Doughty, V. A., Chan, J. W. and Patton, D. L., *J. Am. Chem. Soc.*, 2009, **131**, 14673-14675.

49. Bain, E. D., Dawes, K., Özçam, A. E., Hu, X., Gorman, C. B., Šrogl, J. and Genzer, J., *Macromolecules*, 2012, **45**, 3802-3815.

50. Aucagne, V. and Leigh, D. A., *Org Lett*, 2006, **8**, 4505-4507.

51. Vitérisi, A., Orsini, A., Weibel, J.-M. and Pale, P., *Tetrahedron Lett.*, 2006, **47**, 2779-2781.

52. Cuevas, F., Oliva, A. I. and Pericàs, M. A., *Synlett*, 2010, **2010**, 1873-1877.

53. Himo, F., Lovell, T., Hilgraf, R., Rostovtsev, V. V., Noodleman, L., Sharpless, K. B. and Fokin, V. V., *J. Am. Chem. Soc.*, 2004, **127**, 210-216.

54. Meldal, M. and Tornøe, C. W., *Chem. Rev.*, 2008, **108**, 2952-3015.

55. Nolte, C., Mayer, P. and Straub, B. F., *Angew. Chem. Int. Ed.*, 2007, **46**, 2101-2103.

56. Murata, H., Prucker, O. and Rühe, J., *Macromolecules*, 2007, **40**, 5497-5503.

57. Ulman, A., *Chem. Rev.*, 1996, **96**, 1533-1554.

58. Orski, S. V., Fries, K. H., Sheppard, G. R. and Locklin, J., *Langmuir*, 2009, **26**, 2136-2143.

59. Schuh, C. and Rühe, J., *Macromolecules*, 2011, **44**, 3502-3510.

60. Pearce, E. M., *Journal of Polymer Science: Polymer Letters Edition*, 1977, **15**, 56-56.

CHAPTER 4

DIRECT GRAFTING OF POLY(PENTAFLUOROPHENYL ACRYLATE) ONTO OXIDES: VERSATILE SUBSTRATES FOR REACTIVE MICROCAPILLARY PRINTING AND SELF-SORTING MODIFICATION[1]

[1] Arnold, R.M.; McNitt, C.D.; Popik, V.V.; and Locklin, J. *Chem. Commun,* **2014,** *50*, 5307-5309. Reproduced by permission from The Royal Society of Chemistry.

Abstract

Poly(pentafluorophenyl acrylate) was covalently attached to silicon oxide through the direct coupling of the reactive ester to surface silanol groups. Subsequently, reactive microcapillary printing (R-μCaP) and a one-pot, self-sorting postpolymerization modification reaction were used to generate patterns of spatially resolved chemical functionality.

Introduction

Polymer brushes are generally made using one of two approaches, either a grafting to or a grafting from method.[1] Both protocols have advantages, depending on the desired application. Grafting to tends to be less challenging in terms of both synthesis and methodology. Also, the molecular weight and dispersity of the polymer can be determined *a priori*, allowing the grafting density to be directly calculated from the film thickness and bulk density. Analyzing grafted from polymer is more difficult because of the extremely low quantity of polymer generated on planar surfaces and, in cases where polymer is generated in solution, it is unclear whether the solution polymerization accurately mimics that of the surface.[2, 3] However, one limitation of the grafting to method is the constraint on film thickness. While grafting from has the ability to create films hundreds of nanometers thick, the self-limiting process of grafting to typically yields films with a thickness ranging from five to tens of nanometers.[1, 4, 5]

Silanols, the silicon analog of an alcohol, are typically involved in cross-coupling reactions,[6, 7] organosilane reactions,[8, 9] hydrogen bonding,[10] and acid/base interactions.[11] However, there are very few reports of the direct coupling of a polymer to oxide surfaces containing silanols without the need for extra synthetic steps that add reactive end groups to the polymer backbone.[12-14] Also, modification of the polymer end groups can be troublesome not only because of synthetic difficulties, but also because of limitations due to compatibility issues with other chemical functionalities, such as trichlorosilanes with amine, hydroxyl, or carboxylic acid moieties.[1] Typically, a polymeric anchoring layer, such as poly(glycidal methacrylate) (PGMA), is used as a reactive interfacial layer to circumvent these issues, because it allows further covalent attachment of polymers

bearing (most commonly) carboxy- or amino end-groups.[4, 15] Anchoring layers provide a larger number of functional groups with higher reactivity on the surface towards end-functionalized polymers, and typically result in higher grafting densities. Unfortunately, to complete the entire grafting to process with PGMA as an anchor layer (PGMA to the surface, polymer to PGMA), requires both high temperature (>120 °C) and long annealing times (12 hrs to days).[5, 15]

To overcome these issues, poly(pentafluorophenyl acrylate) (poly(PFPA)), which reacts with surface silanol groups under much milder conditions and shorter reaction times, was utilized to generate an interfacial layer that still contains unreacted pentafluorophenyl ester (PFP) groups that are available for further postpolymerization modification. Because of its high reactivity, poly(PFPA) undergoes rapid conversion with various nucleophiles,[16, 17] which allows techniques such as reactive microcontact[18-20] or microcapillary[21, 22] printing to be used to generate patterns of different chemical functionality. In this report, we have used reactive microcapillary printing (R-μCaP) to fabricate surfaces that contain patterns of dibenzocyclooctyne and PFP as a platform that can undergo a self-sorting, dual click reaction with azides and amines to generate substrates with spatially-separated chemical functionality.

Experimental

Materials

Solvents were purified using an MBraun solvent purification system. Silicon wafers (orientation <100>, native oxide) were purchased from University Wafer. SU-8 2025 photoresist and developer were purchased from MicroChem. PDMS was made

using the SYLGARD 184 silicone elastomer kit from Dow Corning. Microfluidic masks were designed on AutoCAD (Autodesk, Inc., San Rafael, CA) and printed on transparencies at 20000 dpi by CAD/Art services, Inc. (Bandon, ORD). Pentafluorophenyl acrylate (PFPA) was synthesized using previously published methods.[17] It was further purified by distillation, and any residual acrylic acid was removed by passing the PFPA through a plug of neutral alumina with DCM. All other chemicals were purchased from Alfa Aesar, Sigma Aldrich, or TCI, and were used as received. Flash chromatography was performed using 40-63 μm silica gel. All NMR spectra were recorded in $CDCl_3$ (unless otherwise noted) using 400 MHz instrument.

Polymerization of PFPA

4.25 g of PFPA and 25 mL of dry benzene were mixed in a Schlenk flask and degassed with argon for 1 hour at 0 °C. The monomer solution was then transferred with an argon-purged needle to a Schlenk flask containing 0.1 mol% azodiisobutyronitrile (AIBN) that had been evacuated three times and backfilled with nitrogen. The flask was added to an oil bath that was preheated to 70 °C and stirred for 24 hours. Afterwards, most of the benzene was removed and the polymer was precipitated into cold methanol. The polymer was collected, redissolved in benzene, and precipitated again. M_n = 267,062 g/mol, M_w = 364,936 g/mol, Đ = 1.366.

Synthesis of DIBO

See Appendix B.

Spincoating Polymer Films on Silicon Substrates

Silicon wafers cut to approximately 1.5 cm x 1.5 cm were sonicated in hexane, IPA, acetone, and deionized water for 15 minutes each. The substrates were dried in a

stream of nitrogen and argon plasma cleaned (Harrick Plasma, PDC-32-G, 0.8 mbar, 18 W) for 5 minutes. A 20 mg/mL solution of poly(PFPA) in dry THF was spincoated on the clean substrates at 1000 rpm for 15 s (Chemat Technology Spinocoater KW-4A).

Temperature Dependent Annealing Studies

Seven different substrates with an initial polymer layer of approximately 160 nm were annealed on a hot plate in a chemical hood at temperatures ranging from 25-150 °C. After 30 minutes, the substrates were removed, sonicated in THF, and dried with nitrogen. Thicknesses were determined using spectroscopic ellipsometry.

Time Dependent Annealing Studies

A set of eight substrates containing an initial polymer layer of approximately 160 nm were annealed on a hot plate at 110 °C. Individual substrates were removed after different time points (2, 5, 10, 30, 60, 90, 120 min), sonicated in THF, and dried with nitrogen. Thicknesses were determined using spectroscopic ellipsometry.

Postpolymerization Aminolysis of Annealed Substrates with 1-Aminopmethylpyrene

Substrates from the temperature dependent annealing study were placed in a 10 mM solution of 1-aminomethylpyrene (AMP) in dry DMF with an acid scavenger. After four hours, the substrates were removed, rinsed and sonicated in DMF and methanol, and dried with nitrogen.

Lithographic Methodology

Stamp master molds were created on silicon wafers using a mask aligner (MA6, Karl Suss). Negative photoresist, SU-8 2025, (~ 4 mL) was spincoated onto a clean, dry wafer at 3000 rpm for 30 seconds. The photoresist was then exposed to UV light (λ = 365 nm) through a mask at 20 mW/cm^2. The wafer was then heat cured and washed with

SU-8 developer for 30 min under constant agitation. Wafers were rinsed with isopropanol and dried before a final curing on a hot plate at 70 °C for 10 min. The average thickness of the photo-cured SU-8 photo developer was 29 ± 0.4 μm. The stamps were molded out of PDMS using a 10:1 SYLGARD mixture of the base to curing agent. The mixture was degassed before pouring over the master wafer, followed by 4 hours of curing at 70 °C. Prior to stamp formation, the wafers were coated with trimethylchlorosilane through vapor deposition to ensure the PDMS could be easily removed after curing.

Reactive μCaP on Annealed Substrate

A PDMS stamp was fabricated according to literature.[23] The microfluidic-based pattern was designed on AutoCAD and was created to fit within a 2 cm^2 area by using channels with a 100 μm width. Prior to use, the stamps rinsed with ethanol and acetone. The pattern was cut in a manner that resulted in channel openings on at least 2 sides of the stamp in order to allow wicking of the DIBO solution through the channels. Once the stamp was placed in contact with the substrate, 1 μL of a 50 mM solution of DIBO in dry DMF was added to one end of the stamp. The printing setup was left for approximately 3 hours until the solvent had evaporated. The stamp was then removed and the substrate was rinsed and sonicated in DMF. For the one-pot, self-sorting postpolymerization modification reaction, a solution consisting of 5 mM fluoresceinamine and 2 mM azido-Texas Red in 1:1 MeOH:DMF with triethylamine as an acid scavenger was used. The patterned substrates were stirred in the solution at 25 °C overnight. Afterwards, the substrate was removed from the solution, rinsed and sonicated in DMF and MeOH, and dried in a stream of nitrogen.

Characterization

Thickness was determined on a J. A. Woollam M-2000V spectroscopic ellipsometer with a white light source at three angles of incidence (65°, 70°, and 75°) to the silicon wafer normal. A Cauchy model was used to fit the film thickness, with an extinction coefficient of 0 and refractive index of 1.50 for the polymer brush layer. FTIR measurements were taken with a Nicolet Model 6700 with a grazing angle attenuated total reflectance accessory (GATR) at 256 scans with a 4 cm^{-1} resolution. Fluorescence microscopy pictures were taken using a Zeiss AX10 Observer inverted microscope with an X-cite Series 120 fluorescent light source and Zeiss filters 38 HE (470/40 nm excitation, 525/50 nm emission) and 43 HE (550/25 nm excitation, 605/70 nm emission), and Chroma Technology UV filter (350 nm excitation, > 430 nm emission). Differential scanning calorimetry (DSC) (Mettler Toledo, DSC823^e, 400 W) was used to determine the glass transition temperature (T_g) of poly(PFPA). Samples of approximately 3 mg were placed in standard aluminum DSC pans and loaded at room temperature. A temperature range of 20-250 °C was cycled five times with a ramp of 10 °C/min. The first cycle was used to evaporate any remaining solvent or monomer in the polymer. The data collected was analyzed using the STARe software provided by Mettler Toledo. Size-exclusion chromatography (SEC) was conducted on a liquid chromatograph (Shimadzu LC-20AD series) equipped with a RID-10A refractive index detector. Polymer samples were diluted in tetrahydrofuran (THF) mobile phase and passed through three Phenomonex Phenogel (10E3A, 10E4A, and 10E5A) columns at 40 °C under a constant volumetric flow rate (1 mL min^{-1}). Molecular weight characteristics of the samples were referenced to polystyrene standards (Agilent technologies EasiCal PS-2). Dynamic light scattering

(DLS) of the poly(PFPA) at 2 mg/mL in THF was conducted using a Malvern Instruments Zetasizer Nano ZS instrument (Model ZEN3600) equipped with a 4 mV He-Ne laser operating at λ = 633 nm with a measurement angle of 173°. Thickness of the master mold used in soft-lithographic fabrication was determined by profilometry using a Dektak 150 with a 3 mm radius stylus.

Results and Discussion

Thermal Grafting of Poly(PFPA) to Oxide Surfaces in Ambient Conditions

Polymer thin films of poly(PFPA) were directly grafted to silicon oxide surfaces using the reactive pentafluorophenyl-based ester pendant group. A solution of 20 mg/mL poly(PFPA) (M_n = 267,062 g/mol, Đ = 1.366) in dry THF was spincoated onto clean silicon substrates with native oxide, yielding polymer films with a thickness of 162 nm. An initial time dependent study of the annealing process was performed at 110 °C and resulted in a maximum thickness plateau after 30 minutes. Subsequently, the grafting to reaction was examined in terms of annealing temperature. Seven substrates were annealed for 30 minutes at various temperatures ranging from room temperature (25 °C) to 150 °C in ambient conditions.

FTIR spectra of the substrates from the temperature-dependent study display several interesting features. The characteristic C=O stretch of the ester (1785 cm^{-1}) and the aromatic ring stretch (1523 cm^{-1}) of the pendant group for PFPA were not observed for the substrates annealed at room temperature and at 45 °C (Figure 4.3a). Both of these temperatures are below the glass transition temperature of poly(PFPA), which is observed at 55°C by DSC (Figure 4.1). It is likely that below this temperature, there is not enough

thermal energy for polymer mobility to take place, resulting in either no grafted polymer or films with very low grafting density.[24] Films annealed at temperatures above 55 °C exhibit both of these two stretches and result in an exponential increase in thickness from 3.4 nm at 55 °C to 22.3 nm at 150 °C (Figure 4.2). Peaks at 1801, 1762, and 1725 cm^{-1} also become evident, but both their appearance and intensity depend strongly on the annealing temperature (Figure 4.3a). Starting at 70 °C, the peak at 1725 cm^{-1}, which correlates to the carbonyl of a carboxylic acid, begins to appear. At even higher temperatures (~100 °C), two new stretches are observed at 1801 and 1762 cm^{-1}. It is known that active esters containing N-hydroxysuccinimide groups undergo a ring-closing side reaction of adjacent amides that generate *N*-substituted glutarimides.[25] We hypothesize that with the high reactivity of PFPA, a similar ring-closing reaction of an active ester with an adjacent carbonyl can occur (either a carboxylic acid residue present from hydrolysis or through an ester interchange reaction), which generates glutaric anhydride (Scheme 4.1).[26] This side reaction results in crosslinking between polymer chains, causes the exponential increase in thickness, as well as producing films thicker than those typically generated using a grafting to method.[4] A maximum thickness of 22.3 nm was achieved by annealing for 30 min at 150 °C in ambient conditions.

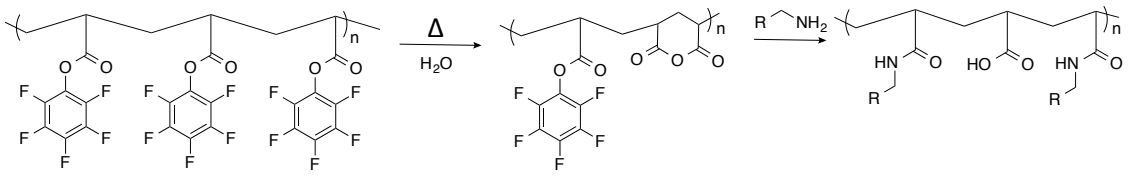

Scheme 4.1. Representation of the ring-closing, anhydride formation reaction followed by ring-opening with an amine.

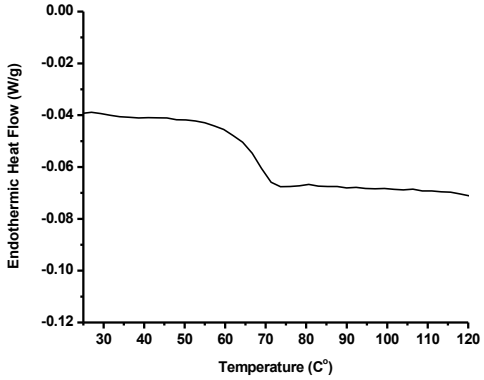

Figure 4.1. DSC scan of poly(PFPA).

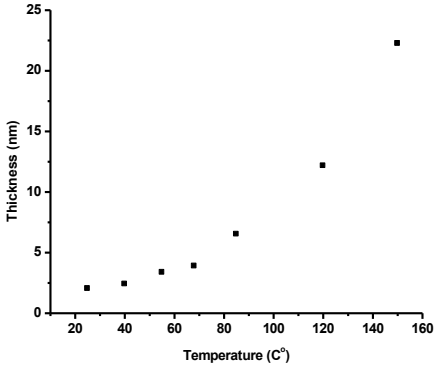

Figure 4.2. Thickness vs. temperature of poly(PFPA) in ambient conditions.

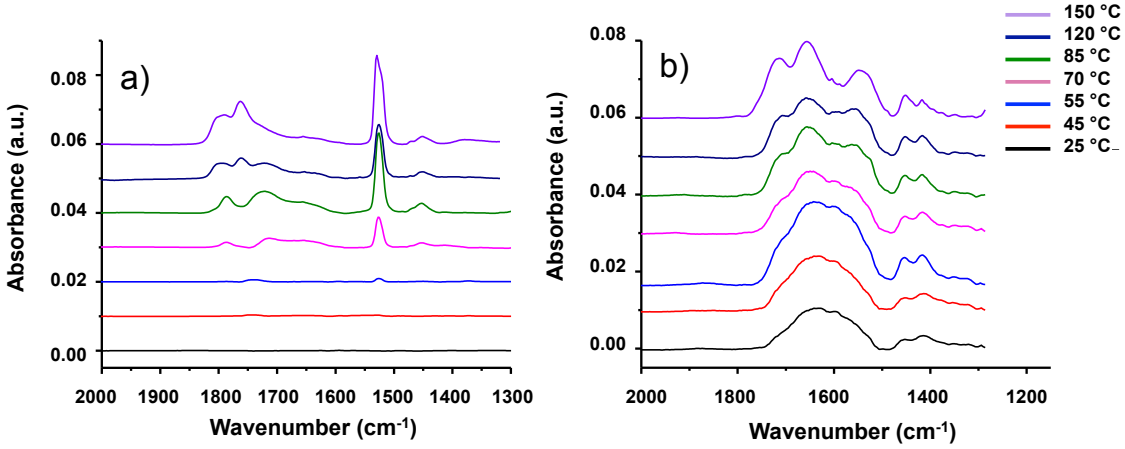

Figure 4.3. FTIR of substrates annealed at various temperatures in ambient conditions. a) After annealing. b) After postpolymerization modification with AMP.

Anhydride Reactivity

The poly(PFPA) films directly grafted to substrates at temperatures above the glass transition of the polymer were subjected to aminolysis using 1-aminomethylpyrene (AMP) in order to examine their reactivity towards postpolymerization modification. The FTIR spectra for all substrates were recorded an analyzed (Figure 4.3b). All substrates annealed at temperatures greater than 55 °C display amide I and II stretches at 1655 and 1530 cm^{-1}, respectively. A small C═O stretch of the carboxylic acid (1726 cm^{-1}) is observed in samples annealed above 70 °C, and this peak increases in intensity with increasing annealing temperature. This is anticipated because films annealed ≥100 °C contain PFPA and glutaric anhydride residues, both of which are susceptible to amidation during postpolymerization modification. However, ring-opening of the anyhydride results in not only an amide linkage, but also a carboxylic acid. (Scheme 4.1).[27] Consequently, the increase in intensity of the carboxylic acid peak after functionalization found in the samples annealed at elevated temperatures is directly correlated to the increase in glutaric anhydride residues in the film.

Thermal Grafting of Poly(PFPA) to Oxide Surfaces in Inert Conditions

To reduce hydrolysis and anhydride formation that occurs during the annealing process in ambient conditions, we annealed poly(PFPA) films for direct grafting at different temperatures under inert atmosphere (N_2 filled glovebox) at a constant annealing time of 30 minutes. The FTIR spectra for these substrates showed the same trends of direct grafting at temperatures above the poly(PFPA) glass transition temperature, but unlike the films generated in ambient conditions, the FTIR spectra were absent of the carboxylic acid and anhydride stretches, and only displayed the

corresponding PFPA peaks (Figure 4.4). Also, the thicknesses of the substrates increased linearly with increasing temperature (Figure 4.5), as compared to the exponential increase observed in an ambient environment. With the removal of H_2O, the hydrolysis of PFP residues is absent, and thus no anhydride formation or polymer crosslinking is observed. Therefore, we hypothesize that the linear increase in thickness at increasing temperatures that is observed results from an increase in grafting density with increased polymer mobility (Table 4.1).[24]

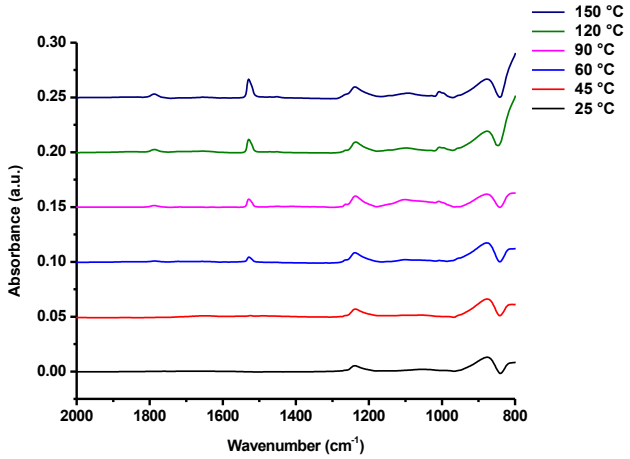

Figure 4.4. FTIR spectra of poly(PFPA) annealed in an inert atmosphere at various temperatures.

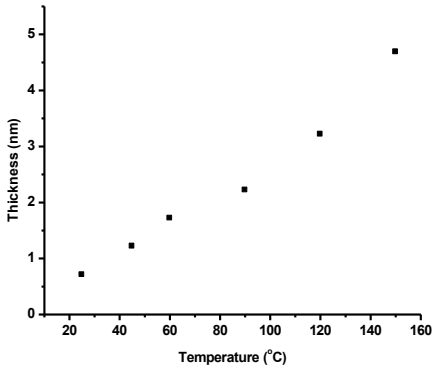

Figure 4.5. Thickness vs. temperature of poly(PFPA) annealed in an inert atmosphere.

Table 4.1 Thicknesses, grafting densities, radius of gyration (R_g) and reduced tethering densities (Σ) of substrates annealed within an inert atmosphere for 30 min.

Temperature	Thickness	σ (chains/nm^2)	R_g	Σ
150 °C	4.69 nm	0.0154	16.64 nm	13.4
120 °C	3.22 nm	0.0106	16.64 nm	9.22
90 °C	2.22 nm	0.0073	16.64 nm	6.35
60 °C	1.72 nm	0.0057	16.64 nm	4.96

R-μCaP and a One-pot, Self-sorting Reaction to Generate a Patterned Surface

To generate patterned surfaces, reactive microcapillary printing (R-μCaP), followed by a one-pot, self-sorting postpolymerization functionalization with two orthogonal reagents, was performed.[21, 22, 28] A PDMS stamp made using conventional lithographic methods was washed with acetone and ethanol and placed directly onto the poly(PFPA) film. It is important to note that the surface of the PDMS stamp was not oxidized using plasma prior to placement. Due to the hydrophobic nature of the polymer, oxidized PDMS would delaminate, causing bleeding of the reacting solution through the channels. Without prior oxidation, the hydrophobic stamp forms an excellent seal when placed in contact with the poly(PFPA) surface. After placing one microliter of a 50 mM solution of a primary amine-containing dibenzocyclooctyne derivative (DIBO)[29] dissolved in DMF at one edge of the stamp, the solution wicks through the channels under capillary action. The substrate was left to react at room temperature until the solvent evaporated. Afterwards, the stamp was removed and the substrate was rinsed thoroughly and placed into a solution containing an azido-Texas Red dye and an aminofluorescein dye to react at room temperature. In one-pot, the orthogonal reagents undergo a self-sorting reaction, the azido-Texas Red dye forms a triazole through strain-promoted azide-alkyne cycloaddition (SPAAC) with the DIBO moiety, and the

aminofluorescein undergoes aminolysis with the free poly(PFPA) that was covered by the PDMS stamp in the previous step (Scheme 4.2). Fluorescence images (Figure 4.6) show little to no cross contamination, as well as sharp resolution. Overall, this patterning method has many benefits over other procedures,[28, 30] including covalent attachment to the surface, its simplicity in a minimal amount of processing steps, and most importantly, mild reaction conditions with short annealing times. This can be compared to our previous work with grafted from poly(PFPA) polymer brushes,[28] in which the patterned substrate fabrication takes several days. With this method, multiple substrates and patterns of different chemical functionality can be made in under an hour.

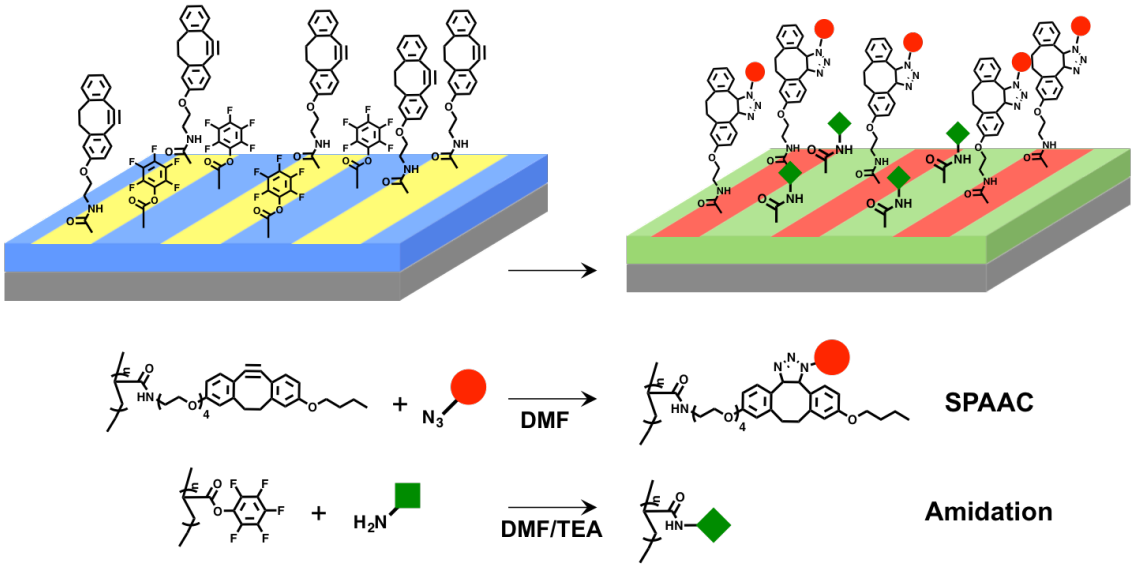

Scheme 4.2 Representative scheme of the one-pot, self-sorting SPAAC/amidation reaction on a patterned surface. After R-μCaP, azido-Texas Red (red ball) undergoes SPAAC with the surface-bound DIBO moieties and aminofluorescein (green squares) reacts with PFPA through aminolysis.

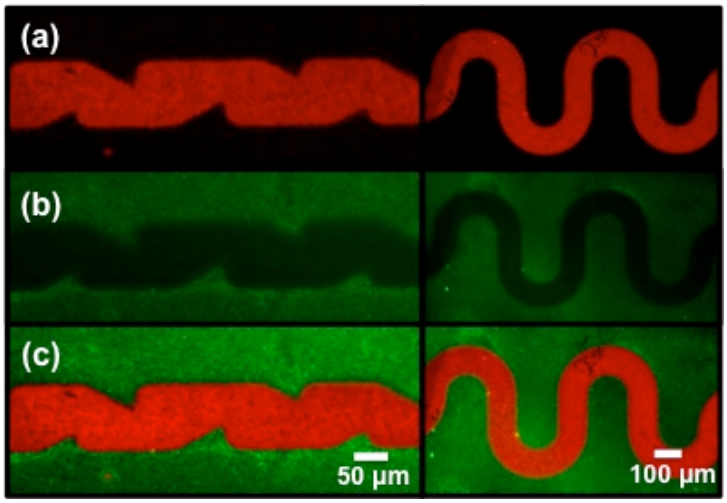

Figure 4.6. Fluorescence microscope images of patterned surfaces generated through R-µCaP followed by a self-sorting click reaction. a) Aminolysis of DIBO with poly(PFPA) followed by SPAAC with azido-Texas Red excited at 550 nm. b) Aminolysis of poly(PFPA) with aminofluorescein excited at 470 nm. c) Excitation of both dyes with broad range UV.

Conclusions

In conclusion, thin films of poly(PFPA) were directly grafted to silicon oxide substrates using surface silanol groups. In ambient conditions, hydrolysis and glutaric anhydride formation occurred at temperatures ≥100 °C, but did not significantly affect postpolymerization functionalization. Under inert atmosphere in the absence of H_2O, this side reaction was completely eliminated. The high reactivity of poly(PFPA) films allowed the used of reactive microcapillary printing, and this was used to pattern DIBO, a strained alkyne, with high fidelity. Spatially-separated chemical functionality with excellent resolution was then generated on the surface using orthogonal reagents in a one-

pot, self-sorting SPAAC/aminolysis reaction at room temperature with fast kinetics. Poly(PFPA) allows the rapid formation of functional polymer interfaces under facile conditions, and opens up new directions for rapid prototyping, as well as for developing surfaces with increasing chemical complexity.

References

1. Rühe, J., in *Polymer Brushes*, Wiley-VCH Verlag GmbH & Co. KGaA, 2004, pp. 1-31.
2. Barbey, R. l., Lavanant, L., Paripovic, D., Schüwer, N., Sugnaux, C., Tugulu, S. and Klok, H.-A., *Chem. Rev.*, 2009, **109**, 5437-5527.
3. Turgman-Cohen, S. and Genzer, J., *J. Am. Chem. Soc.*, 2011, **133**, 17567-17569.
4. Zdyrko, B. and Luzinov, I., *Macromol. Rapid Commun.*, 2011, **32**, 859-869.
5. Iyer, K. S. and Luzinov, I., *Macromolecules*, 2004, **37**, 9538-9545.
6. Denmark, S. E. and Sweis, R. F., *Acc. Chem. Res.*, 2002, **35**, 835-846.
7. Hirabayashi, K., Mori, A., Kawashima, J., Suguro, M., Nishihara, Y. and Hiyama, T., *J. Org. Chem.*, 2000, **65**, 5342-5349.
8. Yoshinaga, K., Yoshida, H., Yamamoto, Y., Takakura, K. and Komatsu, M., *J. Colloid Interface Sci.*, 1992, **153**, 207-211.
9. Ulman, A., *Chem. Rev.*, 1996, **96**, 1533-1554.
10. Tsai, H.-H. G., Jheng, G.-L. and Kao, H.-M., *J. Am. Chem. Soc.*, 2008, **130**, 11566-11567.
11. Bierbaum, K., Kinzler, M., Ch, W., Grunze, M., Haehner, G., Heid, S. and Effenberger, F., *Langmuir*, 1995, **11**, 512-518.
12. Norma, A. A., Eray, S. A. and Jacob, N. I., *J Biomed. Mater. Res.*, 2000, **51**, 343-351.
13. Mansky, P., Liu, Y., Huang, E., Russell, T. P. and Hawker, C., *Science*, 1997, **275**, 1458-1460.

14. Tate, R. S., Fryer, D. S., Pasqualini, S., Montague, M. F., de Pablo, J. J. and Nealey, P. F., *J. Chem. Phys.*, 2001, **115**, 9982-9990.

15. Iyer, K. S., Zdyrko, B., Malz, H., Pionteck, J. and Luzinov, I., *Macromolecules*, 2003, **36**, 6519-6526.

16. Arnold, R. M., Sheppard, G. R. and Locklin, J., *Macromolecules*, 2012, **45**, 5444-5450.

17. Eberhardt, M., Mruk, R., Zentel, R. and Théato, P., *Eur. Polym. J.*, 2005, **41**, 1569-1575.

18. Feng, C. L., Embrechts, A., Bredebusch, I., Schnekenburger, J., Domschke, W., Vancso, G. J. and Schönherr, H., *Adv. Mater.*, 2007, **19**, 286-290.

19. Feng, C. L., Vancso, G. J. and Schönherr, H., *Adv. Funct. Mater.*, 2006, **16**, 1306-1312.

20. Kaufmann, T. and Ravoo, B. J., *Polym. Chem.*, 2010, **1**, 371-387.

21. Geissler, M., Roy, E., Diaz-Quijada, G., Galas, J.-C. and Veres, T., *ACS Appl. Mater. Interfaces*, 2009, **1**, 1387-1395.

22. Diamanti, S., Arifuzzaman, S., Elsen, A., Genzer, J. and Vaia, R. A., *Polymer*, 2008, **49**, 3770-3779.

23. Amit, K. and George, M. W., *Appl. Phys. Lett.*, 1993, **63**.

24. Ionov, L., Zdyrko, B., Sidorenko, A., Minko, S., Klep, V., Luzinov, I. and Stamm, M., *Macromol. Rapid Commun.*, 2004, **25**, 360-365.

25. Devenish, S. R. A., Hill, J. B., Blunt, J. W., Morris, J. C. and Munro, M. H. G., *Tetrahedron Lett.*, 2006, **47**, 2875-2878.

26. Grant, D. and Grassie, N., *Polymer*, 1960, **1**, 125-134.

27. Padwa, A. R., Sasaki, Y., Wolske, K. A. and Macosko, C. W., *J. Polym. Sci., Part A: Polym. Chem.*, 1995, **33**, 2165-2174.

28. Arnold, R. and Locklin, J., *Langmuir*, 2013, **29**, 5920-5926.

29. Orski, S. V., Sheppard, G. R., Arumugam, S., Arnold, R. M., Popik, V. V. and Locklin, J., *Langmuir*, 2012, **28**, 14693-14702.

30. Spruell, J. M., Wolffs, M., Leibfarth, F. A., Stahl, B. C., Heo, J., Connal, L. A., Hu, J. and Hawker, C. J., *J. Am. Chem. Soc.*, 2011, **133**, 16698-16706.

CHAPTER 5

CONCLUSIONS AND OUTLOOK

Conclusions

In this dissertation, the synthesis and design of a new activated ester platform, poly(pentafluorophenyl acrylate) (poly(PFPA)), was outlined. In chapter 1, a literature review discussing each aspect of the platform was presented. The generation of polymer thin films, including the importance of covalent attachment between the polymer and the substrate was examined. An in-depth analysis of free radical polymerization was presented. Postpolymerization modification was surveyed, focusing specifically on click-based functionalization routes. Finally, the generation of complex surfaces through the utilization of the above-mentioned strategies was outlined.

Chapter 2 examined the grafting from surface-initiated photo-polymerization kinetics (poly(PFPA), in regards to reaction time and monomer concentration. The aminolysis of the new active ester polymer brush platform was compared to a different active ester thin film, poly(*N*-hydroxysuccinimide-4-vinylbenzoate) (poly(NHS4VB)). Modification of both surfaces using three different amino dyes of varying nucleophilicity, 1-aminomethylpyrene (AMP), 1-aminopyrene (AP), and $Ru(bpy)_2(phen\text{-}5\text{-}NH_2)(PF_6)$ ($Ru^{+2}A$), was monitored using *ex situ* UV-vis. A pseudo-first order kinetics model enabled the calculation of the pseudo-first order rate constant (k') for each system. Overall, the poly(PFPA) platform showed both faster kinetics and higher reactivity toward poor nucleophiles compared to the poly(NHS4VB) platform.

In chapter 3, two monomers that undergo different, yet orthogonal, click reactions, pentafluorophenyl acrylate (PFPA) and 4-(trimethylsilyl) ethynylstyrene (TMSES), were grafted from a surface using photolithography. Sequential photopolymerizations from an azo-based self-assembled monolayer in the presence of a shadow mask created discreet areas that underwent aminolysis and copper(I)-catalyzed azide-alkyne cycloaddition (CuAAC), respectively. Two dyes, 1-aminomethylpyrene (AMP) and 5-azidofluorescein (AF), were used in a one-pot postpolymerization modification to visualize the 12.5 and 62 micron pitch squares. Deprotection of the terminal alkyne prior to functionalization was not required, as the reaction conditions allowed for dual desilylation/CuAAC through a copper-acetylide intermediate.

Chapter 4 demonstrated the grafting to ability of poly(PFPA). Using thermal annealing, poly(PFPA) directly reacted with the surface silanol groups of different silicon oxide surfaces. In ambient conditions, grafted to films formed anhydrides during annealing due to hydrolysis of some active ester pendent groups, followed by nucleophilic attack on a neighboring ester. However, the anhydrides were found to still be reactive toward a variety of amines. Inert conditions showed no hydrolysis or anhydride formation within the thin films, and thicknesses of 5 nm were achieved. The latent active esters were then used for reactive microcapillary printing (R-μCaP), followed by a one-pot, self-sorting postpolymerization modification reaction, to create a complex surface.

Future work

The fundamental studies required to use poly(PFPA) as a universal platform have been completed within this dissertation. Current work now focuses on using these methods to generate complex surfaces for applications. Several joint projects have been started with departments such as infectious disease and animal and dairy science. In collaboration with the Duncan Krause lab, micropatterned surfaces are being generated to study the gliding mobility mechanism of *Mycoplasma pneumoniae*. Both small molecule analogues and large proteins that are covalently patterned onto glass slides are being studied. Aminolysis is the main functionalization reaction being used for surface patterning. However, a new aldehyde/hydrazide coupling chemistry is being studied in order to attach carbohydrates that contain a reducing end. Reducing sugars have a free anomeric carbon that is in a ring-opened and ring-closed equilibrium. When in the ring-opened form, an aldehyde is present that can act as a reducing agent. Hydrazides that can be synthesized on a poly(PFPA) surface can then capture the open-chain sugar, resulting in a hydrazone linkage. By combining these two coupling reactions with R-μCaP on graft to poly(PFPA) substrates, biological arrays with distinct gliding and non-gliding zones are being developed in order to gain insight into the gliding mechanism of *M. pneumonia*.

In a second collaboration with the Lohitash Karumbaiah lab in the animal and dairy sciences department, the role of the sulfation pattern of chondroitin sulfate (CS) on neuron growth will be studied. Glycosaminoglycans (GAGs) containing sulfated side chains inhibit axon regeneration after injury to the nervous system. By using negative signals, CS acts as a barrier against self-regeneration of damaged nerve endings at the injury site. Different sulfation patterns found on the CS side chains of the GAGs have

shown to have varying effects on this regeneration. By patterning the different CS (CS-A through CS-E), these effects can be directly compared to one another. Also, with the polymer bottlebrush structure that can be generated using grafting to and grafting from methods, the physical structure of the GAGs can be better replicated, making this system a better synthetic mimic compared to others. It is hoped that having more knowledge of the inhibitory signals of different CS can lead to better spinal cord injury treatments.

Other future work will concentrate on surface-attached bottlebrush structures developed from the poly(PFPA) active ester platform in order to create biological mimics of structures such as mucin. Mucins are large, extracellular glycoproteins composed of a protein core with regions of high *O*-glycosylation, yielding a bottlebrush structure. The viscous and elastic gel-like properties of mucins provide many functions in the human body, including exhibiting mucoadhesivity, creating lubrication, and being a diffusive barrier. The unique structure of these glycoproteins allows for a wide range of physical characteristics depending on the chain length of the branches, composition of the branches, and pH and ionic strength of the surrounding environment, making it an interesting model to investigate.

Mucins have recently attracted much attention in research due to their involvement in many respiratory diseases, including asthma, bronchitis, and cystic fibrosis, as well as in cancer and arthritis. Much is known about the cell signaling and biological pathways that result in upregulation of mucin, but little has been studied on the changes in the physical properties of the mucin throughout the progression of these diseases. Mimics have been created in order to try to further understand mucins, but with the complexity of these glycoproteins, it is difficult to extensively study them without

creating multiple substrates through multiple synthetic and polymerization steps. By using the active ester platform developed in this dissertation, a more efficient study of the effects of backbone mobility, side chain length and composition, and hydration on the properties of mucins should be able to be accomplished.

Final Remarks

Polymer-based platforms offer an immense number of advantages over other thin film systems because of the special interfacial properties, high integrity and robustness of the film, and boundless versatility they provide. As disciplines requiring complex, multifunctional surfaces expand, the powerful duo of postpolymerization modification and click-like reactions will continue to advance. This dissertation is comprised of fundamental studies to help overcome the challenges that become apparent when creating such substrates. The development of a single, universal platform that can be used for both complex synthetic and biological studies offers the ability to evolve a wide range of technologies such as lab-on-a-chip, microfluidics, cell proliferation and viability, membranes, sensors, and diagnostic devices. The ability to easily tailor a surface to any application will open up multiple new areas that were once thought to be impossible.

APPENDIX A

UV-VIS SPECTRA AND KINETIC CURVES FOR AMINOLYSIS REACTIONS[1]

[1] Arnold, R.M.; Sheppard, G.R.; and Locklin, J. *Macromolecules,* **2012,** *45* (13), 5444-5450. Reproduced with permission from Arnold, R.M.; Sheppard, G.R.; and Locklin, J. *Macromolecules,* **2012,** *45* (13), 5444-5450. Copyright 2012 American Chemical Society.

Kinetic study

The post-polymerization functionalization of the poly(NHS4VB) and poly(PFPA) kinetics were monitored by taking *ex situ* UV-vis spectra using a spectrometer equipped with a slide holder accessory. The slides were rinsed and dried prior to recording a spectrum from a wavelength of 200 to 800 nm. Spectra were baseline corrected and the absorbance maximum was used to monitor the rate of functionalization. The kinetic curves and UV-vis data for each aminolysis reaction are demonstrated in Figure S2-S6. The kinetic data was fit to a linear form of the pseudo-first order model using a linear regression algorithm in MATLAB (v. 7.1, MathWorks).

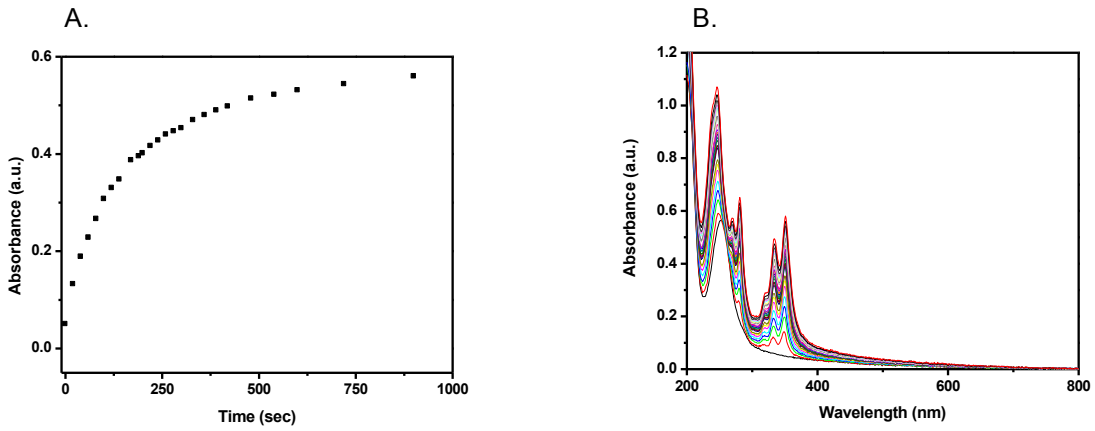

Figure A.1. Poly(NHS4VB) brush on quartz functionalized with AMP. A) Kinetic curve of UV-vis absorbance vs. time at 348 nm. B) UV-vis kinetics spectra.

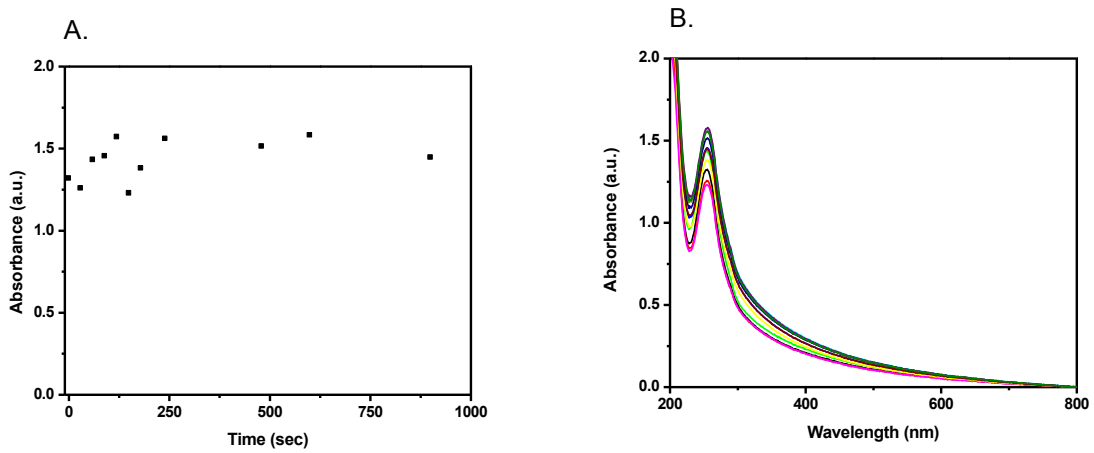

Figure A.2. Poly(NHS4VB) brush on quartz functionalized with AP. A) Kinetic curve of UV-vis absorbance vs. time at 256 nm. B) UV-vis kinetics spectra.

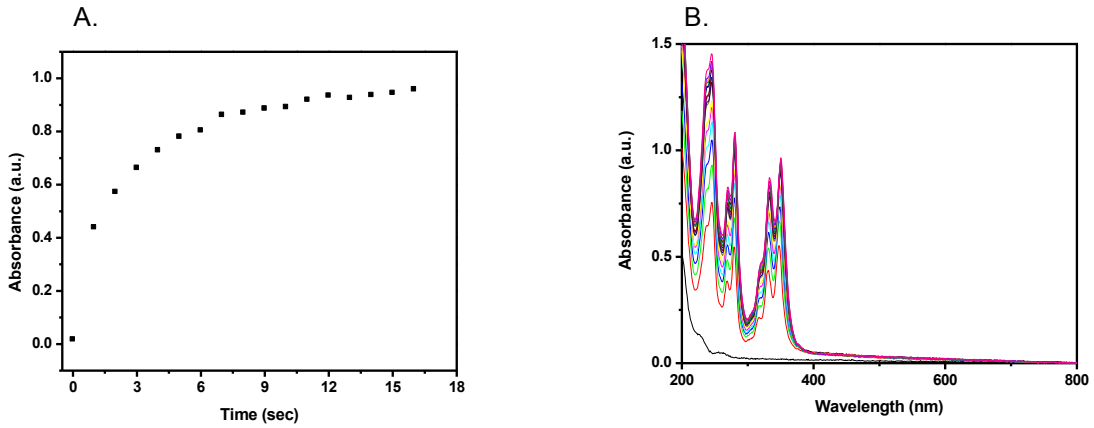

Figure A.3. Poly(PFPA) brush on quartz functionalized with AMP. A) Kinetic curve of UV-vis absorbance vs. time at 349 nm. B) UV-vis kinetics spectra.

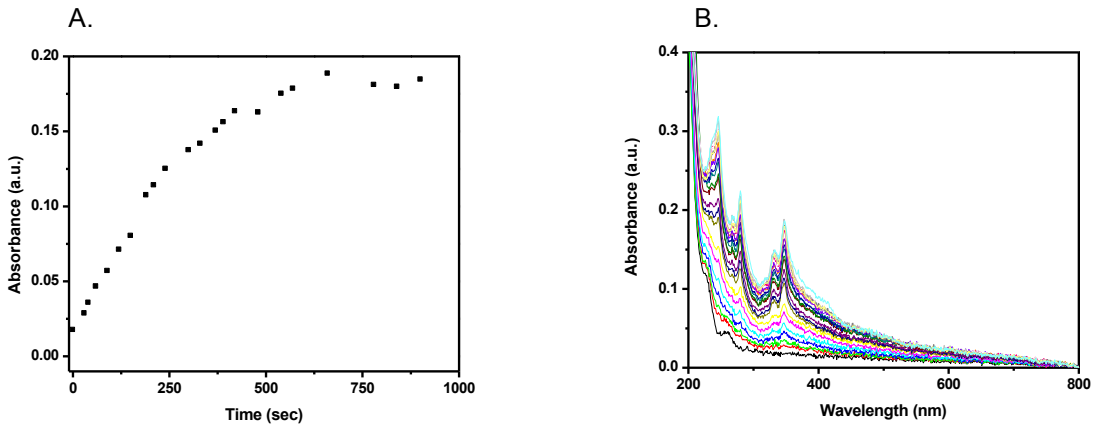

Figure **A.4.** Poly(PFPA) brush on quartz functionalized with AP. A) Kinetic curve of UV-vis absorbance vs. time at 352 nm. B) UV-vis kinetics spectra.

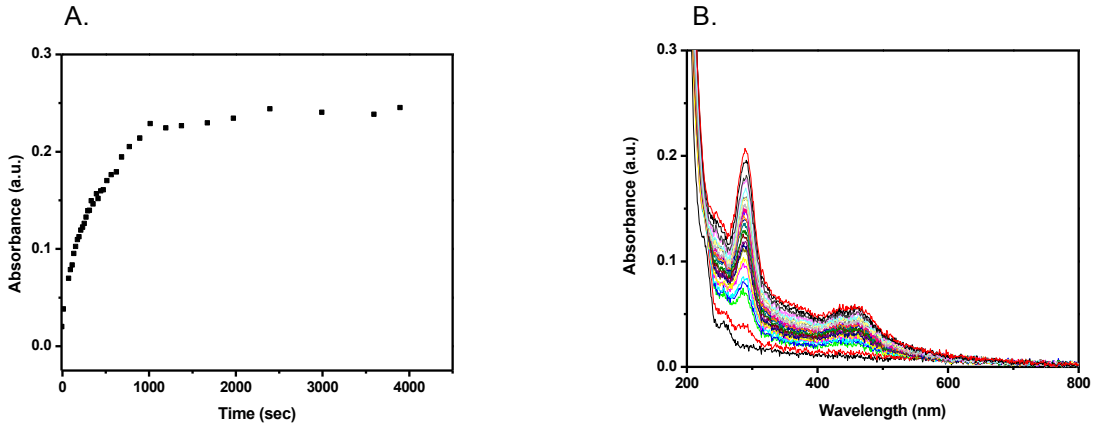

Figure A.5. Poly(PFPA) brush on quartz functionalized with Ru^{+2}A. A) Kinetic curve of UV-vis absorbance vs. time at 291 nm. B) UV-vis kinetics spectra.

APPENDIX B

SYNTHESIS WITH ^{1}H AND ^{13}C NMR OF *2-(2-(2-(2-(2-(9-butoxy-5,6-didehydro-11,12-dihydrodibenzo[a,e]-[8]annulen-2-yl)oxy)ethoxy)ethoxy)ethoxy)ethyl amine* (DIBO-PEG-Amine)[1]

[1]Arnold, R.M.; McNitt, C.D.; Popik, V.V.; and Locklin, J. *Chem. Commun.,* **2014,** *50*, 5307-5309. Reproduced by permission from The Royal Society of Chemistry.

Scheme B.1. Synthesis of Acetamide-PEG-OH.

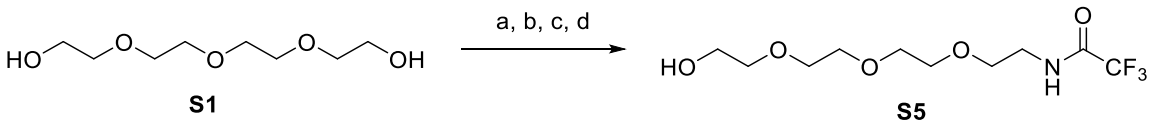

(a) TosCl, DCM; (b) NaN_3, acetonitrile; (c) PPH_3, H_2O, THF; (d) TFAA

p-Toluenesulfonic Acid 2-(2-(2-(2-Hydroxyethoxy)ethoxy)ethoxy)ethyl ester (S2)[1]

Tetra(ethylene glycol) (20.25 g, 104 mmol) and dry triethylamine (15.83 g, 156 mmol) were added to a solution of p-toluenesulfonyl chloride (22.00 g, 115 mmol) in dichloromethane (200 mL) at 0 °C. The reaction was then stirred for 2 hours at 0 °C, and left overnight at room temperature under inert atmosphere. The precipitate was filtered and the reaction mixture was then concentrated in vacuum. The crude mixture was purified by chromatography (hexanes: ethyl acetate 2:8) to provide mono-tosyl tetraethylene glycol (**S2**, 15.28 g, 42%) as a colorless oil. ^{1}H-NMR: 7.79-7.81 (d, J = 8Hz, 2H), 7.33-3.35 (d, J = 4Hz, 2H), 4.15-4.18 (t, 2H), 3.59-3.73 (m, 14H), 2.45 (s, 3H). ^{13}C-NMR: 144.80, 132.83, 129.79, 127.84, 72.43, 70.56, 70.50, 70.31, 70.18, 69.27, 68.54, 61.50, 21.53.

2-(2-(2-(2-Azidoethoxy)ethoxy)ethoxy)ethanol (S3)[1]

A solution of **S2** (15.285 g, 43.9 mmol) and sodium azide (4.28 g, 65.8 mmol) in acetonitrile (150 mL), was refluxed overnight. After cooling to room temperature, water (100 mL) was added and the mixture was extracted with dichloromethane (300 mL). The organic phase was then dried over MgSO4 and concentrated in vacuum. The crude mixture was then purified via silica gel chromatography (ethyl acetate) to provide 2-[2-[2-(2-Azidoethoxy)ethoxy]-ethoxy]ethanol (**S3**, 7.09 g, 74%) as a colorless oil. ^{1}H-

NMR: 3.60-3.74 (m, 14 H), 3.38-3.41 (t, 2H), 2.55-2.58 (t, 1H). ^{13}C: 72.59, 70.76, 70.72, 70.65, 70.40, 70.11, 61.75, 50.72.

2-(2-(2-(2-Aminoethoxy)ethoxy)ethoxy)ethanol (S4)[1]

Triphenylphosphine (9.61 g, 36.7 mmol) was added to a solution of **S3** (5.74 g, 26.2 mmol) subsequently dissolved in THF (53 mL). Once a homogenous solution had been obtained, deionized water (0.660 g, 36.7 mmol) was added to a reaction mixture, and the contents were stirred at room temperature overnight. Next, the solution was concentrated in vacuum and purified by chromatography (chloroform: methanol 1:1) to provide 2-[2-[2-(2-aminoethoxy)ethoxy]ethoxy]ethanol (**S4**, 3.46 g, 68%) as a colorless oil. ^{1}H-NMR: 3.48-3.73 (m, 14H), 2.85-2.87 (t, 2H). ^{13}C-NMR: 73.12, 72.97, 70.54, 70.43, 70.23, 70.07, 61.23, 41.45.

2,2,2-trifluoro-N-(2-(2-(2-(2-hydroxyethoxy)ethoxy)ethoxy)ethyl)acetamide (S5)[2]

Trifluoroacetic anhydride (5.26 g, 25.07 mmol) added dropwise to a solution of **S4** (3.46 g, 17.91 mmol) and triethylamine (4.53 g, 44.8 mmol) in methanol (35 mL) at 0 °C. The mixture was warmed to room temperature and stirred overnight. The solution was then concentrated in vacuum and purified by chromatography (ethyl acetate) to provide acetamide-PEG-OH (**S5**, 4.52 g, 87%) as a colorless oil. ^{1}H-NMR: 8,78 (bs, 1H), 3.55-3.71 (m, 16H). ^{13}C-NMR: 157.82 (q, J= 37 Hz), 116.26 (q, J= 286 Hz), 72.61, 70.82, 70.49, 70.18, 69.86, 69.66, 61.40, 39.99.

Scheme B.2. Synthesis of DIBO-PEG-Amine.

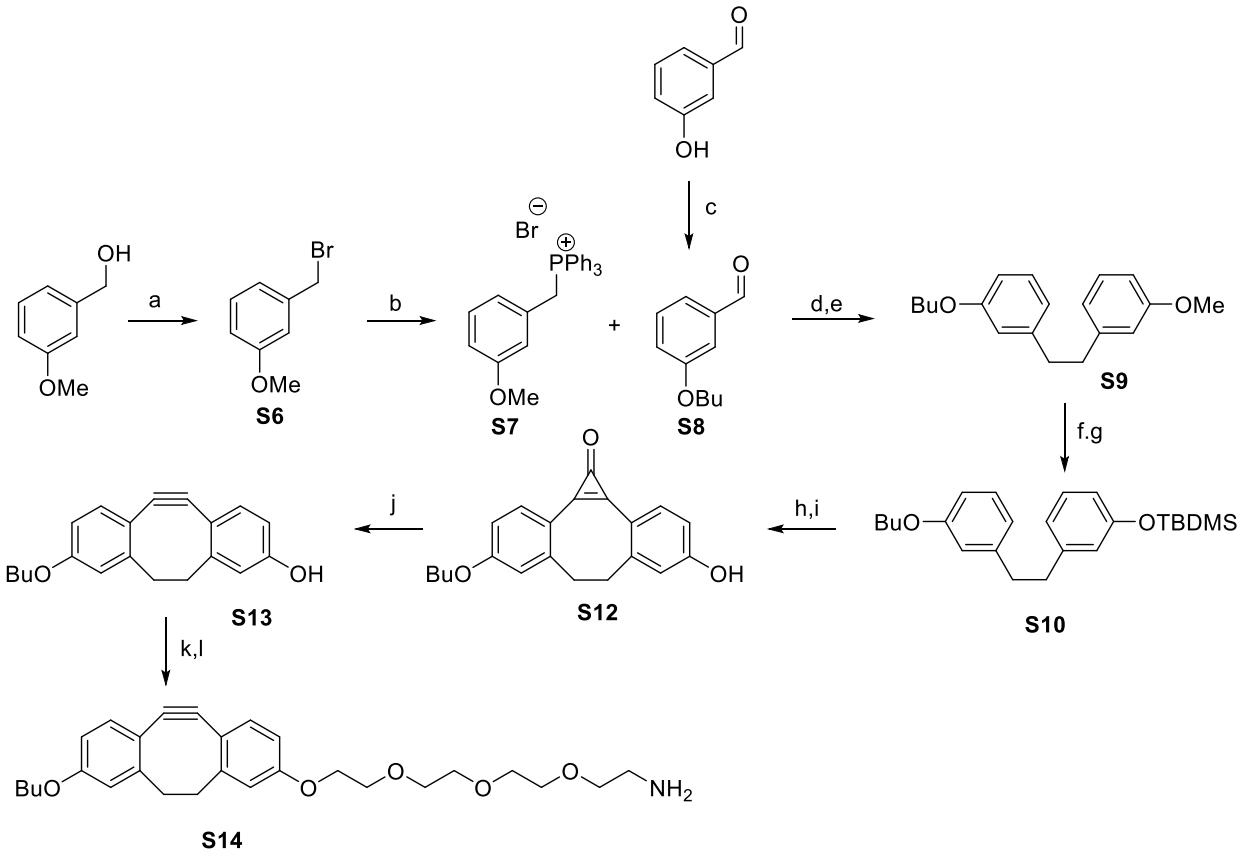

(a) PBr_3 DCM; (b) PPH_3, acetonitrile; (c) butanol, DIAD, THF, PPH_3; (d) n-butylithium, THF; (e) H_2, Pd/C, ethyl acetate; (f) ethanethiol, NaH, DMF, 120 °C; (g) TBDMSCl, imidazole, DCM; (h) aluminum chloride, tetrachlorocyclopropene, DCM; (i) TBAF, THF; (j) MeOH, 350 nm; (k) **S5**, ADDP, PBu_3, THF; (l) K_2CO_3, MeOH, H_2O

1-(bromomethyl)-3-methoxybenzene (S6)[3]

Phosphorus tribromide (11.21 g, 41.4 mmol) was added to a solution of 3-methoxybenzyl alcohol (7.78 g, 55.2 mmol) in dicholormethane (200 mL) at 0 °C. The

reaction mixture was warmed to room temperature and stirred for 30 minutes. The reaction was quenched with saturated sodium bicarbonate (200 mL) and extracted with ether (400 mL). The organic layer was then washed with saturated sodium thiosulfate (200 mL) and brine (200 mL). The organic layer was then dried over $MgSO_4$, filtered, and concentrated in vacuum to provide 1-(bromomethyl)-3-methoxybenzene (10.44 g, 94%) as a colorless oil. ^{1}H-NMR: 7.23-7.27 (t, 1H), 6.97-6.99 (d, J = 7.6 Hz, 1H), 6.93-6.93 (d, J = 2 Hz, 1H), 6.83-6.85 (d, J = 7.6 Hz, 1H), 4.47 (s, 2H), 3.81 (s, 3H).

3-methoxybenzyltriphenylphosphonium bromide (S7)[4]

Triphenylphosphine (40.9, 148 mmol) was added to a solution of **S6** (10.44g, 51.9 mmol) in acetonitrile (210 mL), the reaction mixture was refluxed for 2 hours, concentrated in vacuum, and diluted with toluene. The precipitate was separated to provide (3-methoxybenzyl)triphenylphosphonium bromide (**S7**, 23.60, 98%) as a white solid. ^{1}H-NMR: 7.71-7.78 (m, 9H), 7.60-7.65 (m, 6H), 6.99-7.03 (t, 1H), 6.74-6.78 (m, 2H), 6.63-6.65 (m, 1H), 5.36-5.33 (d, J = 12 Hz, 1H), 3.53 (s, 3H).

3-butoxybenzaldehyde (S8)[5]

Diisopropyl azodicarboxylate (19.87 g, 98 mmol) was added to a solution of 1-butanol (7.28 g, 98 mmol), 3-hydroxybenzaldehyde (12.00 g, 98 mmol), triphenylphosphine (28.8 g, 98 mmol), in THF (200 mL) at 0 °C. The reaction mixture was warmed to room temperature and stirred for 30 minutes. The mixture was concentrated in vacuum, and purified via silica gel chromatography (hexanes: ethyl acetate 10:1) to provide 3-butoxybenzadehyde (12.11 g, 69%) as a colorless oil. ^{1}H-

NMR: 9.97 (s, 1H), 7.38-7.44 (m, 3H), 4.00-4.04 (t, 2H), 176-1.83 (m, 2H), 1.46-1.55 (m, 2H), 0.97-1.01 (t, 3H). ^{13}C-NMR: 192.36, 159.92, 137.98, 130.16, 123.44, 122.12, 112.98, 68.18, 31.37, 19.40, 14.00.

cis/trans-1-(3-butoxyphenyl)-2-(3-methoxyphenyl)ethane

A THF solution of n-butyllithium (22.98 mL, 2.5 M, 60.2 mmol) was added dropwise to a solution of **S7** (24.21 g, 52.3 mmol) in anhydrous THF (450 mL) at -78 °C. The resulting solution was stirred under inert atmosphere for 2 hours, and then **S8** (9.31, 52.3 mmol, 20 mL) was added dropwise. The mixture was then warmed to room temperature and stirred overnight. The reaction mixture was quenched with water (300 mL), extracted with ethyl acetate (3 X 100 mL), and washed with brine (200 mL). The organic layer was then dried over $MgSO_4$ and concentrated in vacuum. The crude product was purified by chromatography (hexanes: ethyl acetate 10:1) to provide 1-(3-butoxyphenyl)-2-(3-methoxyphenyl)ethene (mixture of *cis*- and *trans*- isomers, 11.98 g, 81%) as a colorless oil. ^{1}H-NMR: 7.24-7.33 (m, 3H), 7.03-7.17 (m, 6H), 6.78-6.86 (m, 5H), 6.71-6.75 (m, 1.5H), 6.57 (s, 2H), 3.99-4.02 (t, 1.5H), 3.85 (s, 2H), 3.78-3.81 (t, 2H), 3.66 (s, 3H), 1.75-1.82 (m, 1.5 H), 1.64-1.71 (m, 2H), 1.38-1.57 (m, 3.5 H), 0.92-1.01 (m, 5H). ^{13}C-NMR: 160.07, 159.66, 159.53, 159.12, 138.93, 138.81, 138.77, 138.67, 130.65, 130.41, 129.84, 129.80, 129.39, 129.35, 129.17, 128.96, 121.72, 121.48, 119.46, 119.35, 114.59, 114.12, 113.97, 113.53, 113.46, 112.56, 111.93, 67.87, 67.69, 55.45, 55.26, 31.59, 31.43, 19.50, 19.40, 14.11, 14.03. ESI HRMS: calcd. ($M+H^+$): $C_{19}H_{23}O_2$ 283.1692, found 283.1685.

1-(3-butoxyphenyl)-2-(3-methoxyphenyl)ethane (S9)

A suspension of cis/trans-1-(3-butoxyphenyl)-2-(3-methoxyphenyl)ethene (7.00 g, 24.79 mmol), 10% Pd/C (5.28 g, 2.479 mmol), in ethyl acetate (125 mL) was put on a Parr Shaker at room temperature for 5 hours under H_2 (50 PSI). The reaction mixture was then filtered over celite, concentrated in vacuum, and purified by chromatography (hexanes: ethyl acetate 10:1) to provide 1-(3-butoxyphenyl)-2-(3-methoxyphenyl)ethane (**S9**, 5.63 g, 80%) as a colorless oil. ^{1}H-NMR: 7.16-7.23 (m, 2H), 6.73-6.80 (m, 6H), 3.91-3.94 (t, 2H), 3.77 (s, 3H), 2.88 (s, 4H), 1.72-1.79 (m, 2H), 1.44-1.56 (m, 2H), 0.96-0.99 (t, 3H). ^{13}C-NMR: 159.83, 159.42, 143.64, 143.51, 129.49, 129.44, 121.05, 120.85, 115.03, 114.39, 112.08, 111.49, 67.76, 55.33, 38.07, 31.60, 19.49. 14.07. ESI HRMS: calcd. ($M+H^+$): $C_{19}H_{25}O_2$ 285.1849, found 285.1843.

1-(3-butoxyphenyl)-2-(3-hydroxyphenyl)ethane

Ethanethiol (12.01 mL, 158 mmol) was added to a solution of **S9** (5.60 g, 19.69 mmol) in DMF (280 mL) at 0 °C, followed by sodium hydride (60% suspension in oil, 5.51g, 138 mmol). The solution was warmed to room temperature, stirred for 30 minutes, and heated at 120 °C for 30 h. After cooling to room temperature, the reaction mixture was diluted with ether (200 mL), quenched with water (100 mL), and acidified by the addition of aqueous 5% HCl (100 mL). The organic layer was washed with water (3 x 100 mL), brine (100 mL), dried over $MgSO_4$, filtered, and concentrated in vacuum. The crude mixture was purified by chromatography (hexanes: ethyl acetate 10:1) to provide 1-(3-butoxyphenyl)-2-(3-hydroxyphenyl)ethane (5.01 g, 94%) as a colorless oil. ^{1}H-NMR: 7.15-7.23 (m, 2H), 6.75-6.80 (m, 4H), 6.68-6.69 (m, 2H), 4.93 (s, 1H), 3.94-

3.97 (t, 2H), 2.88 (s, 4H), 1.74-1.81 (m, 2H), 1.46-1.56 (m, 2H), 0.98-1.02 (t, 3H). ^{13}C-NMR: 159.36, 155.71, 143.95, 143.46, 129.72, 129.47, 121.15, 120.89, 115.57, 115.04, 113.05, 112.10, 67.81, 37.94, 37.83, 31.58, 19.48, 14.08. ESI HRMS: calcd. ($M-H^+$): $C_{18}H_{21}O_2$ 269.1547, found 269.1549.

1-(3-butoxyphenyl)-2-(3-(tert-butyldimethylsilyl)oxyphenyl)ethane (S10)

Imidazole (1.100g, 16.16 mmol) was added to a solution of 1-(3-butoxyphenyl)-2-(3-hydroxyphenyl)ethane (4.16 g, 15.39 mmol) in dichloromethane (150 mL) at room temperature. Next, TBDMSCl (2.319 g, 15.39 mmol) was added to the reaction mixture, and the reaction was stirred for 2 hours. The reaction mixture was quenched with saturated ammonium chloride, diluted with ether (400 mL), and layers separated. The organic layer was then washed with brine, dried over $MgSO_4$, filtered, and concentrated in vacuum. The crude mixture was purified by chromatography (hexanes: ethyl acetate 10:1) to provide 1-(3-butoxyphenyl)-2-(3-(tert-butyldimethylsilyl)oxyphenyl)ethane (**S10**, 5.56 g, 94%) as a colorless oil. ^{1}H-NMR: 7.13-7.22 (m, 2H), 6.74-6.82 (m, 4H), 6.68-6.71 (m, 2H), 3.93-3.97 (t, 2H), 2.89 (s, 4H), 1.74-1.81 (m, 2H), 1.49-1.54 (m, 2H), 0.98-1.02 (m, 12H), 0.20 (s, 6H). ^{13}C-NMR: 159.41, 155.83, 143.55, 143.52, 129.43, 129.35, 121.69, 120.86, 120.47, 117.77, 115.02, 112.04, 67.74, 38.08, 37.86, 31.63, 25.93, 19.50, 18.42, 14.10, -4.19. ESI HRMS: calcd. ($M+H^+$): $C_{24}H_{37}O_2Si$ 385.2557, found 385.2549.

4-butoxy-9-((tert-butyldimethylsilyl)oxy)-6,7-dihydro-1H-dibenzo[a,e]cyclopropa[c][8]annulen-1-one (Photo-DIBO-TBDMS, S11)

Tetrachlorocyclopropene (1.887 g, 10.40 mmol) was added to a suspension of aluminum chloride (1.401 g, 10.40 mmol) in dichloromethane (300 mL), stirred for 15 min. and cooled to -78 °C. A solution of **S10** (4.00 g, 10.40 mmol) in 10 mL of DCM was added, and the reaction mixture was stirred for 4 h at -78 °C. The reaction mixture was then warmed to room temperature and stirred for an additional hour. The reaction mixture was then diluted with dichloromethane (300 mL), worked up with a 5% HCl solution (200 mL). The organic layer was washed with water, brine, and dried over $MgSO_4$. The solution was filtered, concentrated in vacuum, and purified by chromatography to provide Photo-DIBO-TBDMS (**S11**, 2.63 g, 58%) as a white amorphous solid. ^{1}H-NMR: 7.94-7.91 (d, J= 12 Hz, 1H), 7.89-7.87 (d, J= 8 Hz, 1H), 6.89-6.86 (m, 2H), 6.83-6.81 (m, 2H), 4.05-4.02 (m, 2H), 3.36-3.26 (m, 2H), 2.63-2.57(m, 2H), 1.82-1.75 (m, 2H), 1.55-1.46 (m, 2H), 1.03-0.97 (m, 12H), 0.25 (s, 6H). ^{13}C-NMR: 162.25, 159.20, 153.96, 148.05, 147.98, 142.76, 142.21, 135.95, 135.76, 121.57, 118.48, 117.20, 116.42, 116.36, 112.38, 68.16, 37.41, 37.17, 31.32, 25.75, 19.37, 18.39, 13.98, -4.13. ESI HRMS: calcd. ($M+H^+$): $C_{27}H_{35}O_3Si$ 435.2350, found 435.2339.

4-butoxy-9-hydroxy-6,7-dihydro-1H-dibenzo[a,e]cyclopropa[c]-[8]annulen-1-one (S12, Photo-DIBO-OH)[6]

Tetrabutylammonium fluoride (7.02 mL, 1.0 M, 7.02 mmol) was added a solution of **S11** (3.05 g, 7.02 mmol) in THF (70 mL), stirred for 30 min, and quenched by saturated ammonium chloride. The reaction mixture was then diluted with

dichloromethane (200 mL), and the aqueous layer was extracted 2x with dichloromethane (50 mL). The combined organic layers were washed with brine, and dried over MgSO4. The solvent was then concentrated in vacuum and purified by chromatography (dichloromethane: methanol 20:1) to provide Photo-DIBO-OH (**S12**) as a white powder. ^{1}H-NMR DMSO: 10.42 (s, 1H), 7.75-7.77 (d, J = 8 Hz, 1H), 7.68-7.70 (d, J = 8 Hz, 1H), 7.08 (s, 1H), 6.98-7.01 (m, 1H), 6.89-6.90 (d, J = 4 Hz, 1H), 6.82-6.84 (dd, 8 & 4 Hz, 1H), 4.06-4.09 (t, 2H), 3.34-3.44 (m, 2H), 2.43-2.7 (m, 2H), 1.70-1.75 (m, 2H), 1.41-1.48 (m, 2H), 0.93-0.96 (t, 3H). ^{13}C-NMR DMSO: 161.36, 161.04, 151.96, 148.13, 147.85, 142.18, 140.78, 135.19, 134.75, 116.94, 116.09, 115.90, 114.48, 113.92, 112.62, 67.57, 36.39, 36.25, 30.60, 18.69, 13.66.

3-butoxy-9-hydroxy-5,6-didehydro-11,12-dihydrodibenzo[a,e]-[8]annulen-2-yl (S13, DIBO-OH)[6]

A solution of Photo-DIBO-OH (**S12**, 0.456 g, 1.423 mmol) in methanol (450 mL) was irradiated for 10 minutes at 350 nm using Rayonet photoreactor. The solution was then concentrated in vacuum, and purified by chromatography (dichloromethane: methanol 40:1) to provide DIBO-OH (**S13**, 0.381 g, 92%) as a white powder (decomp. 74-77 °C) . ^{1}H-NMR: 7.16-7.23 (m, 2H), 6.89 (d, J= 4Hz, 1H), 6.82- 6.83 (d, J= 4 Hz, 1H), 6.76-6.79 (dd, J = 8 & 4 Hz 1H), 6.70-6.73 (dd, J = 8 & 4Hz, 1H), 5.47 (s, 1H), 3.98-4.01 (t, 2H), 3.13-3.22 (m, 2H), 2.41-2.46 (m, 2H), 1.75-1.82 (m, 2H), 1.66-1.56 (m, 2H), 0.98-1.01 (t, 3H). ^{13}C-NMR: 158.84, 155.39, 155.23, 155.04, 127.06, 126.87, 117.46, 116.95, 116.61, 116.13, 113.31, 112.06, 110.75, 110.37, 68.06, 36.76, 36.66, 31.48, 19.43, 14.04. ESI HRMS: calcd. ($M-H^{+}$): $C_{20}H_{19}O_2$ 291.1391, found 291.1376.

2-((2,2,2,-trifluoro-N-(2-(2-(2-(2-(9-butoxy-5,6-didehydro-11,12-dihydrodibenzo[a,e]-[8]annulen-2-yl)oxy)ethoxy)ethoxy)ethoxy)ethyl acetamide (DIBO-PEG-Acetamide)

Tributylphosphine (0.305 g, 1.433 mmol, 2 mL THF) was added to a solution of **S14** (0.381, 1.303 mmol), **S5** (0.415 g, 1.433 mmol), and 1,1'-(Azodicarbonyl)dipiperidine (ADDP) (0.395 g, 1.564 mmol) in THF (10 mL) at room temperature. The reaction mixture was stirred overnight, concentrated in vacuum, and purified by chromatography (dichloromethane: methanol 40:1) to afford DIBO-PEG-Acetamide (0.379 g, 52%) as a yellow oil. ^{1}H-NMR: 7.59 (s, 1H), 7.18-7.20 (d, J = 8 Hz, 2H), 6.88 (s, 2H), 6.75-6.77 (d, J = 8 Hz, 2H), 4.12-4.14 (m, 2H), 3.95-3.99 (t, 2H), 3.83-3.85 (m, 2H), 3.61-3.74 (m, 10H), 3.51-3.55 (m, 2H), 3.15-3.20 (m, 2H), 2.38-2.47 (m, 2H), 1.74-1.81 (m, 2H), 1.45-1.52 (m, 2H), 0.96-1.00 (t, 3H). ^{13}C-NMR: 158.88, 158.24, 157.46 (q, J= 37 Hz), 155.02, 126.81, 126.77, 116.91, 116.85, 116.81, 116.11 (q, J= 286 Hz), 116.01, 112.02, 112.01, 110.82, 110.31, 70.92, 70.72, 70.67, 70.39, 69.83, 68.90, 67.93, 67.63, 39.92, 36.79, 36.77, 31.45, 19.39, 13.99. ESI HRMS: calcd. ($M+H^+$): $C_{30}H_{37}F_3NO_6$ 564.2567, found 564.2550.

2-(2-(2-(2-(2-(9-butoxy-5,6-didehydro-11,12-dihydrodibenzo[a,e]-[8]annulen-2-yl)oxy)ethoxy)ethoxy)ethoxy)ethyl amine (S14, DIBO-PEG-Amine)

A solution of potassium carbonate (0.093 g, 0.672) in water (1.50 mL), was added to a solution of DIBO-PEG-Acetamide (0.379 g, 0.672 mmol) in methanol (3.00 mL) at room temperature. The reaction mixture was stirred overnight, concentrated in vacuum, and the residue was redissolved in dichloromethane/ethyl acetate (1:4). The organic layer was then washed with water, brine, dried over Na_2SO_4, concentrated in vacuum, and

purified by chromatography (dichloromethane: methanol 10:1 to 10:3) to provide DIBO-PEG-Amine (**S14**, 0.259 g, 82%) as a yellow oil. ^{1}H-NMR: 7.18-7.20 (d, J = 8 Hz, 2H), 6.87-6.91 (dd, J= 12 Hz & 4 Hz, 2H), 6.74-6.79 (m, 2H), 4.74 (s, 2H), 4.13-4.16 (t, 2H), 3.96-3.99 (t, 2H), 3.84-3.86 (t, 2H), 3.58-3.74 (m, 10H), 3.15-3.20 (m, 2H), 2.96-2.98 (t, 2H), 2.38-2.47 (m, 2H), 1.74-1.81 (m, 2H), 1.55-1.45 (m, 2H), 1.00-0.96 (t, 2H). ^{13}C-NMR: 158.93, 158.28, 155.11, 155.08, 126.68, 116.99, 116.91, 116.08, 112.25, 112.06, 110.88, 110.36, 70.84, 70.66, 70.62 70.55, 70.36, 69.84, 68.00, 67.81, 40.92, 36.83, 31.51, 19.44, 14.03. ESI HRMS: calcd. ($M+H^+$): $C_{28}H_{38}NO_5$ 468.2744, found 468.2727.

NMR Spectra

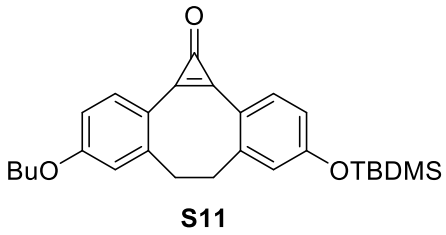

S11

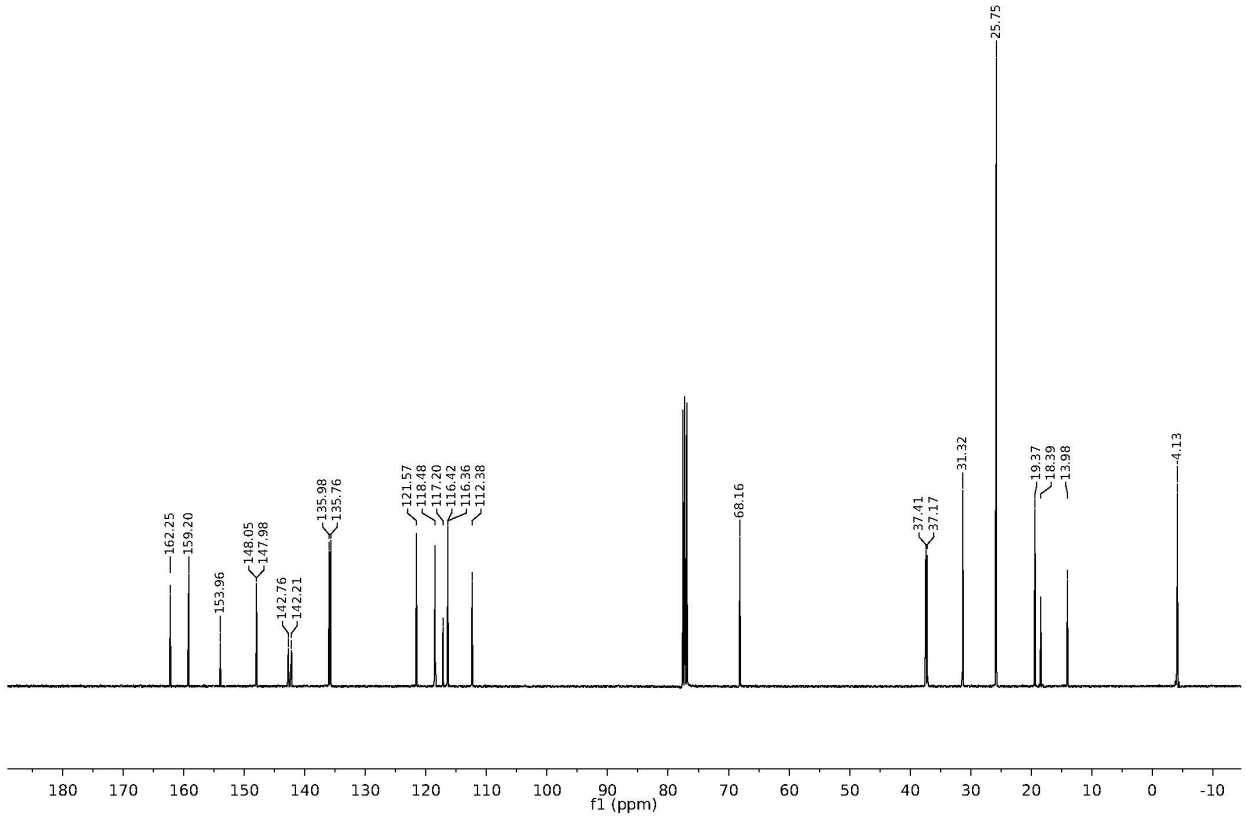

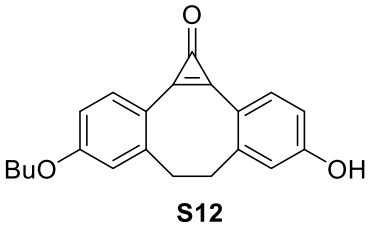
O
BuO
OH

S12

4.09
4.08
4.06
3.42
3.39
3.37
3.34
2.47
2.45
1.74
1.72
1.71
1.47
1.45
1.44
1.42
0.96
0.94
0.93
f1 (ppm)
10.42
7.77
7.75
7.70
7.68
7.08
7.01
7.00
6.99
6.90
6.89
6.84
6.84
6.83
6.82
1.05
1.00
1.01
1.09
1.13
1.12
1.11
2.32
1.92
2.08
2.14
2.09
3.13
f1 (ppm)
161.36
161.04
151.96
148.13
147.85
142.18
140.78
135.19
134.76
116.94
116.09
115.90
114.48
113.92
112.62
67.57
36.39
36.25
30.60
18.68
13.66
f1 (ppm)

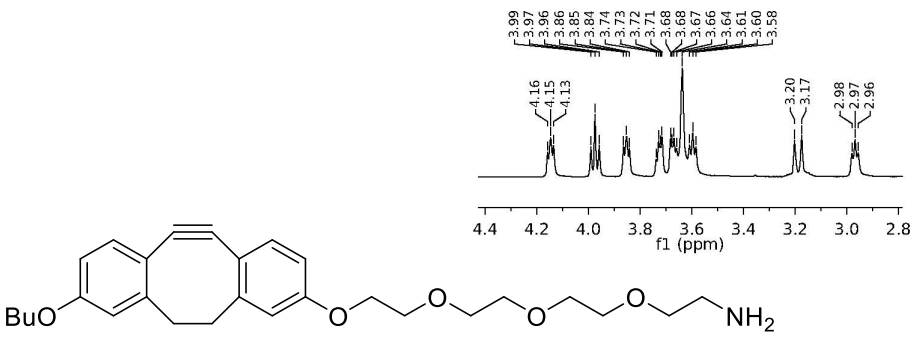

S14

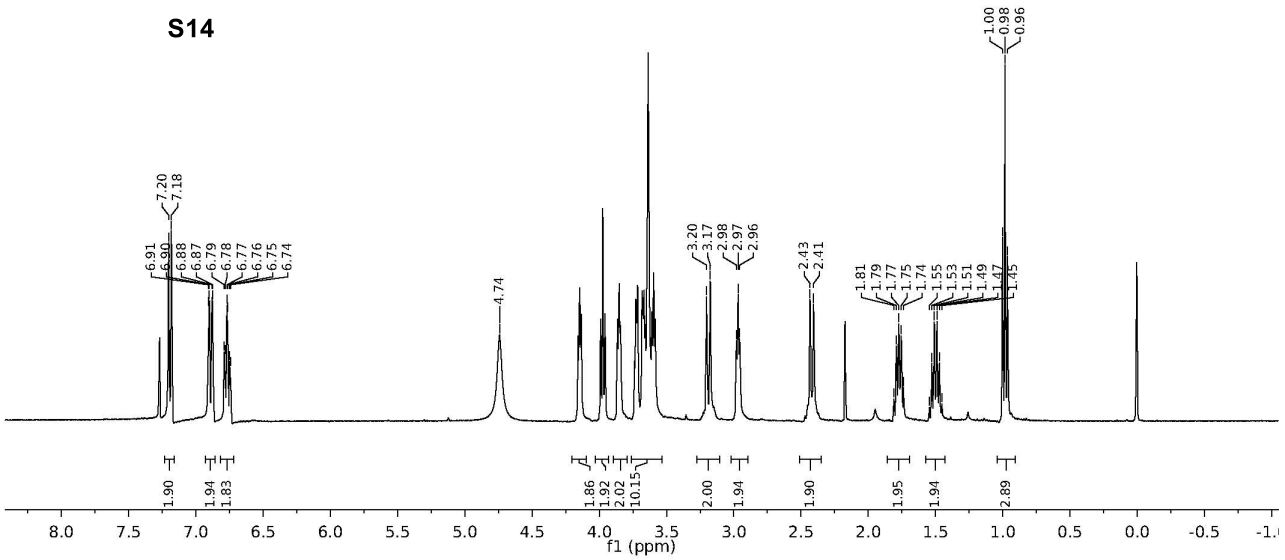

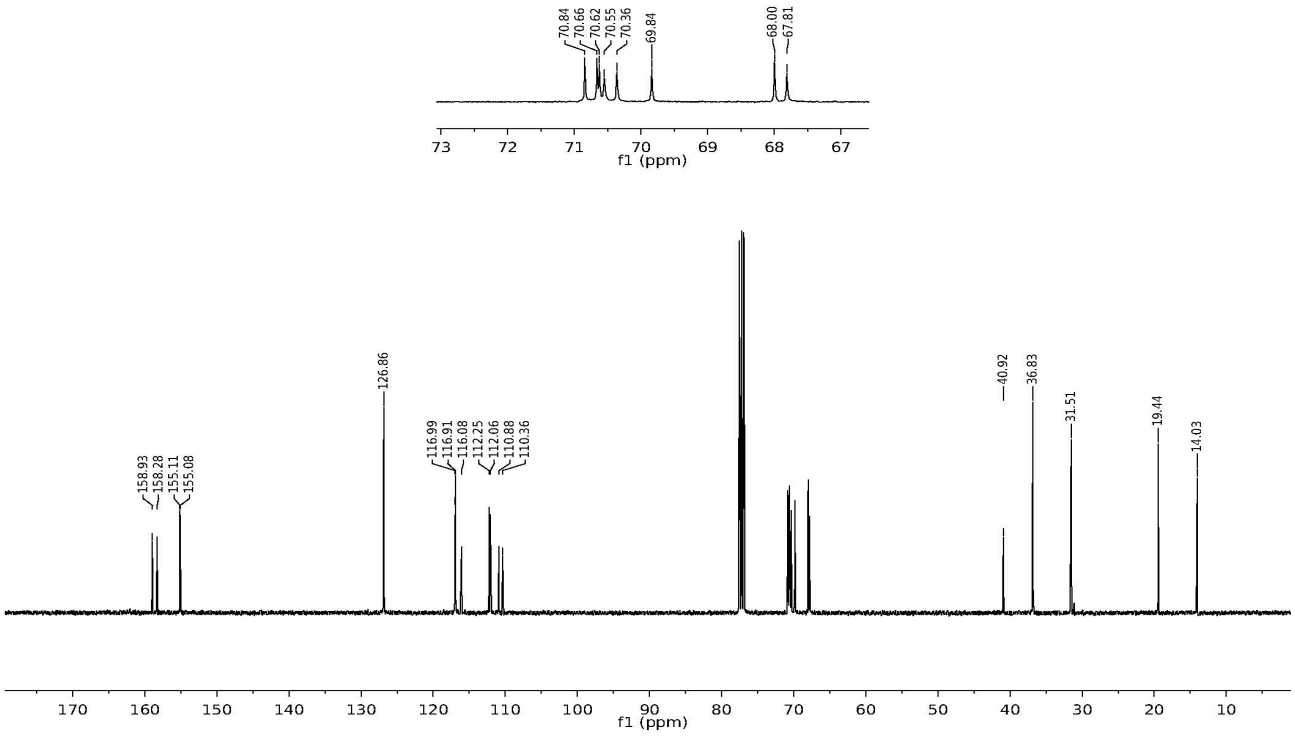

References

1. Wang, W., Li, L.-S., Helms, G., Zhou, H.-H. and Li, A. D. Q., *J. Am. Chem. Soc.*, 2003, **125**, 1120-1121.

2. Dykhuizen, E. C. and Kiessling, L. L., *Org. Lett.*, 2008, **11**, 193-196.

3. McNitt, C. D. and Popik, V. V., *Organic & Biomolecular Chemistry*, 2012, **10**, 8200-8202.

4. Motoshima, K., Noguchi-Yachide, T., Sugita, K., Hashimoto, Y. and Ishikawa, M., *Bioorganic & Medicinal Chemistry*, 2009, **17**, 5001-5014.

5. Lindgren, L. J., Zhang, F., Andersson, M., Barrau, S., Hellström, S., Mammo, W., Perzon, E., Inganäs, O. and Andersson, M. R., *Chem. Mater.*, 2009, **21**, 3491-3502.

6. Poloukhtine, A. A., Mbua, N. E., Wolfert, M. A., Boons, G.-J. and Popik, V. V., *J. Am. Chem. Soc.*, 2009, **131**, 15769-15776.